

---

# Stroke Mimics and In Depth Analysis of Computed Tomography Perfusion in Patients with Acute Ischemic Stroke

by

Liv Jorunn Høllesli

Thesis submitted in fulfilment of  
the requirements for the degree of  
PHILOSOPHIAE DOCTOR  
(PhD)



Faculty of Science and Technology  
Department of Electrical Engineering and Computer Science  
2024

---

University of Stavanger  
NO-4036 Stavanger  
NORWAY  
[www.uis.no](http://www.uis.no)

©2024 Liv Jorunn Høllesli

ISBN: 978-82-8439-250-9

ISSN: 1890-1387

PhD: Thesis UiS No. 772

---

## **Preface**

This thesis is submitted as partial fulfilment of the requirements for the degree of Philosophiae Doctor at the University of Stavanger (UiS), Norway.

The project is initiated and performed in cooperation between the clinical research environment at Stavanger University Hospital and the Department of Electrical Engineering and Computer Science, Faculty of Science and Technology, UiS, both situated in Stavanger, Norway. The work on this thesis has been conducted in the period between October 2019 and March 2024. This project is part of a twin project on computed tomography perfusion (CTP) in acute ischemic stroke, consisting of the current medical PhD project and a connected technical PhD project. The project is placed under the umbrella of Stavanger Medical Imaging Laboratory (SMIL) at the Radiology Department at Stavanger University Hospital, and of the BMDLab (Biomedical data analysis laboratory) at UiS, and Safer Stroke and Safer Healthcare Research Network.

The thesis is based on two published papers, with one additional submitted paper currently under review. The papers are included in the thesis.



University  
of Stavanger



**HELSE STAVANGER**  
Stavanger University Hospital



**SMIL**  
Stavanger Medical Imaging Laboratory



---

## Acknowledgements

First, I would like to thank my supervisor and good colleague and friend, Professor Kathinka Dæhli Kurz. Thank you for having introduced me to research and guiding me into the academic world, for your many ideas and encouragement. Thank you for always being available, for all the work you have laid down in this project, for scientific guidance, and for always staying positive.

Thank you to my co-supervisors Professor Kjersti Engan, Professor Martin W. Kurz and Professor Kim Beuschau Mouridsen for invaluable support. Your different focuses and personalities combined led to a perfectly matched supervision team to guide me through the complex topics and tasks of this work.

Thank you also to Jörn Schulz for important contribution with statistics, and to Hauke Bartsch at Haukeland University Hospital and our contacts in Cercare Medical for crucial help with data implementation in the startup phase of the project.

Management of acute stroke patients is complex and involves an acute stroke treatment team with both paramedics and nurses, radiographers and medical doctors. I want to express my gratitude to the entire team at Stavanger University Hospital for your excellent work and your effort. A special thanks goes to all colleagues at the Radiology Department for your important contribution in imaging in acute stroke patients and for supporting me in the work with the thesis. I am grateful to

---

Siri Fagerheim, Head of the Radiology Department, for finding solutions that made it possible to combine clinical work with research, and to the Department of Research at SUS for support and help. I will also extend my gratitude to SAFER for their effort in the stroke management and research at SUS.

Thank you to the University of Stavanger. A special thanks to Dr. Luca Tomasetti (my PhD twin) for invaluable collaboration. This twin project would not have been possible without your great effort, encouragement, and your skills in analyzing the data. Thank you for being so friendly and positive. Additionally, I want to thank all members of the BMD lab and all colleagues at the Department of Electrical Engineering and Computer Science for your support and guidance. A special thank goes to Head of Department Tom Ryen for always finding solutions to challenges and for facilitating a friendly, open, and forward-looking research environment, which it has been a pleasure to be a part of during the last 4 ½ years.

I will also express my gratitude to all my co-authors for your important contributions, for sharing your knowledge and for your support, and to the committee members for your effort on reading my dissertation and attending my defense.

Thank you to family and friends for having patience with me during busy periods, for being there for me, for your support and for encouraging me during the work on my thesis.

---

Thank you most of all to my precious Lord and Savior, Jesus Christ, who is forever faithful and watches over me every day and guides me in all things.

*Liv Jorunn Høllesli, March 2024*

---

## Summary

Globally, neurological disorders are the leading cause of disability-adjusted life years (DALYs) and the second leading cause of death<sup>1</sup>. Cerebral stroke is a major contributor to this burden, being the second leading cause of death and the third leading cause of death and disability combined<sup>2</sup>. 85 % of acute cerebral strokes are caused by ischemia<sup>3</sup>. In eligible patients with acute ischemic stroke (AIS), treatment with intravenous thrombolysis (IVT) alone or in combination with mechanical thrombectomy (MT), or MT alone, is indicated<sup>4-6</sup>. Whether treatment is applied depends on individual patient characteristics, but also largely on imaging results. Importantly, clinical outcomes of therapy are highly time dependent<sup>7,8</sup>. Therefore, neuroimaging in acute stroke patients should provide rapid, necessary, and precise diagnostic information. Computed tomography (CT) is the preferred imaging modality at many centers<sup>3</sup>.

In AIS, ischemic brain tissue is usually divided into two levels of ischemia: Ischemic penumbra and ischemic core. Ischemic penumbra is hypoperfused but still viable and potentially salvageable ischemic tissue if blood flow is restored timely. The ischemic core is irreversibly damaged ischemic tissue, which cannot be saved, with inevitable development of infarction<sup>9</sup>. The lack of a perfectly reliable definition for ischemic core presents a major challenge in current stroke imaging. Imaging plays a central role in treatment decision in patients with a suspected AIS<sup>4-6</sup>. Currently used imaging in AIS, including most



---

commonly used perfusion-based parameters, struggle to accurately differentiate between salvageable and non-salvageable tissue<sup>10-12</sup>. Calculation tools exploring the microvascular environment in AIS has shown to have the capacity to more accurately describe the ischemic brain tissue compared to conventional methods<sup>13,14</sup>. A better understanding of the microvascular environment during an ischemic event has the potential to select patients for treatment more precisely and to create the possibility for improving recovery after recanalization therapies<sup>14-17</sup>. Given the vital importance of imaging in the management of AIS patients, there is a growing need of more studies on tissue viability visualization.

At Stavanger University Hospital, patients with a suspected AIS are routinely investigated with a stroke imaging protocol, usually a non-contrast computed tomography (NCCT) of the head, CT angiography (CTA) of precerebral and intracranial arteries, and CT perfusion (CTP)<sup>7,18</sup>. Additionally, magnetic resonance imaging (MRI) including diffusion-weighted imaging (DWI) is performed in most patients, usually within 24 hours after IVT treatment. All consecutive patients with a suspected AIS having received intravenous thrombolysis are prospectively included in a local thrombolysis registry.

Minimizing time from symptom onset to treatment is of great importance in AIS, as clinical outcomes of therapy are highly time dependent<sup>7,8</sup>. It has been shown that simulation-based team-training can improve team performance<sup>19-21</sup>. A revised AIS treatment protocol along with weekly

---

simulation-based team-training for the stroke treatment team was implemented at our institution, leading to reduced treatment times, including a reduction of the median door-to-needle time (for IVT treatment) from 27 to 13 minutes<sup>7</sup>.

This thesis is based on three papers. The overall objective for paper I and II was to assess ischemic brain tissue in patients with acute ischemic stroke by utilizing the CTP dataset, MRI and clinical data. Segmentation of the ischemic lesion was the primary objective for paper I, characterization of the ischemic lesion for paper II. In paper III, possible unwanted effects of simulation training were assessed, including the proportion of SMs among IVT-treated patients for presumed AIS, and the proportion of intracranial hemorrhage (ICH) among IVT-treated SMs. The thesis demonstrated the feasibility of using CTP as input to segment the ischemic regions in AIS (paper I), and the potential for a more accurate delineation of the ischemic core using additional parametric calculations (transit time coefficient variation, CoV) compared to conventional parametric measures alone (paper II). Further, implementation of in situ simulation-based team-training for the acute stroke treatment team seems to be safe, but was associated with a significant increase in the proportion of patients treated with IVT who were later diagnosed as SMs, constituted mainly of patients with peripheral vertigo (paper III).

---

## List of papers

Paper I: Tomasetti L, Høllesli LJ, Engan K, Kurz KD, Kurz MW, Khanmohammadi M. **Machine Learning Algorithms Versus Thresholding to Segment Ischemic Regions in Patients With Acute Ischemic Stroke.** IEEE J Biomed Health Inform 2021;Pp (In eng). DOI: 10.1109/jbhi.2021.3097591. (Tomasetti and Høllesli with shared first authorship.)

Paper II: Høllesli LJ, Tomasetti L, Mouridsen KB, Schulz J, Engan K, Khanmohammadi M, Kurz MW, Kurz KD. **Is the parametric calculation “transit time coefficient variation” capable of predicting tissue outcome in patients with acute ischemic stroke?** Submitted. Journal of Cerebral Blood Flow & Metabolism, March 2024. (Høllesli and Tomasetti with shared first authorship.)

Paper III: Høllesli LJ, Ajmi SC, Kurz MW, Tysland TB, Hagir M, Dalen I, Qvindesland SA, Ersdal H, Kurz KD. **Simulation-based team-training in acute stroke: Is it safe to speed up?** Brain Behav 2022;12(12):e2814. (In eng). DOI: 10.1002/brb3.2814.

---

## **Abbreviations**

AI: Artificial intelligence

AIF: Arterial input function

AIS: Acute ischemic stroke

ANN: Artificial neural network

ASL: Arterial spin labeling

ASPECTS: The Alberta Stroke Program Early CT Score

CBF: Cerebral blood flow

CBV: Cerebral blood volume

CC: Collateral circulation

CNN: Convolutional neural network

CoV: The transit time coefficient variation

CT: Computed tomography

CTA: Computed tomography angiography

CTH: Capillary transit time heterogeneity

CTP: Computed tomography perfusion

DALYs: Disability-adjusted life years

---

DECT: Dual energy computed tomography

DSA: Digital subtraction angiography

DSC: Dynamic susceptibility contrast

DWI: Diffusion-weighted imaging

EICs: Early ischemic changes

EVT: Endovascular therapy

FLAIR: Fluid-attenuated inversion recovery

ICH: Intracranial hemorrhage

IVT: Intravenous thrombolysis

LVO: Large vessel occlusion

mCTA: Multiphase computed tomography angiography

MIP: Maximum intensity projection

ML: Machine learning

MRA: Magnetic resonance angiography

MRI: Magnetic resonance imaging

MRP: Magnetic resonance perfusion

mRS: Modified Rankin Scale

---

MT: Mechanical thrombectomy

mTICI: Modified Thrombolysis in Cerebral Infarction

MTT: Mean transit time

NCCT: Non-contrast computed tomography

NIHSS: National Institute of Health Stroke Scale

Non-LVO: Non-large vessel occlusion

PET: Positron emission tomography

PI: Perfusion imaging

PMs: Parametric maps

PtO<sub>2</sub>: Tissue oxygen tension

QI: Quality improvement

rCBF: Relative cerebral blood flow

rCBV: Relative cerebral blood volume

RCTs: Randomized-controlled clinical trials

RTH: Relative transit time heterogeneity

rtPA: Recombinant tissue plasminogen activator

sICH: Symptomatic intracranial hemorrhage

---

SLIC: Simple linear iterative clustering

SMs: Stroke mimics

SWI: Susceptibility-weighted imaging

TIA: Transient ischemic attack

Tmax: Time-to-maximum

TOF: Time-of-flight

TSE: Turbo spin echo

TTP: Time-to-peak

---

# Table of Contents

Preface .....	iii
Acknowledgements.....	v
Summary.....	viii
List of papers .....	xi
Abbreviations.....	xii
Table of Contents.....	xvi
1 Introduction.....	1
1.1 Definition of acute cerebral stroke.....	1
1.2 Etiology of acute ischemic stroke .....	1
1.3 Clinical manifestations of cerebral stroke .....	4
1.4 Epidemiology.....	5
1.5 Pathophysiology of acute ischemic stroke .....	6
1.6 Neuroimaging in acute stroke patients .....	9
1.6.1 Computed tomography .....	11
1.6.2 Magnetic Resonance Imaging .....	19
1.6.3 Advanced imaging.....	23
1.6.4 Ultrasonography.....	28
1.6.5 Nuclear medicine.....	29
1.6.6 Digital subtraction angiography .....	29
1.7 Artificial intelligence and machine learning methods.....	30
1.8 Challenges in neuroimaging in acute stroke patients .....	33
1.9 Management of acute ischemic stroke patients.....	38
1.9.1 Prehospital management.....	39
1.9.2 Neuroimaging.....	39
1.9.3 Treatment of AIS.....	40
1.9.4 Clinical scoring tools.....	48
1.10 Stroke mimics and simulation training .....	51
2 Aims of the Studies .....	54
3 Materials and Methods.....	56



---

3.1	Context.....	56
3.2	Dataset .....	56
3.3	Methods .....	59
3.4	Statistics .....	64
3.5	Ethical considerations .....	65
4	Results of Papers .....	67
5	Discussion and Future Perspectives .....	72
6	References .....	84
	Appendices .....	115
	Paper I: Machine Learning Algorithms Versus Thresholding to Segment Ischemic Regions in Patients With Acute Ischemic Stroke. ....	115
	Paper II: Is the parametric calculation “transit time coefficient variation” capable of predicting tissue outcome in patients with acute ischemic stroke? ...	115
	Paper III: Simulation-based team-training in acute stroke: Is it safe to speed up? .....	115

# **1 Introduction**

## **1.1 Definition of acute cerebral stroke**

Acute cerebral stroke is characterized as a sudden loss of neurological function due to brain or retinal ischemia (85%) or intracerebral hemorrhage (15%)<sup>3</sup>. Among ischemic strokes, impairment of the arterial blood flow is by far the most common etiology, with venous strokes accounting for <1% of all strokes<sup>3</sup>.

## **1.2 Etiology of acute ischemic stroke**

Ischemic strokes are caused by focal or systemic hypoperfusion. Focal hypoperfusion is usually caused by stenosis or occlusion of one or several intracranial arteries or extracranial arteries giving blood supply to the brain. This can be caused by different mechanisms, with thrombosis, embolism and atherosclerosis being the most common<sup>22-24</sup>:

- **Thrombosis:** A focal thrombotic clot is formed in an intra- or extracranial artery causing stenosis or occlusion of the affected artery.
- **Embolism:** A focal occlusion is caused by an embolic clot from a distant location outside the cranium, that is carried to the brain via the blood stream and causes occlusion or stenosis of an intracranial artery. The most common form is an embolic blood clot from the heart, aorta or cervical arteries. Other potential sources are also important to be aware of, like septic emboli from infective endocarditis and patent foramen ovale.

- Occlusive or stenotic vascular disease caused by atherosclerosis of intra- or extracranial arteries.

Small lacunar infarcts due to small vessel disease are also a common cause of ischemic stroke.

Systemic hypoperfusion can lead to impaired blood supply to the brain. Cerebral infarctions caused by systemic hypoperfusion will typically start in watershed regions between the vascular territories of large cerebral arteries and will eventually spread to affect the whole brain if brain perfusion is not restored. Brain tissue in the vascular territory of stenotic arteries are particularly vulnerable to ischemia if blood pressure drops<sup>25</sup>.

Acute ischemic stroke (AIS) is often divided into different subtypes by The Trial of Org 10172 in Acute Stroke (TOAST) classification, which defines five subtypes of ischemic stroke based on the anticipated etiology<sup>23</sup>:

- Large artery atherosclerosis (embolus/thrombus)
- Cardioembolism
- Small vessel occlusion
- Stroke of other determined etiology
- Stroke of undetermined etiology

A more recent publication using more advanced techniques with vessel wall imaging, showed the potential to better determine the etiology in

acute ischemic stroke, in which stroke etiology was classified with a modified TOAST classification<sup>26</sup>:

- Cervical atherosclerotic disease
- Cardioembolism
- Small vessel occlusion
- Stroke of other determined etiology
- Stroke of undetermined etiology
- Intracranial atherosclerosis
- Intracranial arterial dissection
- Vasculitis
- Reversible cerebral vasoconstriction syndrome
- Intracranial arteriopathy not otherwise specified

Patients presenting with AIS are often categorized according to level of vessel occlusion: Large vessel occlusion (LVO) and non-large vessel occlusion (non-LVO). The definitions used in the literature exhibit noticeable variability<sup>27</sup>. At our institution, the following definitions have been adopted:

- LVO: Occlusion of the internal carotid artery, M1 and proximal M2 segment of the middle cerebral artery, A1 segment of the anterior cerebral artery, P1 segment of the posterior cerebral artery, basilar artery and vertebral artery<sup>5,27-29</sup>.
- Non-LVO: Acute ischemic stroke patients with occlusion of more distal arteries or with perfusion deficits or cytotoxic

edema on diffusion weighted imaging (DWI) without visible artery occlusion<sup>28</sup>.

Patients presenting with LVO are less common compared to non-LVO. The prevalence of LVO is estimated to range between approximately 10-30% among patients presenting with AIS<sup>30-32</sup>. Still, patients with LVO clearly represent a clinically significant share of patients with AIS, considering the tendency to present with large ischemic lesions and the grim natural course of this condition<sup>33</sup>.

### **1.3 *Clinical manifestations of cerebral stroke***

Cerebral strokes manifest as a sudden loss of neurological function and have a wide range of clinical manifestations, from transient to permanent and from mild to fatal presentation. Clinical presentation depends among other factors on size and site of the affected brain tissue. Impairment of motor and sensory functions as well as language and visual disturbances are common manifestations in acute stroke. Ischemic and hemorrhagic strokes share a lot of common clinical manifestations, though acute onset of symptoms with headache, increased systolic blood pressure and vomiting might indicate hemorrhage<sup>34</sup>.

#### **1.4 Epidemiology**

Globally, neurological disorders are the leading cause of disability-adjusted life years (DALYs) and the second leading cause of death<sup>1</sup>. Cerebral stroke is a major contributor to this burden, being the second leading cause of death and the third leading cause of death and disability combined<sup>2</sup>. The global burden of stroke is increasing<sup>2</sup>. Despite significantly reduced age-standardized rates over the past years, the annual number of strokes, DALYS and deaths from stroke has increased substantially, with the highest contributor to the global stroke burden found in lower-middle income younger age groups with increasing rates<sup>2</sup>. Globally, there were 12.2 million incident strokes (62.4% constituted by AIS), 101 million prevalent strokes, 143 million DALYs due to stroke and 6.55 million deaths from stroke in 2019<sup>2</sup>, with 89% of stroke-related DALYS and 86% of stroke-related deaths occurring in lower-middle income countries. The positive trend of falling age-adjusted stroke rates is outweighed by an increasing ageing population in European countries<sup>35</sup>. Changes in demography with an increasing population of old age groups will result in a predicted increase in stroke incidence in the European Union, which is likely to be mirrored in many other parts of the world. Different studies have shown some discrepancies when it comes to future trajectories of stroke incidence and prevalence, probably due to methodological differences. The Stroke Alliance for Europe anticipates a 34 % increase in incident stroke events between 2015 and 2035<sup>35</sup>, while another study forecasts a modest increase of 3 % between 2017 and 2047 and an increase in stroke

survivors (prevalence) by 27 % in the same period<sup>36</sup>. This is largely due to an expected increase in the population aged  $\geq 70$  years old in which stroke risk is the highest, which is expected to compromise 23 % of the population in 2047 compared to 14% in 2017<sup>36</sup>.

The reduced incidences of stroke over the past years are largely due to prevention and better control of risk factors<sup>37</sup>. Risk factors for developing cerebral strokes include both modifiable and nonmodifiable factors<sup>38</sup>. Among nonmodifiable risk factors are age, sex and race/ethnicity, among modifiable risk factors are hypertension, high body mass index, smoking, unhealthy diet, low physical activity, hyperlipidemia, diabetes mellitus (high fasting plasma glucose), alcohol consumption and cardiac causes with especially atrial fibrillation being a major risk of stroke<sup>38</sup>. Genetic predisposition is also a well-recognized risk factor, often placed in an overlapping position between nonmodifiable and modifiable risk factors due to its increasingly recognition as potentially modifiable<sup>38</sup>. In 2019, 87 % of total stroke-related DALYs were attributable to 19 risk factors, with high systolic blood pressure, high body mass index and high fasting plasma glucose as top three risk factors<sup>2</sup>.

### **1.5 Pathophysiology of acute ischemic stroke**

In acute ischemic stroke, one common differentiation is to divide the ischemic brain tissue into two levels of ischemia: Ischemic penumbra and ischemic core. It was Astrup et al who first defined the ischemic

penumbra as electrically silent functionally impaired tissue with residual perfusion sufficient to maintain a close to normal concentration of adenosine triphosphate and sustained energy metabolism, with possible potential for recovery<sup>9</sup>. Ischemic penumbra is hypoperfused but still viable and potentially salvageable ischemic tissue if blood flow is restored timely. If blood flow is not restored, however, the tissue will eventually develop into irreversibly damaged ischemic tissue. The ischemic core is irreversibly damaged ischemic tissue, which cannot be saved, with inevitable development of infarction. The term “benign oligemia” in AIS is occasionally encountered in the literature. This refers to a phenomenon sometimes found in AIS, with a temporary decrease in blood flow in brain tissue surrounding the primary affected regions, which typically resolves spontaneously without causing significant or permanent damage<sup>39</sup>. The original notion that in AIS, occlusion of an artery causes an ischemic lesion with a centrally located irreversibly injured core with surrounding potentially salvageable penumbra<sup>40</sup>, is useful and is also supported by imaging findings with often confluent infarcted regions on follow-up imaging. However, recent imaging and experimental findings suggest that in the early minutes and hours after onset of ischemia, the ischemic lesion actually consists of several “mini-cores” surrounded by “mini-penumbra” with further coalescence of the mini-cores as time goes by if blood flow is not restored<sup>41</sup>.

Research over the last decades has led to an increasing though not yet full understanding of the underlying factors such as hemodynamics and cellular and molecular pathways involved in ischemic brain injury.



Cerebral autoregulation is the mechanism that leads to a relatively constant level of cerebral blood flow within moderate changes in perfusion pressure, i.e., a perfusion pressure of typically 60-150 mm Hg<sup>42</sup>. Different mechanisms are thought to participate in maintaining a relatively constant blood flow, like vasoconstriction and vasodilatation in response to increased or decreased perfusion pressure, respectively. Hence, under normal conditions, cerebral blood flow is primarily determined by the degree of vascular resistance in cerebral blood vessels<sup>42</sup>. If perfusion pressure exceeds the autoregulation limits, the ability to maintain constant blood flow through autoregulation is lost. This poses a risk of ischemia if perfusion pressure is reduced, and a risk of edema if perfusion pressure is increased. Reduced perfusion pressure will eventually lead to a decrease in cerebral blood flow. Initially, oxygen delivery to the brain is maintained through increased oxygen extraction fraction<sup>13,42</sup>. With further reduced blood flow, other factors are involved. Several conditions, including ischemic stroke, are known to cause impairment of cerebral autoregulation<sup>43</sup>. This may lead to injured brain tissue being even more vulnerable to changes in perfusion pressure. There are some critical levels of cerebral blood flow (CBF), with inhibition of protein synthesis by blood flow below 50 mL/100 g/minute and ceasing completely at 35 mL/100 g/minute. The last value corresponds to the same level at which the utilization of glucose and energy metabolism is disturbed. Failure of neuronal electrical activity occurs at CBF below 16-18 mL/100 g/minute, with further reduction below 10-12 mL/100 g/minute leading to failure of membrane ion

homeostasis<sup>42,44</sup>. This level is typically referred to as the threshold for development of infarct.

Despite not performing mechanical work, the human brain is one of the most metabolically active organs in the body. It requires about 20 % of the cardiac output despite only possessing 2 % of the total body weight<sup>42</sup>. With no own energy storage, the brain depends on preserved blood flow for the supply of oxygen and glucose to maintain its metabolic demands. This fails during an ischemic stroke. With CBF below 10-12 mL/100 g/minute, a cascade of cellular events eventually leads to cell death: The release of unregulated glutamate, depletion of ATP, impairment of ionic pumps leading to changes in concentrations of sodium, potassium and calcium, increased lactate, acidosis, accumulation of oxygen free radicals, cell swelling due to intracellular water accumulation (cytotoxic edema) and activation of proteolytic enzymes<sup>45-47</sup>. Cerebral ischemia and infarction cause loss of structural integrity of the affected brain tissue<sup>47</sup>. Vascular injury causes impairment of the blood-brain-barrier leading to brain edema and in some cases hemorrhage in the ischemic region (hemorrhagic conversion). With breakdown of the blood-brain-barrier, proteins and other macromolecules enter the extracellular space followed by increased extracellular fluid volume (vasogenic edema)<sup>46,47</sup>.

## **1.6 Neuroimaging in acute stroke patients**

In eligible patients with acute ischemic stroke, intravenous thrombolysis (IVT) alone or in combination with mechanical thrombectomy (MT), or

MT alone, is indicated<sup>4-6</sup>. Whether treatment is applied depends on individual patient characteristics, but also largely on imaging results. Importantly, clinical outcomes of therapy are highly time dependent<sup>7,8</sup>. Therefore, neuroimaging in acute stroke patients should provide rapid, necessary, and precise diagnostic information.

Imaging approach may differ according to patient characteristics and local availability of stroke expertise and imaging capabilities. According to current guidelines, diagnostic imaging with computed tomography (CT) or magnetic resonance imaging (MRI) is recommended in all patients with suspected acute cerebral stroke<sup>5,48</sup>. MRI with DWI is superior to CT for detection of acute infarctions and identification of some stroke mimics<sup>49,50</sup>. Still, CT is the preferred imaging modality at most centers for acute stroke patients due to its widespread availability, rapid scan times, and its high sensitivity for detecting hemorrhage<sup>3</sup>.

The goals of imaging in patients with acute cerebral stroke are to confirm the diagnosis and provide guidance for treatment decisions by the following<sup>51</sup>:

- Exclude hemorrhage and stroke mimics
- Assess the large extracranial and intracranial arteries
- Identify potentially salvageable brain tissue at risk of developing into infarction (ischemic penumbra) and irreversibly damaged ischemic tissue (ischemic core)

- Uncover possible etiology (e.g., embolic stroke, lacunar stroke, dissection, atherosclerosis)

### *1.6.1 Computed tomography*

Computed tomography (CT) is a radiological imaging modality that involves the rotational projection of a series of x-ray beams onto a targeted area of the body, resulting in images through computer processing. Currently used CT-scanners typically use spiral/helical scan techniques, where the table moves continuously while the x-ray source and detectors rotate, allowing for fast scanning times. The resulting volumetric tomographic images offer the creation of three-dimensional images and contain detailed information. CT images are highly useful in various medical scenarios and can provide valuable information in detection, therapy planning and monitoring of many different diseases<sup>52,53</sup>.

#### **1.6.1.1 Non-contrast computed tomography**

Non-contrast computed tomography (NCCT) has high sensitivity for detecting hemorrhage and early signs of acute ischemic stroke can be detected. Common early ischemic changes (EICs) are subtle hypoattenuation of the brain tissue, loss of grey-white matter differentiation, sulcal effacement and poor delineation of the basal ganglia and insular ribbon<sup>54</sup>. The Alberta Stroke Program Early CT Score (ASPECTS) is used to quantify the extent of EICs. Here,

segmental estimation of the middle cerebral artery vascular territory is performed by subtracting 1 point from the initial score of 10 for each predefined region with hypoattenuation involved<sup>55</sup>. ASPECT score has been shown to correlate inversely with the National Institute of Health Stroke Scale (NIHSS) score and predict functional outcome and symptomatic intracerebral hemorrhage, with a score of 7 or less highly associated with poor outcome<sup>55</sup>. Therefore, it can be used prognostic and in treatment decision. Current guidelines advise against performing MT in AIS patients with an ASPECTS <6<sup>5,6</sup>.

A normal NCCT scan does not rule out an AIS. Though hypodensity on NCCT is regarded highly specific for irreversibly damaged brain tissue, there is limited sensitivity for detecting early ischemic changes and interobserver variability is common<sup>56-58</sup>. Although rare, hypodensity on NCCT may in some cases be reversible after recanalization<sup>59</sup>. Recent advancement in scanning techniques have demonstrated capability of improved diagnostic accuracy, such as dual energy CT (DECT)<sup>60</sup>. DECT using X-map has shown greater sensitivity in detecting EICs compared with simulated 120-kVp mixed-CT and may also provide additional information in DWI-negative acute ischemic regions<sup>61</sup>. NCCT can also yield diagnostic information concerning acute intravascular thrombi; a blood clot can be seen as a hyperdensity within a blood vessel, the “dense artery sign”<sup>62</sup>.

### **1.6.1.2 Computed tomography angiography**

Computed tomography angiography (CTA) is well suited for assessing the status of large cervical and intracranial arteries and is used for selecting patients eligible for endovascular treatment, i.e., patients with LVO. CTA is performed by injecting iodinated contrast through an intravenous line with image acquisition from the aortic arch to skull vertex during the arterial peak phase of contrast. Filling defects in both intracranial and extracranial arteries are visualized.

During CTA acquisition, reduced contrast filling in the brain microvasculature can be detected in infarcted regions. These regions appear hypodense compared to normal brain tissue. This can be depicted on the CTA source images, and the sensitivity to detect early ischemia is higher compared to NCCT<sup>63</sup>.

#### **1.6.1.2.1 Collateral circulation imaging**

Collateral circulation (CC) imaging is based on multiphase CTA (mCTA) with CTA in three distinct phases through the whole brain; peak arterial (from aortic arch to vertex), peak venous and late venous phase<sup>64</sup>. Imaging in different phases of contrast allow time-resolved assessment of pial collateral arterial filling in the ischemic region, by which temporal delay in the filling of vessels in addition to the extent of contrast filling of the vessels can be evaluated. The technique is used for patient selection for MT by comparing the pial arterial filling in the ischemic

region to the contralateral hemisphere. Good CC has been shown to be associated with greater likelihood for successful recanalization and better clinical outcomes compared to patients with poor CC<sup>64,65</sup>. Compared to single phase CTA, mCTA provides better sensitivity for detection of vessel occlusions<sup>66,67</sup>, improved evaluation of internal carotid artery stenosis<sup>68</sup>, assessment of thrombus length<sup>69</sup>, improved tolerance for motion and poor hemodynamics, higher interrater reliability<sup>70</sup>, requires only a small increase in radiation dose, no additional contrast injection, no need for image post processing and provides whole-brain coverage<sup>64</sup>.

### **1.6.1.3 Computed tomography perfusion**

Computed tomography perfusion (CTP) provides information about tissue viability and has proven useful for outcome prediction and for detection of the ischemic lesion<sup>71-73</sup>. One study yielded a sensitivity of 80 % and a specificity of 95 % for the detection of acute ischemic lesions, with 2/3 of the missed lesions caused by small lacunar infarcts and the remainder mainly due to limited coverage of the ischemic region<sup>71</sup>. In addition, visualizing the ischemic lesion helps to detect vessel occlusions by targeting where occlusions are located. This is especially useful in distal medium vessel occlusions, which can be challenging to detect on CTA alone, especially for less experienced radiologists/residents on call<sup>74,75</sup>. The technique is used to aid treatment decisions in acute stroke patients, especially those presenting in the extended time window. CTP

is also useful in stroke mimics, with the ability to show perfusion abnormalities in certain conditions like seizure, migraine and tumors<sup>76</sup>.

In CTP, a time series of three-dimensional datasets are acquired with repeated scans through the brain during the passage of contrast through the brain vasculature. Typically, only a distinct region of the brain is included, corresponding to where the ischemic lesion is suspected to be located based on the clinical presentation. Color-coded parametric maps (PMs) are then generated by analyzing alterations in tissue density over time. The different PMs highlight spatio-temporal information from the passage of the contrast agent within the brain tissue<sup>77-79</sup>. Generally, CTP PMs are generated in two steps: The first step acquires a time-density curve for each pixel based on the track of the contrast agent. The second step consists of extracting specific information from the generated time-density curves. Time-to-peak (TTP), mean transit time (MTT), time-to-maximum (Tmax), cerebral blood volume (CBV) and cerebral blood flow (CBF) are examples of different commonly used parametric maps. TTP reflects the time it takes until the contrast bolus reaches maximum concentration in the tissue (the apex of the time-density curve) and is highly sensitive to ischemia. Increased TTP indicates ischemia, as it takes longer time for the contrast medium to reach the ischemic region compared to normal brain tissue. MTT represents the time from wash in to wash out of the contrast media in the brain tissue, which is also increased during ischemia. Time-to-maximum of the flow-scaled residue function is obtained by deconvolution of the arterial input function (AIF) and is also prolonged during ischemia. This parameter is not fully



understood and is influenced by a complex interaction of many factors, but it represents the arrival delay between the contrast bolus arriving in the proximal large arterial circulation (AIF) and the tissue, and should be considered a measure of macrovascular characteristics<sup>80,81</sup>. Tmax is highly sensitive to ischemia, and has been shown to reliably identify critically hypoperfused tissue<sup>82</sup>. TTP, MTT and Tmax are usually measured in seconds. CBV is the blood volume present in a distinct region of the brain (e.g., as ml blood/100 ml brain tissue) and is calculated from the area under the time attenuation curve (figure 1). CBF is the blood supply to a distinct region of the brain for a given time (e.g., as ml blood/100 ml brain tissue/minute) and is derived from the slope of the wash in of the time-density curve (figure 1). Absolute values for these two parameters can only be calculated if there is no recirculation of contrast and no capillary permeability, of which the second claim is difficult to fulfil as permeability can vary a lot. Hence, relative values are calculated representing CBV or CBF relative to an internal control like contralateral white matter or an AIF. This is referred to as relative cerebral blood volume (rCBV) and relative cerebral blood flow (rCBF). The relationship between MTT, CBV and CBF is represented by the following equation (the central volume theorem):  $MTT = CBV/CBF$ <sup>83</sup>.

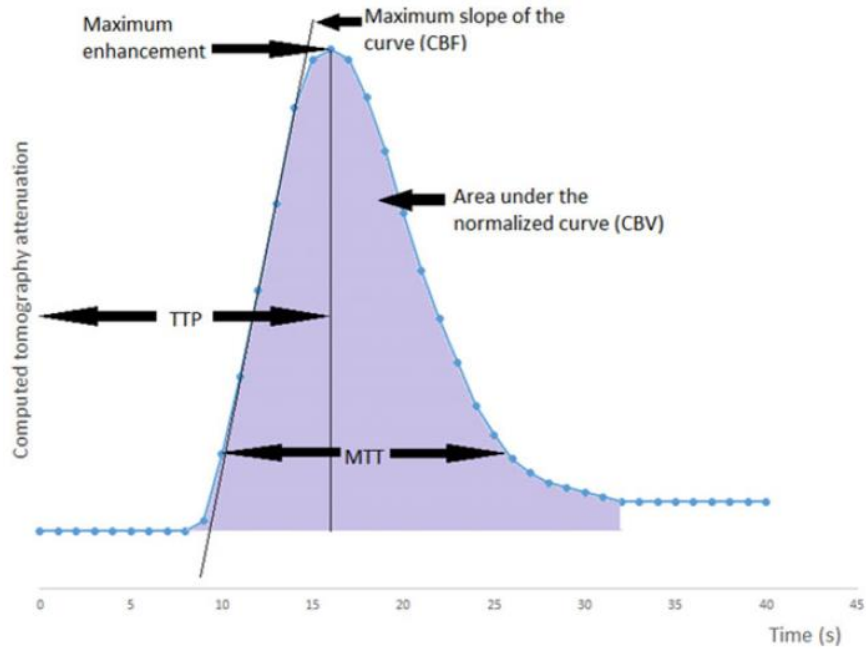


Figure 177: CTP time-density curve. TTP is defined as the time it takes until the contrast bolus reaches maximum concentration in the tissue. MTT represents the time from wash in to wash out of the contrast media in the brain tissue. The area under the curve represents CBV, which is the blood volume present at a given time in a distinct region of the brain, and CBF is the blood supply to a distinct region of the brain and is derived from the slope of the wash in of the time-density curve. Figure text is slightly modified.

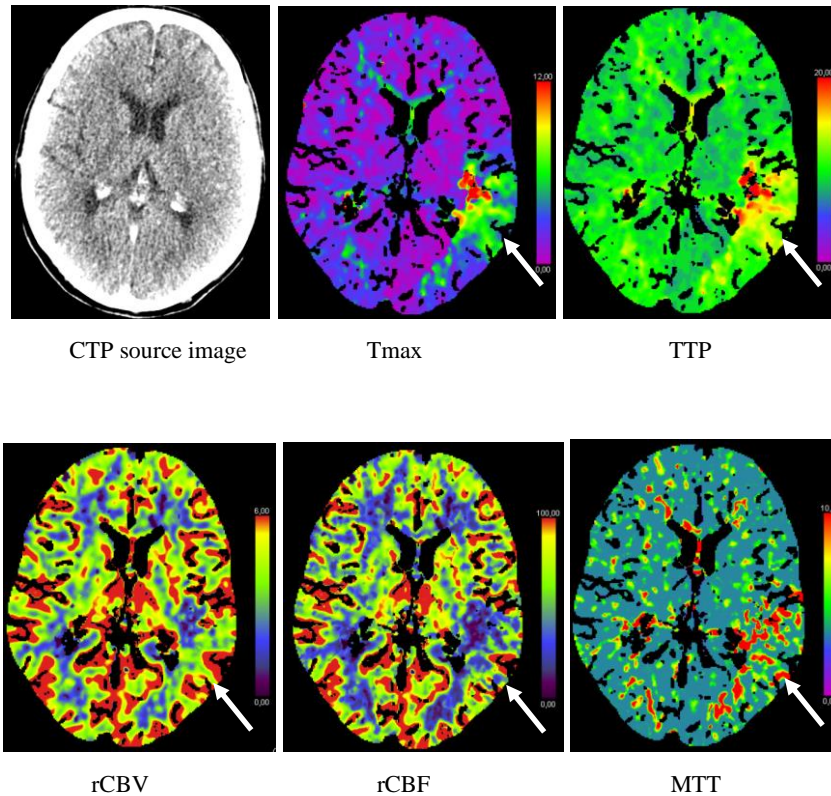


Figure 2: CTP source image and different conventional PMs from a CTP scan in an AIS patient. There is an ischemic lesion in the vascular territory of the left middle cerebral artery (arrow).

To estimate penumbra and core on CTP, different approaches are used, both automatic and manual. One method is to presume that areas with reduced CBF and increased TTP/Tmax represent penumbra<sup>84,85</sup>, while areas with additionally significantly reduced CBV represent the ischemic core<sup>86,87</sup>. A wide variety of different thresholds are used for different PMs to estimate penumbra and core<sup>85,88-96</sup>. One commonly used definition for core is CBF reduced to <30 % compared to the contralateral hemisphere, and penumbra as Tmax >6 s<sup>4,84,94-96</sup>.

CTP source images can also be used to identify infarcted brain regions, which appear hypodense compared to normal brain tissue, and has been shown to predict neurological outcome and final infarct volume better compared to NCCT<sup>97</sup>.

### *1.6.2 Magnetic Resonance Imaging*

Like CT, magnetic resonance imaging (MRI) is also highly sensitive for detecting hemorrhage. It is equivalent to NCCT for the detection of acute hemorrhage and has higher sensitivity for the detection of chronic hemorrhage<sup>98</sup>. It is also superior to CT for detection of acute infarctions and identification of some stroke mimics<sup>99-105</sup>. In many stroke centers, MRI is not as easily accessible as CT for the initial assessment of patients with suspected acute stroke, and MRI is often not available fast enough on a 24/7 basis. MRI is also limited by other contraindications, higher costs and longer scan times leading to potential delayed treatment compared to CT<sup>106,107</sup>. The standard MRI-based stroke protocol does not include the aortic arch or the precerebral arteries, and anatomical variations and pathology that is relevant for treatment decisions might therefore be missed initially. Nevertheless, MRI is superior to CT in AIS in several aspects, such as detection of AIS. There is a growing number of reports indicating that the use of MRI in the acute setting does not cause delays. Initial assessment with MRI has proven to be feasible within the time constraints for guidelines-based treatment times<sup>108</sup>, and outcomes in AIS patients initially evaluated

with acute MRI has been shown not to differ from those evaluated with CT<sup>107</sup>. Ultrafast MRI protocols have also been developed with scan times below five minutes, with the potential of selecting patients for treatment in the acute setting and to provide an alternative diagnostic tool in patients who do not tolerate long scan times<sup>109</sup>. If not performed in the acute stage, MRI should be performed in all patients with a suspected ischemic stroke as part of the in-hospital diagnostic follow-up within one to three days to determine exact infarct distribution and to evaluate potential differential diagnoses.

#### **1.6.2.1 MRI protocols in patients with suspected cerebral stroke**

In patients with a suspected cerebral stroke, a MRI protocol typically includes DWI, a T2-weighted turbo spin echo (TSE) sequence, a fluid-attenuated inversion recovery (FLAIR) sequence, a T2\*-weighted Turbo Field Echo or susceptibility-weighted imaging (SWI) sequence and a 3D arterial MR angiography (MRA). Time-of-flight (TOF) is the most widely used technique, though contrast enhanced MRA can also be performed. Both a T2-weighted TSE and a FLAIR sequence can be included or just one of them. Especially in patients with suspected stroke with unknown time of onset, a FLAIR sequence should be included.

DWI is an important sequence in stroke imaging, with high sensitivity and specificity for detecting acute ischemia<sup>110</sup>. DWI reflects the

random, Brownian movement of diffusion of water. In an ischemic lesion with cytotoxic edema, the intracellular water content increases, causing the cells to swell. Enlargement of the cells leads to narrowing of the extracellular space, causing restricted diffusion as the free movement of extracellular water molecules are impeded. Due to anisotropy in the brain, diffusion is measured in three directions, and restricted diffusion corresponds to reduced movement in all three directions<sup>111</sup>. This is visualized as a hyperintense signal on the DWI images with corresponding low ADC values. DWI has potential for detecting ischemic changes within minutes after onset<sup>101</sup>. Infarcted brain tissue continues to demonstrate restricted diffusion until the end of the first week, then ADC values start to increase, and at approximately 1-4 weeks, normal ADC values are measured in the infarct. The time for ADC normalization is dependent on the infarct size, among other factors<sup>101</sup>. During this development, the DWI hyperintense signal gradually decreases.

Vasogenic edema, in which the blood-brain-barrier is disrupted, causes extracellular edema. In this setting, the diffusion of extracellular water molecules is not restricted as in cytotoxic edema.

Whereas restricted diffusion is visible almost immediately when an ischemic stroke develops, it takes more time for acute ischemic changes to be visible on conventional sequences. Vasogenic edema typically appears within hours after onset, visualized with hyperintense signal on FLAIR and T2-weighted sequences.

The DWI-FLAIR mismatch, with early ischemic changes on DWI but without visible changes on FLAIR, has been found to identify patients within 4.5 hours with high specificity and positive predictive value<sup>112</sup>, corresponding to the 4.5 hours' time window for which thrombolytic treatment has been proven safe and effective<sup>4,8,112,113</sup>. T2\* or SWI are highly sensitive to detect intracranial hemorrhage<sup>98,114</sup>. Moreover, it is also useful for the early detection of acute thrombosis in large intracranial arteries with hypointense signal from the thrombosed vessel, the so-called “susceptibility-sign” corresponding to the “dense-artery sign” on NCCT<sup>115,116</sup>. MRA is performed to evaluate intracranial vessels with the capability to detect stenosis and occlusions in acute ischemic stroke.

#### **1.6.2.2 Perfusion imaging**

Similar to CTP, viability of ischemic brain tissue can also be assessed with MRI through perfusion imaging (PI). PI can be performed by utilizing the magnetic susceptibility effect from the passage of an intravenously administered gadolinium-based contrast agent through brain tissue, called dynamic susceptibility contrast (DSC) MR perfusion (MRP). DSC MRP has been shown to correlate with severity and outcome in AIS<sup>117</sup>. Similar PMs as those derived from CTP can be calculated, like TTP, MTT, Tmax, CBF and CBV. Alternatively, arterial spin labeling (ASL), without the use of contrast agent, can be used to depict perfusion deficits in ischemic regions of the brain. In

ASL, blood is magnetically labeled at the level of the neck before entering the brain. To assess the perfusion of labeled blood throughout the brain vasculature, subtraction images are generated by subtracting labeled images from control images (acquired before labeling). The remaining signal in the subtraction images is linear to the perfusion and proportional to the cerebral blood flow.

To support treatment decision in acute ischemic stroke, the PI-DWI mismatch is commonly used. PI-DWI mismatch corresponds to a larger PI-lesion (i.e., penumbra) than DWI-lesion (i.e., core), representing patients with salvageable tissue who might benefit from reperfusion therapy<sup>96,118-122</sup>.

### *1.6.3 Advanced imaging*

Advanced imaging is used to provide information about tissue viability, i.e., information about the irreversibly damaged ischemic core and the hypoperfused but still viable and potentially salvageable ischemic penumbra. This can be performed with either multimodal CT (multiphase CTA or CTP) or multimodal MRI (DWI and PI)<sup>4</sup>. A correlation between imaging and clinical symptoms can also be a part of the assessment<sup>123</sup>.



### 1.6.3.1 The capillary environment in ischemic brain tissue

The environment on the capillary level is thought to influence the spatiotemporal evolution of tissue damage during an ischemic event in the brain<sup>13,17,124,125</sup>. Tissue oxygenation is related to blood flow, but also depends on capillary flow patterns<sup>126,127</sup>. Capillary flow velocities are highly heterogeneous in a normal, resting brain<sup>128</sup>. This can give rise to *functional shunting*, where extraction of substances like oxygen and glucose through the brain tissue becomes less efficient as capillary flow becomes more heterogeneous<sup>14,124</sup>. It has been shown that capillary flow becomes more homogenous when there is hyperemia caused by brain activation, which contributes to more sufficient oxygen extraction and seemingly ensures sufficient oxygen extraction across a wide range of blood flows and metabolic needs in the brain<sup>14,124,127</sup>. *Capillary dysfunction* relates to the failure of homogenization of capillary flow during episodes of increased blood flow<sup>14</sup>, i.e., a gradual increase in resting capillary flow heterogeneity during episodes of increased blood flow<sup>129</sup>. In response to ischemia, capillary vasoconstriction causes limited flow and increased capillary dysfunction. To some degree, lower velocity of blood through the microvasculature compensates for this by maintaining oxygen levels in the tissue through increased oxygen extraction, though widespread vasoconstriction may also prevent sufficient oxygen levels and cause ischemia. Higher blood flow velocities cause impaired oxygen extraction. Capillary dysfunction tends to cause increased functional shunting by increased blood flow induced by brain activation or hypercapnia, which can lead to so-called

*luxury-perfusion* causing a paradoxical reduction in tissue oxygenation after reperfusion in ischemic tissue<sup>127,130</sup>. The effects of capillary dysfunction on tissue oxygenation can be evaluated by capillary flow and transit times through the capillary bed<sup>124,127</sup>. Two calculations have been developed to characterize the distribution of capillary transit times: The mean of capillary transit times (MTT) and the standard deviation of capillary transit times, the capillary transit time heterogeneity (CTH)<sup>124,127,131</sup>. These parameters have been used to calculate the oxygen extraction efficacy for different transit time distributions. CTH is an indicator of microvascular distribution of blood and changes in proportion to MTT in normal anatomical microvascular networks; a passive increase in proportion to MTT is expected in response to reduced perfusion pressure during an ischemic event<sup>13</sup>. Additionally, the ratio between these two parameters, the transit time coefficient variation (CoV), also called the relative transit time heterogeneity (RTH), a measure of capillary dysfunction, has been used to distinguish between passive changes due to hypoperfusion and deterioration of the autoregulation of the vasculature<sup>124,127</sup>.

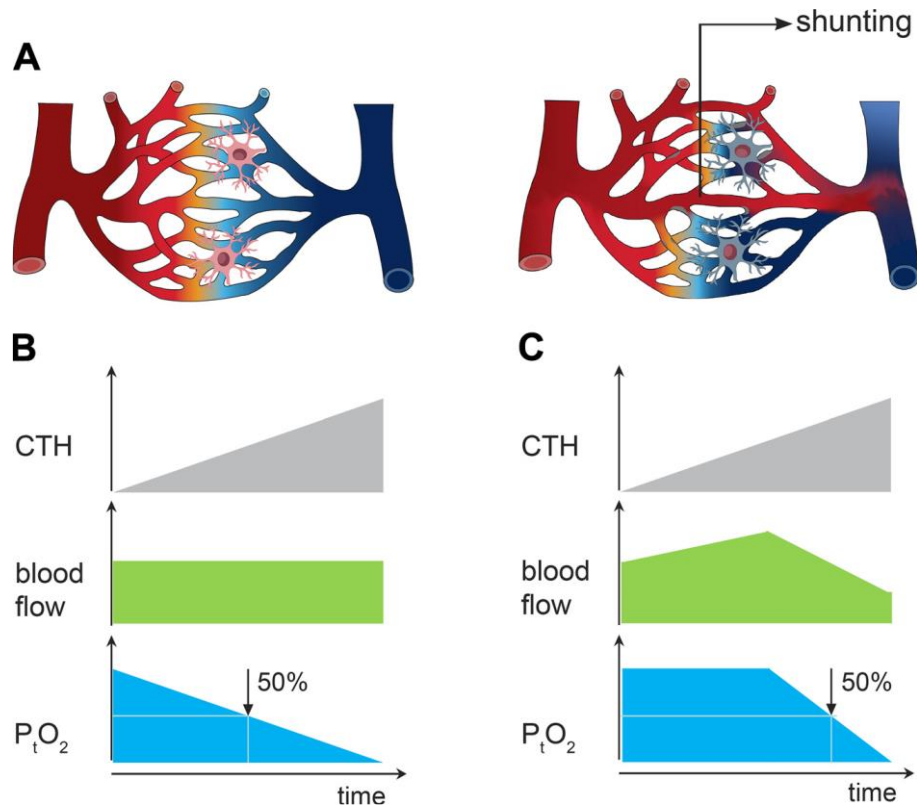


Figure 3<sup>129</sup>: Tissue oxygen tension ( $P_{tO_2}$ ) is influenced by capillary patency. A: During increased blood flow, disruption in capillary patency can disturb capillary flow patterns and prevent normal homogenization. B: Cumulative disturbances lead to gradual increase in capillary transit times (CTH), lowering oxygen uptake, and causes  $P_{tO_2}$  to decrease unless compensatory changes in blood flow occur. C: Compensatory hyperemia can maintain normal  $P_{tO_2}$  for mild capillary dysfunction, but for severe dysfunction, this “shunting” of oxygenated blood can only be alleviated by increased oxygen extraction, which is achieved by prolonging blood transit times through limiting blood flow. These compensatory flow changes can only temporarily delay symptoms and tissue damage, as illustrated by the time at which  $P_{tO_2}$  starts to drop and reaches 50% of normal values (B+C). Figure text is slightly modified.

CBF is adjusted in relation to the metabolic needs of the tissue by the *neurovascular coupling mechanism*<sup>14,132</sup>. As capillary dysfunction increases and oxygen extraction drops, the neurovascular coupling mechanism would be expected to adjust CBF accordingly<sup>124,133</sup>. With

only minor capillary dysfunction, a small increase of CBF is thought to compensate for minor impaired oxygen extraction. This explains why capillary dysfunction is expected to cause hyperemia in some preclinical conditions like stroke and certain types of dementia<sup>124</sup>. As capillary dysfunction worsens, sufficient oxygen extraction can only be maintained by limiting flow responses, until a certain limit<sup>124</sup>. This limit corresponds to the highest CTH value for which the brain's metabolic needs can be met. Above this, attempts to increase CBF will not be sufficient to maintain the tissue's metabolic needs due to excessive functional shunting. The neurovascular coupling mechanism explains the low CBF found in capillary dysfunction<sup>124</sup>. Interestingly, this corresponds to CBF <20 mL/100 mL/min, which is commonly referred to as an ischemic threshold<sup>124,134</sup>. It is thought that cerebral ischemia causes widespread capillary no-flow, and that transit time homogenization represents capillary no-flow<sup>13,135</sup>. Accordingly, severe homogenization of flow, in terms of its corresponding low RTH values, is associated with low CBV and CBF and increased risk of infarction<sup>13</sup>. Capillary dysfunction has been explored experimentally. In one computational model, different grades of microvascular failure were related to changes in PI-based parameters, including CBF, MTT, CTH, RTH, oxygen extraction fraction and cerebral metabolic rate of oxygen<sup>13</sup>. Voxel-wise transit times can be derived from perfusion imaging using the concentration time curve from voxels within the image slices (CTP or MRP)<sup>13,124</sup>, which further allows calculation of oxygen extraction in the tissue<sup>127,136</sup>. Voxel-wise MTT, CTH and RTH

have been used to examine how acute ischemia and subsequent recanalization affect tissue outcome on follow-up MRI<sup>13</sup>. It has been shown that there is high risk of infarction in perfusion-diffusion mismatch tissue when perfusion drops below a certain level (MTT >5 s and CBF  $\leq$ 6 mL/100 mL/min), regardless of recanalization status<sup>13</sup>. However, low RTH predicts high risk of infarction if recanalization is not achieved, also in tissue with preserved CBF<sup>13</sup>. Hence, RTH could represent a novel biomarker for microvascular failure<sup>13</sup>.

One important aspect of the capillary dysfunction phenomenon is the gradual accumulation of microvascular changes. It is thought that mechanisms leading to an ischemic event in some stroke patients evolve over several decades, with capillary dysfunction being central, to finally present as an acute event<sup>124</sup>. Still, many strokes are clearly caused by an acute thromboembolic event, wherein capillary dysfunction may become important after recanalization with the possibility of impaired microvascular reperfusion persisting despite successful recanalization<sup>17</sup>.

#### *1.6.4 Ultrasonography*

Color flow guided duplex ultrasonography of the carotid and vertebral arteries is an established noninvasive method for the evaluation of cervical atherosclerotic disease. Typically, it is used in patients with suspected transient ischemic attack (TIA), or with ischemic stroke with possible large artery origin. Transcranial Doppler ultrasonography can

be used to evaluate intracranial vessel stenosis and occlusions, but has poorer sensitivity and accuracy and is more operator dependent compared to CTA and MRA<sup>137</sup>.

### **1.6.5 Nuclear medicine**

Nuclear medicine techniques, especially positron emission tomography (PET), has shown to give detailed information and provide better understanding of the underlying pathophysiology in ischemic stroke<sup>138</sup>, including mechanisms responsible for neurological and functional recovery after stroke<sup>139</sup>. However, the utilization of PET in the management of acute stroke patients has received limited investigation due to the long time needed to perform the examination. Regarding rapid scan times being of vital importance for neuroimaging in patients with suspected acute ischemic stroke, PET is not expected to be part of routine clinical practice in the near future<sup>140</sup>.

### **1.6.6 Digital subtraction angiography**

Digital subtraction angiography (DSA) is an invasive procedure providing excellent visualization of cervical and intracranial arteries. The technique uses the acquisition of pre-contrast images followed by images acquired after the injection of a contrast agent. Radiopaque structures like bone visualized on pre-contrast images are digitally subtracted from the following post-contrast images, with resulting

subtracted images providing accurate visualization of the contrast-filled blood vessels. DSA is the gold standard for detection of cerebrovascular stenosis and occlusions<sup>141</sup>, and provides equal or slightly higher resolution, sensitivity and specificity compared to CTA or MRA for detecting stenosis and occlusions<sup>142</sup>. However, as an invasive technique, DSA carries the risk of potentially serious complications like stroke and even lethal complications. Fortunately, the risk of serious complications is low, with the occurrence of deaths being reported as low as 0.06 % and stroke with permanent disability 0,14 %<sup>143</sup>. Due to high sensitivity and specificity of CTA and MRA for the detection of cerebrovascular stenoses and occlusions, along with their accessibility, non-invasiveness, and additional information about the brain parenchyma provided by CT and MRI, noninvasive techniques are recommended in the acute evaluation of patients with suspected acute cerebral stroke<sup>5,48,142</sup>. If large vessel occlusion is present and there is indication for endovascular therapy (EVT), DSA with EVT is performed.

### **1.7 Artificial intelligence and machine learning methods**

In recent years, machine learning (ML) methods, particularly neural network algorithms, have demonstrated promising results in numerous medical image analysis applications, including stroke applications<sup>28,78,144,145</sup>.

*Artificial intelligence* (AI) is a term used for a wide range of technological methods having in common the use of a computer to model

intelligent behavior with minimal human interference<sup>146</sup>. The term is frequently applied for systems that hold the intellectual processes characteristic of humans, like the ability to reason, discover meaning, generalize, or learn from past experience<sup>147</sup>. ML is a certain application of AI that deals with the implementation of computer software that can learn autonomously<sup>148</sup>. By learning from experience, which consists of large sets of data, algorithms used in ML are improved. *Deep learning* are methods based on *artificial neural networks* (ANNs) inspired by networks in the human brain<sup>149</sup>. It is one of the most commonly used approaches in ML algorithms<sup>148</sup> aiming to perform cognitive functions like problem solving by mimicking the brain's capability of pattern recognition<sup>149</sup>. The algorithms consist of several layers of ANNs. The input layer receives input from the external environment, while the output layer conveys the ultimate outcome. Between these two layers, one or more layers of artificial neurons are found, where most of the information processing takes place. Especially *Convolutional neural networks* (CNNs) have been proven useful in medical imaging analysis<sup>150</sup>. CNNs consist of multiple artificial neuronal layers, in which all neurons in one layer are connected to all the neurons in the next layer. In CNNs, a feature detector (kernel/filter) is used to detect certain features in one convolution layer, a process called convolution. Convolution of one layer can follow outputs from previous layers, where pixels from previous layers can be seen in later layers<sup>151</sup>. The high connectivity between the layers makes CNNs prone to “overfitting data”, i.e., the model corresponds so close to a certain data set that it is unable



to fit additional data reliably. This is limited by different types of regulation.

Several ML methods have been used in stroke applications. In one study, a general linear model based on CTP and clinical data was used to quantify tissue infarction depending on recanalization<sup>152</sup>. The resulting time-adjusted multivariate prediction of infarction may identify patients who could benefit from recanalization therapy in the extended time window<sup>152</sup>. Another study found that the ischemic core could be accurately predicted by using ANNs with implementation of clinical and CTP data<sup>145</sup>. Our research group, as part of the current twin project, have studied the use of CTP in acute stroke patients. In one study, the entire 4D CTP dataset was used as input to a neural network to segment both penumbra and core<sup>78</sup>. In another study, color-coded PMs were used to automatically segment the penumbra and core using three different ML-based methods<sup>28</sup>. It was found that the best random forest-based method outperforms classical thresholding approaches<sup>28</sup>. ML has also been applied to other modalities than CTP. In one study, ML was used for automated prediction of ischemic brain tissue fate from mCTA-derived tissue maps in patients with acute ischemic stroke<sup>153</sup>. The method showed comparable results to CTP in terms of prediction of tissue perfusion abnormality and follow-up infarction<sup>153</sup>.

### **1.8 Challenges in neuroimaging in acute stroke patients**

Rapid recognition of stroke symptoms, patient transfer and acute treatment, including immediate thrombolytic treatment (medication administered to restore cerebral blood flow) and/or thrombectomy (catheter approach to restore cerebral blood flow), are of vital importance in the acute setting and significantly improve outcomes in acute stroke patients<sup>4,5</sup>. Whether treatment is applied depends on time from symptom onset to hospital admission, but also largely on imaging results with, especially in extended time windows, perfusion imaging often being fundamental in estimation of the penumbra, ischemic core and outcome prediction<sup>120</sup>. However, current techniques are far from accurate in determining hypoperfused but still salvageable tissue and irreversibly damaged tissue.

The lack of a definite gold standard for ischemic core is a challenge in current stroke imaging. DWI is often used as gold standard for ischemic core in clinical trials, with high sensitivity and specificity to detect irreversibly injured tissue (ischemic core)<sup>99-101,105</sup>. However, DWI is not a perfectly reliable measurement for the ischemic core<sup>10,56</sup>. One study showed that DWI might be negative in as many as 8 % of AIS patients, while adding PI increased sensitivity to 97.5%<sup>110</sup>. False-negative DWI may be due to very small lacunar deep grey nuclei or brain stem infarction<sup>100,102</sup>, or very early after onset<sup>154</sup>. Also, changes in the acute setting can be potentially reversible<sup>155</sup>. One meta-analysis found that DWI reversal ranged from 0.9-50% and the extent of reversal ranged from 1.8-72.7% after thrombolytic treatment, with greater reversibility

associated with younger patients<sup>156</sup>. Hence, caution should be taken in recanalized patients, as early DWI changes may not represent the definite ischemic core.

In addition to the lack of a gold standard for ischemic core, the definition of ischemic core is up for debate. Although there is broad agreement to define ischemic core as irreversibly damaged ischemic tissue, which cannot be saved, the definition could refer to both already infarcted tissue and tissue not yet infarcted but inevitable destined to develop into infarction regardless of treatment<sup>10</sup>. Perfusion imaging in acute ischemic stroke provides only a short time measurement. There is unavoidably a time delay between baseline imaging and reperfusion, and reperfusion can be complete or incomplete, causing a greater burden of cell death at time of reperfusion. Hence, follow-up imaging has certain limitations if final infarct on follow-up imaging is used as gold standard for ischemic core on baseline imaging. One paper addresses uncertainty with the current ischemic core concept due to no uniform definition of ischemic core, lack of standardized and validated quantitative measures of irreversibly injured tissue (threshold values) and lack of a reliable gold standard to validate image parameters, and the ischemic core concept being an inadequate measure of the burden of cell death<sup>10</sup>.

Hypodense tissue on NCCT is regarded highly specific for irreversibly damaged brain tissue, but there is limited sensitivity for detecting early ischemic changes and interobserver variability is common<sup>56-58</sup>. Although rare, hypodense tissue on NCCT could also be potentially reversible after

recanalization<sup>59</sup>. Current guidelines advise against performing MT in AIS patient with an ASPECTS <6<sup>5,6</sup>. However, there is growing evidence indicating that even patients with ASPECTS <6 can benefit from EVT<sup>51,157-160</sup>.

In CTP, different approaches and thresholds result in variable estimation of penumbra and core, causing a challenge in the acute setting<sup>85,88-94</sup>. Some studies have found good correlation between CBV and final infarct core<sup>86,87</sup>, while others consider CBF more accurate<sup>95</sup>. CTP may overestimate infarct core on initial imaging, especially in patients in the early time window and short time to recanalization<sup>12,161</sup>. This phenomenon is called “ghost infarct core” and has been defined as initial core minus final infarct. It is regarded significant by a ghost core larger than 10 ml<sup>12,161</sup>. One study used CTP CBF to define infarct core, which resulted in ghost infarct core found in 16 % of patients who underwent thrombectomy of the middle cerebral or intracranial internal carotid artery<sup>12</sup>. CTP CBV based infarct core has resulted in even higher frequency of ghost infarcts, found in 38 % of the patients in one study<sup>161</sup>. Hence, CTP should be carefully evaluated in the acute setting to prevent withholding treatment in patients who might benefit from it, especially in early time windows.

Current CTP based calculations are far from perfect in diagnostic accuracy and further improvement of the methods in use is needed<sup>10,162</sup>. Automated solutions have contributed to reduce heterogeneity in the application of different thresholds, but still ischemic core volumes vary substantially between different software packages<sup>51,85,93,94</sup>. RAPID is a

fully automated software to segment the ischemic region and has been shown to identify patients in whom reperfusion is associated with good outcome<sup>144</sup>. Several recent large clinical trials have used the RAPID software to estimate volume of ischemic lesions to select patients for treatment<sup>4,96,119,120,123</sup>. However, many hospitals do not have access to this software, leading to challenges on how to select patients for treatment based on selection criteria from clinical trials. With RAPID, core is defined as CBF reduced to <30 % compared to the contralateral hemisphere, and penumbra is the tissue outside the core with Tmax >6 s<sup>94,96</sup>. A study from 2019 compared three commonly used perfusion software systems (RAPID, IntelliSpace Portal CT Brain Perfusion and syngo.via CT Neuro Perfusion) in patients with acute ischemic stroke<sup>94</sup>. Here, best agreement with RAPID was found with the use of syngo.via with default settings and an additional smoothing filter.

Neural network algorithms and ML methods have shown promising results in medical image analysis applications in acute stroke patients, with the capacity to accurately predict tissue outcome<sup>28,78,144,145,163,164</sup>. This could help reducing sources of error in the interpretation of CTP. By taking these promising results into account, the applications are expected to have the capacity to select AIS patients for treatment more accurate, and on the other hand, better identify patients who are unlikely to benefit from reperfusion therapy in the future. It is also expected that patients with stroke mimics will be identified better. The goal is to provide automated decision support with recommendations for personalized treatment plans<sup>28,125,165</sup>.

During an ischemic event in the brain, current diagnostic approaches to assess cerebral hemodynamics in acute stroke, like conventional PMs from CTP and MRP, rely on temporal dynamics in changes of image density and intensity. Microvascular patency only affects these parameters in cases where plasma, and thereby CT and MRI contrast media, fails to reach large proportions of the microvasculature within an image voxel<sup>13</sup>. Accordingly, conventional PMs mainly reflect blood supply and the vascular volume perfused by plasma, and not the microvascular distribution of blood, which might affect the availability of oxygen in the tissue<sup>13</sup>. Clinical evidence indicates that reperfusion (restoration of microcirculatory blood flow) is better than recanalization (reopening of the occluded artery) in terms of predicting tissue outcome after recanalization therapy<sup>17,166,167</sup>. After recanalization therapy, there might be incomplete restoration of the microcirculatory flow in some parts of the ischemic tissue despite reopening of the occluded vessel, called the *no-reflow* phenomenon<sup>17,168-170</sup>. Hence, despite complete recanalization, microvascular impairment might prevent microcirculatory reperfusion sufficient to meet the tissue's metabolic needs<sup>17,171</sup>. In the DEFUSE study, where MRI imaging profiles were used to predict clinical response to early reperfusion, four of nineteen patients had recanalization, but no reperfusion assessed on PI<sup>172</sup>. In a review paper on the no-reflow phenomenon after reperfusion therapy in stroke patients, where thirteen studies with a total of 719 patients were included, the no-reflow phenomenon was observed in one-third of stroke patients with successful macrovascular reperfusion, which in turn was

associated with reduced rates of functional independence<sup>169</sup>. This study was limited by a considerable heterogeneity in the definitions used for no-reflow and the inclusion of patients with TIC12b reperfusion, with some persisting vessel occlusion. Still, the pooled estimates after trying to account for this heterogeneity indicates that no-reflow might be quite common<sup>169</sup>. Incomplete reperfusion may be one of the factors contributing to limited efficacy of recanalization therapy and has been suggested as a potential target for preventive and therapeutic treatment to improve outcome after recanalization<sup>17,124,173-175</sup>. CTH and CoV describe the microvascular environment and are promising calculation tools having the capacity to more accurately describe the ischemic brain tissue compared to conventional methods<sup>13,14</sup>. A better understanding of the microvascular environment during an ischemic event has the potential to select patients for treatment more precisely and to create the possibility for improving recovery after recanalization therapies<sup>14-17</sup>.

### **1.9 Management of acute ischemic stroke patients**

In patients with suspected acute ischemic stroke, current guidelines provide recommendations regarding the whole stroke care chain; from prehospital systems including emergency medical services to diagnostics and treatment at the hospital, with recommendations concerning organization and integration of the different stroke care chain components<sup>3-5,48,176</sup>.

### *1.9.1 Prehospital management*

Prehospital educational programs should focus on stroke symptoms and highlight the importance of seeking emergency care urgently<sup>5</sup>. One central goal is to decrease the interval between stroke onset to arrival at the emergency department and treatment<sup>5</sup>.

### *1.9.2 Neuroimaging*

All patients with suspected acute cerebral stroke, who might be candidates for recanalization therapy, should receive emergency imaging with CT or MRI as quickly as possible before any specific AIS therapy is initiated<sup>5,48</sup>. CT and MRI are both effective to exclude ICH before IVT<sup>98</sup>. If ICH is present, CTA may be performed in certain patients to help identify an underlying vascular cause<sup>177</sup>. Either CTA or MRA is recommended for detection of cerebrovascular stenosis and occlusions in the acute evaluation of patients with suspected acute ischemic stroke, thereby identifying patients with LVO being potential candidates for EVT<sup>5,48</sup>. For patients presenting in the extended time window (i.e., 4.5/6 hours after symptom onset), CT or MRI core/perfusion mismatch evaluation is recommended to determine treatment eligibility<sup>4,5</sup>. However, in many stroke centers, perfusion imaging is also performed in early time windows, both from a logistical point of view for streamlining and thereby shortening the time needed for the examination, as well as for providing additional information for diagnostic certainty<sup>7,18,51</sup>.



### **1.9.3 Treatment of AIS**

Restoring blood flow to prevent further tissue damage is the main treatment goal in AIS. For patients presenting with AIS, intravenous thrombolysis or mechanical thrombectomy are the two main options for recanalization therapy. It is recommended that patients eligible for intravenous thrombolysis and/or mechanical thrombectomy receive treatment in the fastest achievable onset-to-treatment time<sup>5</sup>.

#### **1.9.3.1 Intravenous thrombolysis**

IVT was approved for treatment of AIS in 1996<sup>178</sup> after the National Institute of Neurological Disorders and Stroke (NINDS)-2 trial that showed improved clinical outcome at three months after treatment with intravenous recombinant tissue plasminogen activator (rtPA) within the 3 hours-time window<sup>179</sup>. It was the first possible treatment for the occluding thrombus or embolus causing AIS. The findings from the NINDS-2 trial have later been confirmed in subsequent trials testing the 0-6 hours' time window, demonstrating clear trends in favor of rtPA, which was highly significant in the first meta-analysis up to 4.5 hours after onset<sup>180,181</sup>. Later studies have also shown benefit from treatment with IVT up to 4.5 hours after onset<sup>4,8,182</sup>, and for selected patients in the extended time window (4,5 hours-9 hours' time window and for patients with wake-up stroke or stroke with unknown onset time)<sup>96,113,118,120,121</sup>.

Wake up stroke refers to patients with AIS upon awakening from sleep, creating uncertainty regarding the exact time when the stroke symptoms began.

The use of rtPA, Alteplase, has been the standard thrombolytic agent used for treatment of AIS for several years<sup>183</sup>. It was approved for treatment of AIS by the US Food and Drug Administration (FDA) in 1996 and is the only thrombolytic agent approved for this indication<sup>183</sup>. rtPA is a powerful drug and the benefit from treatment is time dependent with higher likelihood of better outcome the sooner treatment is initiated. rtPA works by its binding to fibrin, which induces the conversion of plasminogen to plasmin, which further acts to dissolve the fibrin-containing blood clot. Treatment with rtPA entails a certain risk for hemorrhage. The rate of hemorrhage in the NINDS-2 trial was found to be 6.4 % in the tPA group. However, since this trial was published, the definition of hemorrhage after AIS has evolved, with the definition of symptomatic intracranial hemorrhage (sICH) being important. Following trials have shown variable rates of hemorrhage depending on the definition used, with rates of sICH being reported as low as 2,4 %<sup>184</sup>. Due to the risk of hemorrhagic complications after IVT, there are various contraindications to this therapy in addition to presenting outside the therapeutic time window (like use of oral anticoagulants, intracranial hemorrhage (ICH) and a bleeding disorder)<sup>5</sup>. Alteplase is administered as a 10% bolus followed by a 1-hour continuous injection.

Tenecteplase is a genetically modified form of Alteplase, with increased plasminogen activator inhibitor 1 resistance, greater fibrin specificity and a longer half-life, which allows for single bolus administration<sup>185,186</sup>.

In 2023, Tenecteplase was also included in the European Stroke Organization guidelines as a thrombolytic agent for treatment of AIS<sup>186</sup> after the results from four RCTs that compared the use of Alteplase and Tenecteplase in AIS. These guidelines recommend the use of Tenecteplase (0.25 mg/kg) over Alteplase for patients with AIS <4.5 hours duration<sup>186</sup>. Also, it is suggested that Tenecteplase could be a reasonable alternative to Alteplase (0.9 mg/kg) for eligible patients with wake-up stroke and for stroke with unknown onset time<sup>186</sup>.

### **1.9.3.2 Endovascular therapy**

IVT alone has shown low reperfusion rates in AIS with LVO, with rates reported up to around 30 %<sup>187-190</sup>. Endovascular therapy (EVT) has been shown to provide better reperfusion rates in these patients, with reperfusion rates above 80 %<sup>191-193</sup>. Today's gold standard for EVT is MT, and both stent retrievers and catheter aspiration devices can be used<sup>5,6,194,195</sup>. Among available AIS therapies, MT constitutes the most effective acute treatment option for patients with acute LVO with very low number needed to treat, sometimes as low as 2<sup>196</sup>. In catheter aspiration, catheterization is performed (often femoral artery puncture), and a catheter is placed directly proximal to the thrombus. Suction is then used to aspirate and remove the thrombus. If reperfusion is not achieved,

or as a first choice of method, a stent retriever can be employed to perform thrombectomy. For stent retrievers, the catheter containing the stent, is guided distal to the site of the thrombus. The stent retriever is then inserted through the catheter to reach the clot. The catheter is pulled back, and the stent retriever adheres to the clot. With the clot adherent to the stent, the stent retriever is pulled back into the catheter, and the clot is removed.

The degree of reperfusion after thrombectomy is often defined by the modified treatment in cerebral infarction (mTICI) scale, with grade 2b and 3 defining successful reperfusion in terms of antegrade reperfusion in more than half, yet incomplete reperfusion, or complete reperfusion, in the downstream target arterial territory, respectively<sup>5,197</sup>.

As an invasive procedure, MT involves inherent risks that may potentially harm the patients. Device-related serious adverse effects are uncommon, but can have severe consequences and be potentially lethal. Adverse effects include hemorrhage and pseudoaneurysm formation at the site of catheterization, arterial perforation with bleeding complications, arterial dissection, transient vasospasm, embolism, and the induction of new ischemic lesions<sup>192</sup>. However, the rates of intracranial hemorrhage and mortality in patients receiving MT are not increased compared to standard medical treatment alone<sup>198-201</sup>.

According to current guidelines, MT is recommended in eligible patients with anterior circulation LVO AIS<sup>6</sup>, typically referred to occlusion of the intracranial carotid artery and/or the proximal middle cerebral artery

(M1/proximal M2 segments)<sup>6,119,123</sup>, in which clinical trials have shown clear benefit from treatment<sup>5,6,119,123,198-200,202-204</sup>. A clear benefit from MT has not been shown after MT in patients with vertebrobasilar occlusion<sup>205,206</sup>. However, this is thought at least partly to be due to results being confounded by poor recruitment and implementation of the study design<sup>205,206</sup>. With respect to the grim natural course of basilar artery occlusion, it is also recommended that IVT and MT should be strongly considered in these patients<sup>5,6</sup>. According to current guidelines from the American Heart and American Stroke Associations for the early management of acute ischemic stroke, although uncertainty regarding potential benefit, it is recommended that MT may be reasonable for selected patients within 6 hours and occlusion of the anterior cerebral arteries, vertebral arteries, basilar artery or posterior cerebral arteries<sup>5</sup>.

MT can be performed isolated or in combination with IVT (“bridging therapy”). Current guidelines recommend MT in LVO AIS within 6 hours of symptom onset, and for selected patients in the extended time window (6-24 hours after symptom onset)<sup>5,6</sup>.

### 1.9.3.3 Treatment criteria in acute ischemic stroke patients

Early time window:

- For patients presenting with acute ischemic stroke <4.5 hours, intravenous thrombolysis with Tenecteplase is recommended<sup>4,8,182,186</sup>.
- For patients presenting with acute ischemic stroke with LVO, MT is recommended <6 hours<sup>5,6,199,200,202,203</sup>.
  - *Bridging therapy in selected patients†.*

Extended time window\*:

- For patients presenting with acute ischemic stroke in the 4.5-9 hours' time window (with known time of onset), and for patients with wake-up stroke or stroke with unknown onset time, IVT is recommended in selected patients<sup>4,5,96,113,118,120,121</sup>.
- For patients presenting with acute ischemic stroke with LVO in the 6-24 hours' time window, MT is recommended in selected patients<sup>5,6,119,120,123</sup>.
  - *Bridging therapy (IVT before MT) is recommended in selected patients†.*

\*For patients in the extended time window, the following criteria are used to determine treatment eligibility:

- IVT: DWI/FLAIR mismatch or perfusion imaging (CTP/MRP), with core/perfusion mismatch defined as follows<sup>4,96,113,118,120,121</sup>:

- Infarct core\*\* volume <70 ml
- Critically hypoperfused volume\*\*\*/ Infarct core\*\* volume (mismatch ratio) >1.2
- Mismatch volume (penumbra) >10 ml
- \*\* rCBF <30% (CTP) or ADC<620  $\mu\text{m}^2/\text{s}$  (DWI)<sup>96,207</sup>
- \*\*\*Tmax >6 s (CTP or MRP)<sup>4,84,96</sup>
- MT: Perfusion imaging or DWI<sup>5,6,119,120,123</sup>
  - In two trials, which provided evidence for benefit of mechanical thrombectomy up to 24 hours after onset in patients with occlusion of the intracranial internal carotid artery or the proximal middle cerebral artery, the following criteria were used for treatment eligibility:
    - DAWN (6-24 hours' time window)<sup>123</sup>:
      - Patients with mismatch between the severity of the clinical deficit and infarct volume, «clinical-imaging mismatch», defined as follows (infarct volume was assessed with DWI or CTP):
        - Group A:  $\geq 80$  years of age + NIHSS score  $\geq 10$  + infarct volume <21 ml
        - Group B: <80 years of age + NIHSS score  $\geq 10$  + infarct volume <31 ml

- Group C: <80 years of age +  
NIHSS score  $\geq 20$  + infarct  
volume 31-50 ml
- DEFUSE-3 (6-16 hours' time window)<sup>119</sup>:
  - Infarct core\* volume <70 ml
  - Critically hypoperfused volume\*\*/  
infarct core\* volume (mismatch ratio)  $\geq$   
1,8
  - Mismatch volume (penumbra)  $\geq 15$  ml

\*rCBF <30%, \*\*Tmax >6 s (CTP or MRP +  
DWI)

†*Bridging therapy* (IVT before MT): In the latest European guidelines, bridging therapy is recommended over MT alone in patients eligible for both treatments with a  $\leq 4.5$  hours or wake-up AIS and anterior circulation LVO<sup>208</sup>. Bridging therapy is also recommended for both of these patients groups when admitted to a non-thrombectomy capable center followed by rapid transfer to a thrombectomy-capable center for MT<sup>208</sup>.

Current guidelines provide clear recommendations on reperfusion treatment to only a proportion of AIS patients. Some guidelines/expert opinions provide recommendations regarding reperfusion therapy to patients presenting with borderline indications<sup>5,6,209</sup>, based on experience and recent literature, such as performing MT in patients with occlusion



more distal in the M2 and M3 segment of the middle cerebral artery<sup>210-212</sup>, in the posterior circulation<sup>205,206</sup>, in patients with large ischemic core<sup>157-160</sup>, pre-existing illness or deficits on mRS<sup>213</sup>, milder strokes (NIHSS<6)<sup>214</sup> and in children<sup>215,216</sup>. Still, a significant number of patients presenting with AIS is excluded from reperfusion therapy, and present guidelines that include borderline indications often provide weak recommendations due to the lack of randomized controlled trials on these patients. This is increasingly recognized, and there are many recent and ongoing trials focusing on expanding indications for reperfusion therapy<sup>209</sup>. Further development, along with improved imaging precision, will likely be required in acute stroke patients.

#### *1.9.4 Clinical scoring tools*

In stroke patients, two clinical scoring tools are commonly used both in the clinical setting and in clinical trials: The National Institutes of Health Stroke Scale (NIHSS) and the Modified Rankin Scale (mRS).

##### **1.9.4.1 National Institutes of Health Stroke Scale**

The NIHSS is a tool used by healthcare personnel to measure stroke severity by measuring the neurological impairment caused by a stroke<sup>217</sup>. It was developed in 1989<sup>218</sup> for use in acute stroke therapy trials<sup>218</sup>, and has been used both for clinical evaluation and as an outcome measure in clinical trials<sup>217</sup>, including recent trials dealing with the use of IVT and

MT in the extended time windows<sup>96,113,119,123</sup>. The scale assesses stroke severity by including the following domains: Level of consciousness, eye movements, integrity of visual fields, facial movements, arm and leg muscle strength, sensation, coordination, language, speech and neglect<sup>217</sup>. The original developed scale from 1989 assessed 15 items<sup>218</sup>, but modified versions have been developed later, with the 11-items modified NIHSS commonly used in recent years<sup>219,220</sup>. In this scale, each of the 11 items scores a specific grade of impairment, with 0 indicating normal function and higher score indicating higher degree of impairment<sup>221</sup>. The individual scores are then summarized, with the maximum possible score being 42, and the lowest being 0<sup>221</sup>. Minor stroke is often defined by NIHSS, often as a score <5, though there is no unified definition<sup>222</sup>. In the WAKE-UP trial, a severe stroke was defined as NIHSS >25<sup>113</sup>.

The NIHSS has been shown to possess high prospective reliability and validity<sup>218,220,221</sup> and high retrospective reliability<sup>223</sup>. It provides both high interrater reliability and test-retest reliability for a given examiner or patient, and high correlation between scoring by a neurologist and other examinees<sup>218,224</sup>. It has a high predictive validity in AIS, with the initial score being a robust predictor of in-hospital complications and outcome at 3 months<sup>179</sup>. NIHSS score at 3 months is strongly associated with degree of dependency<sup>225,226</sup>. One important limitation for the stroke scale is certain limitations in detecting all stroke-related impairments, particularly with posterior circulation<sup>227</sup> and in certain nondominant-hemispheric strokes<sup>221,228</sup>.

The NIHSS score is part of the initial assessment in acute stroke patients and, although a unified practice is lacking, aids in determining treatment eligibility. In the WAKE-UP trial, patients with severe stroke (NIHSS >25) were excluded from the trial<sup>113</sup>. In the DAWN trial, among the eligibility criteria for MT was NIHSS score  $\geq 10$ <sup>123</sup>, while the DEFUSE 3 trial included a NIHSS score  $\geq 6$ <sup>119</sup>. In the European Stroke Organization and European Society for Minimally Invasive Neurological Therapy (ESMINT) Guidelines on Mechanical Thrombectomy in Acute Ischaemic Stroke, an upper NIHSS score for decision-making is not recommended<sup>6</sup>. Regarding patients with low NIHSS score, an expert opinion states that MT, in addition to IVT in eligible patients, may be reasonable in patients with enabling deficits (e.g., aphasia) and in the case of clinical worsening despite IVT<sup>6</sup>.

#### **1.9.4.2 Modified Rankin Scale**

Dr. John Rankin developed the original Rankin scale to describe outcome in stroke patients in 1957<sup>229,230</sup>. A modified Rankin scale (mRS) was developed in the 1980s<sup>231</sup>, and its value in the assessment of handicap in stroke patients was confirmed with its reproducibility for the first time being examined a few years later<sup>232</sup>. The mRS measures functional independence on a seven-grade scale (score 0-6), with higher score indicating more severe disability<sup>230,231</sup>. How outcome based on the mRS score is referred to vary somewhat, though excellent outcome is often defined as a mRS score of 0-1 (no symptoms or symptoms without

significant disability), good outcome as a score of 0-2 (functional independency), and worst outcome as a score of 5-6 (bedridden or dead)<sup>7,96,113,119,123</sup>.

The scale was in little use during Rankin's lifetime. It was not until the development of multicenter intervention trials that Rankin's scale was rediscovered<sup>229</sup>. Since then it has become the most widely used<sup>233</sup> scale for stroke-related disability in trials<sup>229,230</sup>. The mRS has been shown to be a reliable and reproducible measure of outcome in stroke patients<sup>233</sup>. A systemic review from 2009 found just a moderate overall reliability, but the reliability was highly variable among the included studies<sup>234</sup>. The scale serves as a global functional health index with high emphasis on physical disability<sup>233,235</sup>. mRS score at 90 days after IVT or MT in acute stroke patients is in general accepted as standard for assessing recovery from ischemic stroke and has been used in numerous large, randomized trials<sup>8,96,113,119,123,233</sup>.

### **1.10 Stroke mimics and simulation training**

Patients with stroke mimics (SMs) present with neurological symptoms thought to be of cerebrovascular origin, but diagnostic work-up proved that the symptoms were not caused by a cerebrovascular event. SMs are common and comprise up to 43 % of patients presenting with acute neurological symptoms in the acute phase<sup>236</sup>. The number of SMs are more common in stroke centers using CT as a first line diagnostic tool<sup>237</sup> and in centers with a focus on reducing treatment times<sup>238</sup>. IVT-treatment

of SMs poses a potential risk due to the possibility for bleeding complications<sup>184</sup>, and the treatment is associated with an increased resource and cost burden to hospitals and society<sup>239</sup>.

Minimizing time from symptom onset to treatment is of great importance in AIS, as clinical outcomes of therapy are highly time dependent<sup>7,8</sup>. At Stavanger University Hospital, patients with a suspected AIS are met by a round-the-clock on-call stroke treatment team. An initial assessment, including imaging, usually CT (NCCT of the head, CTA of precerebral and intracranial arteries, and CTP) is performed prior to determining the treatment tailored to the specific patient<sup>7,18</sup>. It has been shown that simulation-based team-training can improve team performance by refining technical skills like communication, teamwork and leadership<sup>19</sup>. Improvement in both simulated, and to some extent clinical performance, has been demonstrated for various emergencies, including AIS<sup>20,21</sup>. Recent research points out human factors as a key limit in the management of AIS<sup>240</sup>.

Translational simulation is used in quality improvement (QI) projects, and refers to improving healthcare systems and improving patient care with the potential to both diagnose system performance and deliver interventions<sup>7,241</sup>. As part of a QI project in our institution, a revised AIS treatment protocol along with weekly simulation-based team-training for the stroke treatment team was implemented. Our primary aim was to reduce treatment times, to enhance protocol adherence, and to improve communication skills. We performed clusters of in situ simulation-based

team-training using acute stroke scenarios, including all inn-hospital stroke treatment team members and paramedics on-call. This led to reduced treatment times, including a reduction of the median door-to-needle time (for IVT treatment) from 27 to 13 minutes, and reduced patient morbidity and mortality<sup>7</sup>. There is a tradeoff between short door to needle time in stroke patients and avoiding IVT treatment of too many patients with SMs<sup>18,242</sup>. It is not desirable to treat patients with SMs with IVT from a patient safety<sup>179,243</sup> and from a cost of health care perspective<sup>239</sup>. However, if there are only very few SM patients that are treated with IVT, there is a higher risk of giving too few patients with real AIS IVT, or after too long delay. Quality improvement focusing on reducing treatment times in patients with suspected AIS should therefore additionally focus on unintended, potentially negative effects of speeding up the treatment times<sup>18,244</sup>.

## **2 Aims of the Studies**

The overall objective for paper I and II was to assess ischemic brain tissue in patients with acute ischemic stroke by utilizing the CTP dataset, MRI and clinical data. Further, segmentation of the ischemic lesion was the primary objective for paper I, characterization of the ischemic lesion for paper II.

### Paper I:

The aim of the study was to compare fully-automated methods based on ML with thresholding approaches to segment the ischemic regions (penumbra + core) in patients with AIS.

### Paper II:

The primary aim of the study was to evaluate if the parametric calculation CoV, calculated from CTP, adds value to the conventional parametric measures CBF and CBV in the prediction of DWI-based tissue outcome in patients with LVO AIS.

Paper III:

In situ simulation-based team-training led to significantly reduced treatments times in our stroke center. To analyze possible unwanted effects of simulation training, the proportion of SMs among IVT-treated patients for presumed AIS, and the proportion of intracranial hemorrhage (ICH) among IVT-treated SMs, were identified.



## **3 Materials and Methods**

### **3.1 Context**

Stavanger University Hospital serves a population of 369.000. Close to 450 patients with AIS are annually admitted to the hospital. All consecutive patients with a suspected AIS having received intravenous thrombolysis are prospectively included in a local thrombolysis registry. The registry contains multiple variables, including patient demographics, cerebrovascular risk factors, information about neurological impairment assessed by the NIHSS on admission and discharge, in-hospital mortality and mRS at baseline and 3 months post stroke measuring long-term functional outcome<sup>7,28</sup>.

### **3.2 Dataset**

#### Paper I + II:

An overview of the patients included in paper I + II are shown in figure 4 and 5.

The study group was IVT-treated AIS patients with visible perfusion deficits on CTP. The dataset comprises CTP scans from patients extracted from a population-based cohort between January 2014 and August 2020. All patients were examined with NCCT of the head, CTA of precerebral and intracranial arteries, and CTP immediately after hospital admission. Additionally, MRI including DWI was performed in

most patients in paper I and in all patients in paper II, in most cases within 24 hours after IVT treatment. The patients were divided into different groups based on level of vessel occlusion on CTA. LVO was defined as occlusion of any of the following arteries: The internal carotid artery, M1 and proximal M2 segment of the middle cerebral artery, A1 segment of the anterior cerebral artery, P1 segment of the posterior cerebral artery, basilar artery and vertebral artery occlusion. Non-LVO was defined as patients with perfusion deficits with more distal artery occlusion or with perfusion deficits without visible artery occlusion. Both groups, and additionally 15 patients without ischemic stroke (patients admitted under the suspicion of stroke, but after diagnostic work-up were determined not to have suffered from a stroke episode) were included in paper I. The latter group served as control group. Only LVO AIS patients, with a follow up MRI, were included in paper II. In paper II, recanalization status was also evaluated based on DSA or TOF angiography. Patients were grouped according to recanalization status on the mTICI scale (mTICI $\leq$ 2a not recanalized, mTICI >2a recanalized)<sup>245</sup>.

*Materials and Methods*

---

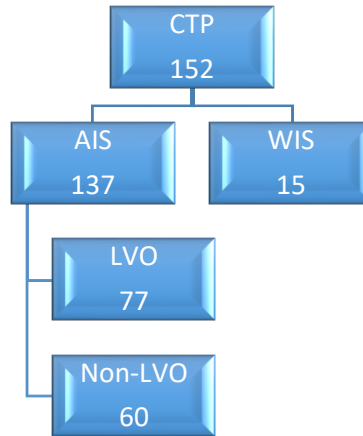


Figure 4: Patients included in paper I.

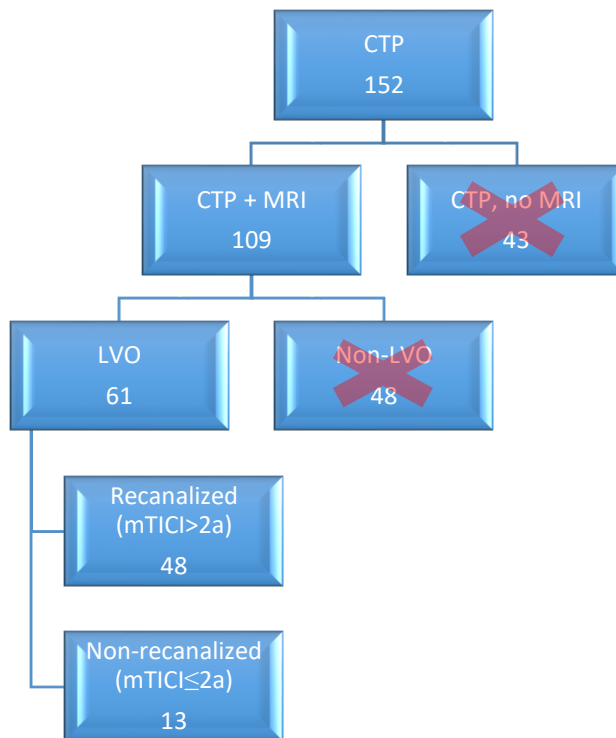


Figure 5: Patients included in paper II.

Paper III:

The study period was between January 1, 2015, and December 31, 2020. All patients with suspected AIS treated with IVT in this period were prospectively registered in a local research database. All relevant data-endpoints including ICH and the final diagnosis were registered in this database. On February 1st, 2017, repeated clusters with weekly in situ simulation-based team-training involving the stroke treatment team was introduced. Patients treated before introduction of the simulation training served as control group.

**3.3 Methods**

Paper I:

CTP-based conventional parametric maps (Tmax, TTP, CBF, CBV), MIP images and NIHSS score were used as input. In all the experiments, the predictions were compared with the ground truth and multi-class confusion matrices were generated. Ground truth images were manually annotated from CTP-derived parametric maps and MIP in assistance with the follow-up MRI examination by using an in-house developed software in MATLAB. CTP images from 33 randomly selected patients (19 from the LVO, 11 from the non-LVO, and 3 from the WIS subset) were manually annotated by two experienced neuroradiologists, and images from the remaining patients were manually annotated by one of the neuroradiologists. The criteria to select the best method for

classification of penumbra and core were based on a study of various implemented experiments and their relative statistical results. Our proposed multi-classification methods consist of the following steps (also illustrated in figure 6):

1. Brain extraction.
2. Simple linear iterative clustering (SLIC) algorithm whereby 3D superpixel versions of the PMs are obtained.
3. ML algorithm: Feeding the features (PMs + MIP images + superpixel images + NIHSS) to our implemented ML algorithms to predict the ischemic regions. The ML methods used were support vector machines, decision tree and random forest, in a single- or two-step approach. A final post-processing step using a 3D mode filter was also implemented.

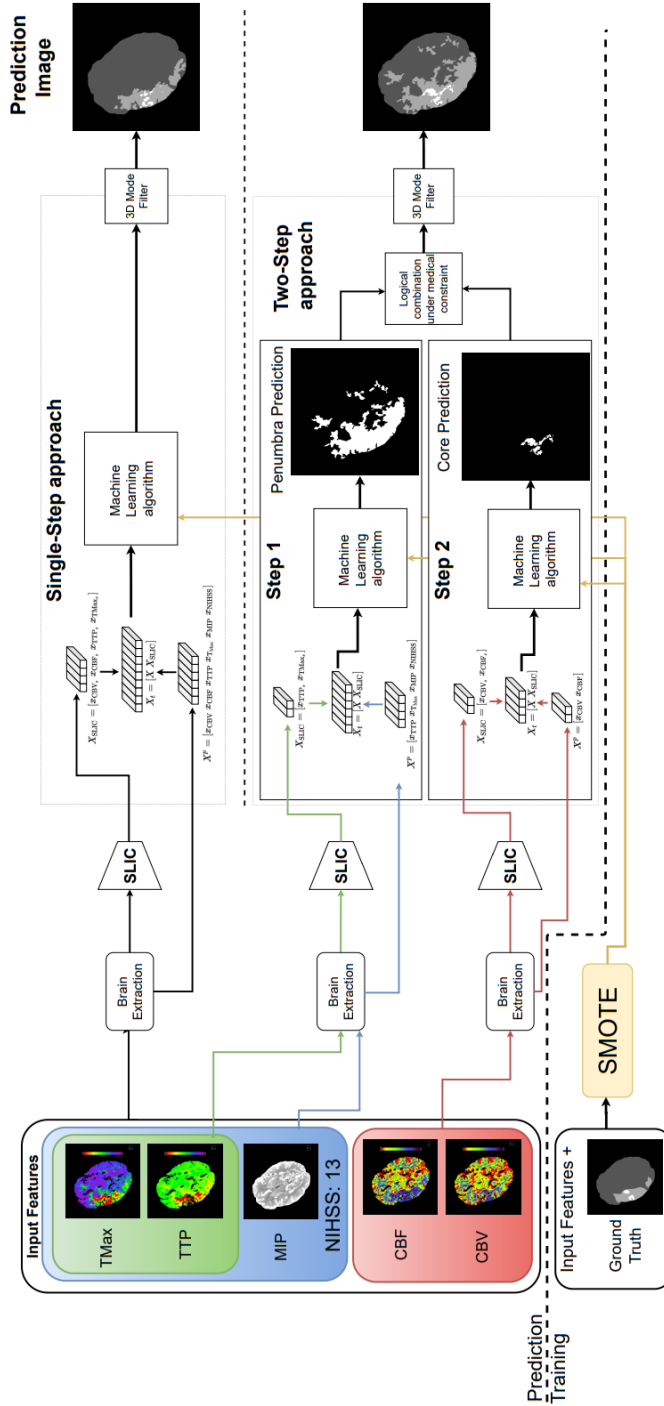


Figure 6: Visual description of the proposed multi-classification methods. SLIC refers to the algorithm to extract superpixel regions.

Paper II:

CTP derived parametric maps and DWI were assessed in acute stroke patients. Ground truth ischemic regions were outlined by manual annotations by an experienced neuroradiologist, and for some patients by two experienced neuroradiologists (as described in Material and Methods for paper I). An in-house developed software in MATLAB was used<sup>28</sup>. The CTP conventional parametric maps were used for delineating the hypoperfused lesion (penumbra + core), whereas DWI was used for core delineation. Co-registration of each DWI-slice and the corresponding CTP slice for the parametric maps was performed using the first and last slice in the ischemic region as a frame of reference. CTP voxel-wise tissue outcome was assessed for the parametric maps CoV, CBF and CBV. The primary outcome for our analysis was tissue outcome according to infarction on follow-up DWI.

## Materials and Methods

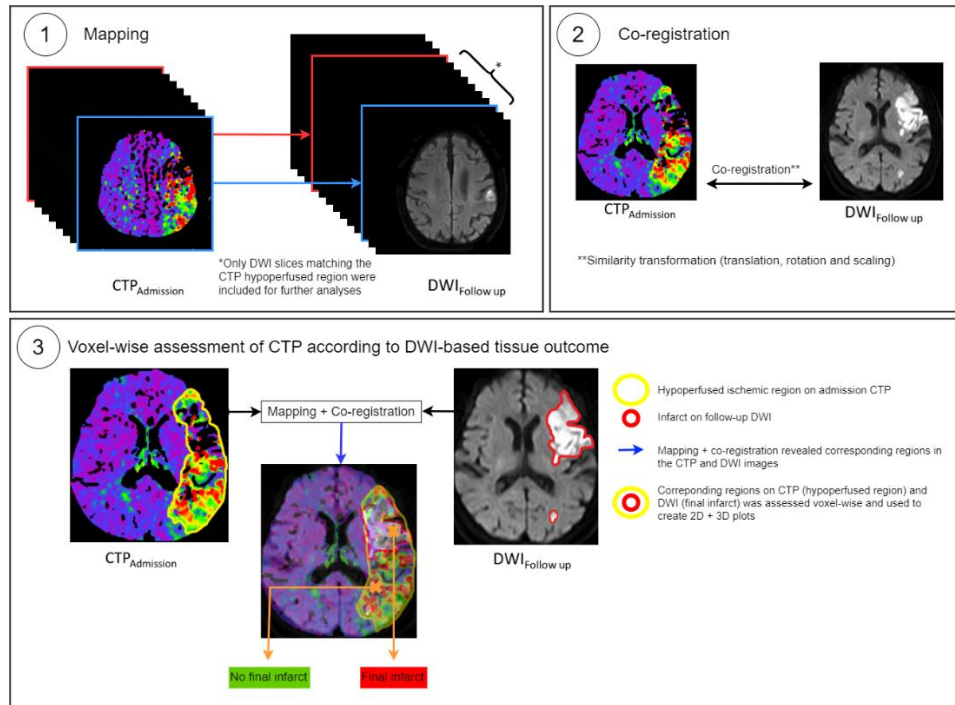


Figure 7: General overview of the processing steps involved: Step 1) maps the hyperperfused region on the CTP scans with the corresponding region on follow-up DWI scans. In step 2, image co-registration was performed slice-by-slice using a similarity transformation, consisting of translation, rotation and scaling. In step 3, voxel-wise assessment of CTP was done according to DWI-based tissue outcome.

### Paper III:

The proportion of SMs among patients that received IVT for presumed AIS, and the extent of intracranial hemorrhage in IVT-treated SM patients, were identified by clinical and radiological evaluation. SMs were diagnosed during their hospital stay and then retrospectively categorized into eight different sub-groups: Psychiatric disorders,



peripheral vertigo, epilepsy, migraine, infectious diseases, intoxication, peripheral facial palsy, and others.

### **3.4 Statistics**

#### Paper I:

In all the experiments, the predictions were compared with the ground truth and multi-class confusion matrices were generated. Our dataset comprised three classes (core, penumbra and healthy brain). Multi-class confusion matrices were created for the different classes, including pixels classified as true positive/negative and false positive/negative. From each confusion matrix, the recall, the precision and the Dice coefficient were calculated. The range for these values was [0, 1]. We also considered the Hausdorff distance between predictions and ground truth regions, and the absolute difference in the volume among the predictions, both with a range of [0,  $\infty$ ]. Bland-Altman plots were used to illustrate mean differences and limit of agreement between predicted volume and volume calculated from ground truth images.

#### Paper II:

Patients with LVO were grouped according to recanalization status. Statistical analyses were performed using SPSS Statistics version 24 (IBM Cooperation, Armonk, NY, USA) and MATLAB (R2020a, Update

1, The MathWorks, Inc., Natick, USA). Categorical variables are presented as count (percent, %) and continuous variables as median (interquartile range, IQR). Changes in ratios were evaluated using Fisher's exact test or Pearson Chi-Square, as appropriate. Changes in continuous variables were evaluated using Mann-Whitney test. Statistical significance was set at  $p < 0.05$  (two-sided).

Paper III:

All statistical analyses were performed using SPSS Statistics version 24 (IBM Cooperation, Armonk, NY, USA). Categorical variables are presented as count (percent, %) and continuous variables as median (interquartile range, IQR). Changes in proportions were evaluated using Pearson Chi-square test or Fisher's exact test, as appropriate. Changes in continuous variables were evaluated using Mann-Whitney test.

**3.5 Ethical considerations**

Paper I+II:

The studies are approved by the Regional ethic committee project 2012/1499, and by Sikt, the Norwegian Agency for Shared Services in Education and Research, reference number 953392.

All procedures involving human participants were performed in accordance with the ethical standards of the institutional and/or national

research committee and with the 1964 Helsinki Declaration and its later amendments or comparable ethical standards, including the ARRIVE guidelines.

Paper III:

All procedures involving human participants were performed in accordance with the ethical standards of the institutional and/or national research committee and with the 1964 Helsinki Declaration and its later amendments or comparable ethical standards. This study was approved by the regional ethical committee and the local hospital authorities. Informed consent was waived, after approval of the regional ethical committee.

## **4 Results of Papers**

### Paper I:

The results that showed best alignment with the manually annotated delineations of penumbra and infarct core were calculated with random forest and single-step approach (called Mdl-5.2), with an average Dice coefficient of 0.68 for penumbra and 0.26 for core, for the three groups analyzed together. The average in volume difference was 25.1 ml for penumbra and 7.8 ml for core, for all groups together. The best result was found for penumbra prediction in patients with LVO, with a Dice coefficient of 0.69. We found some inter-observer variability in the manual annotations for ground truth images between the two neuroradiologists, e.g., a Dice coefficient of 0.80 was found for interobserver-variability for penumbra in the LVO subset, and of 0.67 for penumbra in the non-LVO subset.

### Paper II:

The combination of CoV versus CBF and CBV for the ischemic lesion on admission according to final outcome on follow-up DWI, is shown in the voxel-based 2D and 3D plots in figure 8 and 9. In patients with subsequent recanalization, both CBF and CBV showed a clear association with infarct risk. Low CBF and CBV were associated with high risk of infarction across a broad range of CoV values (figure 8). Conversely, in patients without recanalization, infarct risk was largely

dependent on CoV. In these patients, there was a tendency towards lower CoV values, where a large proportion of tissue with reduced CoV developed into infarction, also in regions with higher CBF and CBV values (figure 9). In Figure 8 and 9, areas with red color on the 3D curves, represent combinations of voxel values associated with a high risk of infarction. These voxels were predominantly located beside the peaks for both CBF and CBV, most evident in recanalized patients.

Figure 8: Recanalized patients

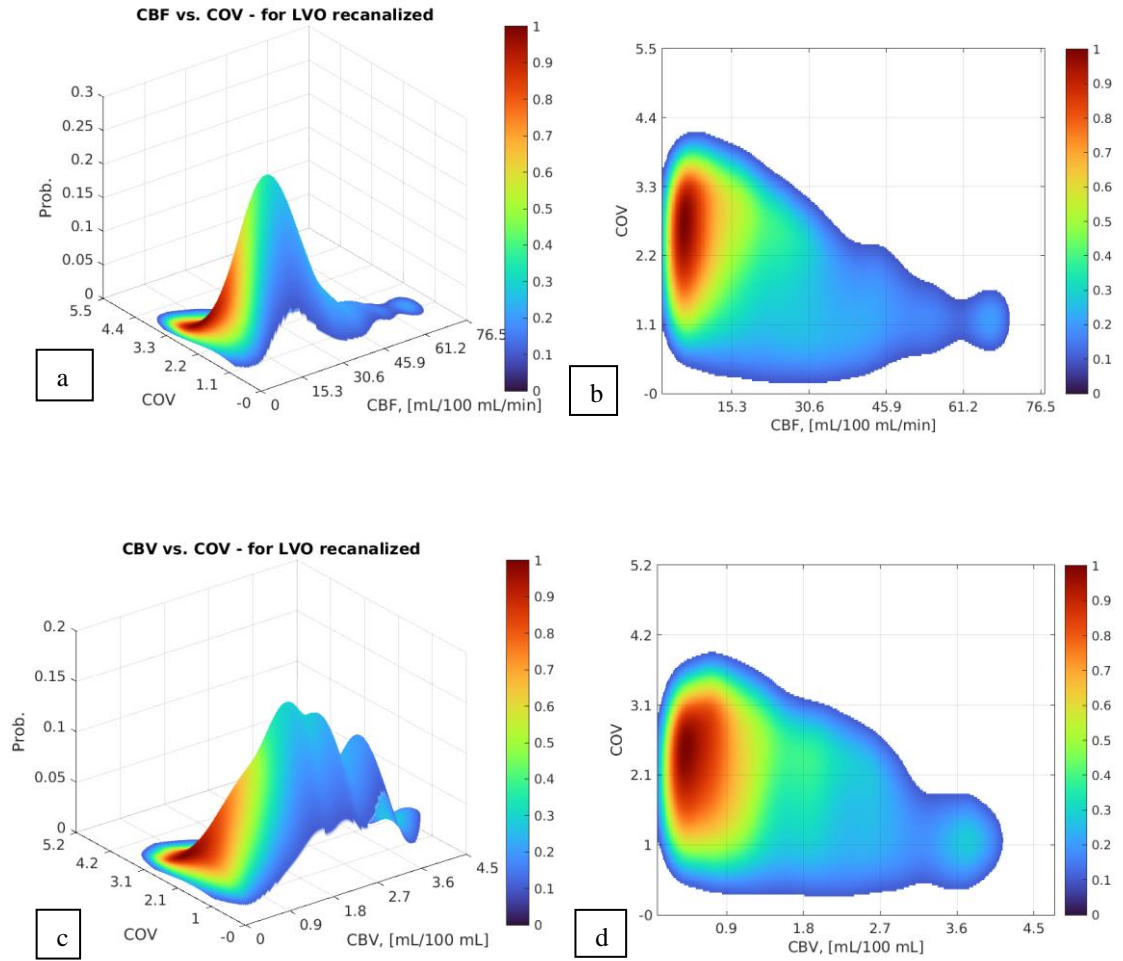
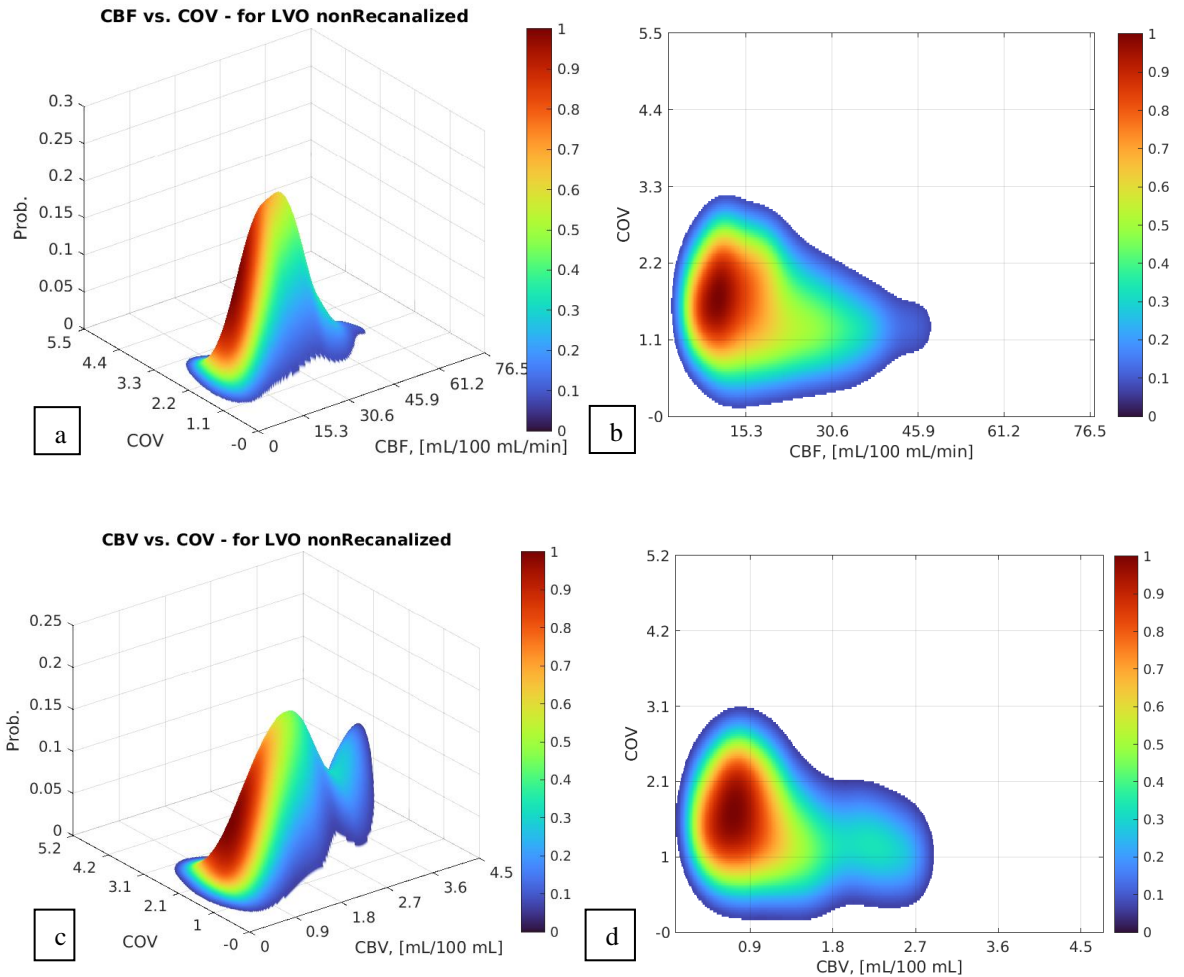


Figure 9: Non-recanalized patients



**Figure 8 and 9:** The plots show the CTP parametric measures on admission in the hypoperfused region in recanalized (figure 8) and non-recanalized patients (figure 9). The results are presented as 3D plots (a+c) and 2D plots (b+d). Values of the parametric measures are defined in the first two dimensions of each 2D and 3D plot. The third dimension in the 3D plots indicates the distribution of value combinations for the parametric measures analyzed (given as probability, values ranging between 0 and 1). Final infarct was defined as the union between the hypoperfused

region from a CTP scan and the infarct area visible on a follow-up DWI scan (step 3 in Figure 7). The color dimension illustrates the likelihood of final infarct (given as probability, with values weighted to lie between 0 and 1) across all subjects in the dataset, i.e., the likelihood of having a particular combination of values in the CTP hypoperfused region, overlapping the DWI-based final infarct area.

Abbreviations: CBF, cerebral blood flow (ml blood/100 g brain tissue/minute); CBV, cerebral blood volume (ml blood/100 g brain tissue); CoV, transit time coefficient variation.

### Paper III:

From 2015 to 2020, 959 patients were treated with IVT for symptoms of AIS. After introduction of simulation training the proportion of patients treated with IVT that were later diagnosed as SMs increased significantly (15.9% before vs. 24.4% after,  $p=0.003$ ). There were no ICH complications in the SM patients treated before, while two SM patients suffered from asymptomatic ICH after introduction of simulation training ( $p=1.0$ ). When sub-grouping SMs into pre-specified categories, only the group diagnosed with peripheral vertigo increased significantly (2.5 vs 8.6%,  $p<0.001$ ).



## **5 Discussion and Future Perspectives**

### Paper I:

In this study, we propose an automatically ML-based classification of penumbra and core. Early treatment is vital in AIS, hence, an automatic approach can help medical doctors in rapid recognition of ischemic lesions. Fast and precise visualization of ischemic lesions have the potential to better guide treatment decisions by improving diagnostic accuracy.

The best results were achieved with random forest and single-step approach. Applying superpixel regions to our models improved the results. Different numbers of superpixels were applied to our model, and increasing the number of superpixel regions slightly improved the statistical measures for both groups (LVO and non-LVO). Patients with non-LVO tend to have smaller ischemic lesions compared to LVOs, making precise classification more challenging in these patients. This applies particularly to the core and might be caused by limited number of samples for core since patients with non-LVO do not always present with a core. Our proposed model performed better for all classes compared to threshold-based approaches, especially for LVO and penumbra, with the core-class for non-LVO being the only exception where our method performed about as poorly as thresholding. This indicates a reliable agreement between ML predictions and manual annotations created by neuroradiologists.

Our study inherits limitations. Our ground truth images rely on CTP upon hospital admittance combined with the results of the follow-up MRI examination. In many studies, MRI is used as the initial diagnostic modality, with cytotoxic edema on DWI used as ground truth for ischemic core<sup>88-90</sup>. However, in many countries, MRI is not performed simultaneously with CTP. The CTP examination shows a delineation of penumbra and core that is highly dependent on the exact time at which the images are acquired. The development of the ischemic lesion in acute ischemic stroke is a dynamic process, contingent upon numerous factors, such as whether thrombectomy was performed, duration and severeness of ischemia and patient-related factors like age, blood pressure and comorbidity<sup>10</sup>. This poses a challenge, as the size of the core might have changed between the time of the CTP examination and the subsequent MRI scan. Still, follow-up DWI is commonly used as a measure for the ground truth of the ischemic core in lack of a more precise measure<sup>88-90</sup>. Our ground truth, however, relying on both CTP and MRI, might provide a reasonable alternative.

Our study is also a single center study, and there might be unintended, unknown factors that could constrain its generalizability (like local institutional practices, limited size of the study population, population characteristics and different confounding variables). Yet, we present data gathered over several years from the sole stroke-treating hospital in the geographic area for our study, and thus limiting biases related to patient selection and transfer. Being a single center study also applies to paper II and III.

For both paper I and II, manually annotated images constitute a quite small portion of the patients included. In paper I, we found some inter-observer variability between the two neuroradiologists. In general, ML-based approaches for the segmentation of medical images, including ischemic lesions, are supervised learning methods and require large amounts of manually annotated data<sup>255</sup>. This is challenging, as manual annotations are scarce since the labeling process is often time-consuming. Inter-observer variability is common in manual annotations in medicine<sup>256</sup> and may also be influenced by the frequent lack of a universal ground truth, which also applies for ischemic core<sup>10</sup>. Hence, increasing the number of manual annotations by two neuroradiologists has the potential to enhance the observer confidence and further increase the impact of computer-aided analysis in the assessment of the ischemic lesions, with further implications for clinical decision-making processes.

In summary, our proposed method calculating the penumbra and core based on ML algorithms, performed better for all classes compared to threshold-based approaches, especially for LVO and penumbra, with the only exception being the core-group for non-LVO where our method performed about as poorly as thresholding. However, there is still room for improvement. Given the central role of imaging in the management of AIS patients, and the overwhelming evidence of the benefit from early treatment in AIS<sup>7,246,247</sup>, more studies on fast and precise tissue viability visualization is wanted. Rapid and improved diagnostic accuracy in AIS holds the potential to enhance treatment decision-making with the goal to tailor the acute treatment to each patient<sup>165</sup>. Better analyses using

techniques such as artificial intelligence and deep neural networks, will probably and hopefully lead to a better worldwide access to personalized treatment for AIS patients in the future<sup>78,144,145</sup>, including stroke units who do not have access to highly qualified radiologists for radiologic image interpretation<sup>257</sup>.

Paper II:

The lack of a perfectly reliable definition for ischemic core presents a major challenge in current stroke imaging. Imaging plays a central role in treatment decision in patients with a suspected AIS<sup>4-6</sup>. Currently used imaging in AIS, including most commonly used perfusion-based parameters, struggle to accurately differentiate between salvageable and non-salvageable tissue<sup>10-12</sup>. Most previous imaging-based studies, exploring microvascular distribution of blood in ischemic brain tissue, are MRP based<sup>13,15,125,136,248</sup>. Given the widespread use of CTP, there is a growing need of CTP-based studies on tissue viability visualization.

We assessed the CTP-based parametric maps CoV, CBF and CBV voxel-wise according to DWI-based final infarct. In patients with subsequent recanalization, a distinct correlation between infarct risk and both CBF and CBV was observed. Conversely, in patients without recanalization, infarct risk was largely dependent on CoV.

Our study has inherent limitations. Adding a more quantitative assessment of the imaging parameters could further explore our data and

strengthen our findings. To further assess the risk of infarction, such as employing a logistic model, are in alignment with our intended focus for further work on the topic.

It should also be mentioned that we did not include all patients referred to the hospital with AIS in the study period, as the presence of a visible and acute ischemic lesion on the CTP dataset, and collecting high-quality data on combinations of parameters, was our primary focus and among our inclusion criteria. A more unselected group, including all LVO-patients with an ischemic lesion on CTP, is a planned expansion of the study, as soon as the selection of parameters is explored more thoroughly. There is also some heterogeneity in our study population (e.g., patients in both early and extended time windows), partly because the data are acquired over several years, and the selection criteria for treatment have changed over time due to results of studies<sup>96,113,119,123,199</sup>. As in clinical daily life, patients with AIS are an inhomogeneous group of patients. This does not necessarily need to be a drawback for a study exploring the delineation of penumbra and core, on the contrary, the results might prove to be more robust.

As for paper I and III, this is also a single center study, with potential unintended, unknown factors that could constrain its generalizability. As for paper I, only a relatively small proportion of the ground truth images used were manually annotated by two neuroradiologists.

In summary, our findings suggest the potential for a more accurate delineation of the ischemic core using CoV, compared to conventional

parameters alone. If the delineation of the ischemic core and penumbra is more accurate in the future, it will have a tremendous value for treatment decisions in the acute clinical setting. Due to inaccuracies with today's core-penumbra calculations<sup>10,12,71,160</sup>, patients that probably could profit from MT are not selected for treatment<sup>157,203,207,208,211,212</sup>. On the other hand, there are patients that are selected for treatment by today's recommendations, but who do not profit, even by technical optimal procedures<sup>196</sup>. Obviously, there is a need for other or additional selection criteria, and parameters exploring the microvascular environment might add support in better core and penumbra delineation.

Paper III:

Introduction of in situ simulation-based team-training in 2017 was accompanied by a significant increase in the proportion of patients treated with IVT for a presumed AIS that were later diagnosed as SMs (15.9% vs 24.4%,  $p=0.003$ ). The increase was mainly accounted for by patients diagnosed with peripheral vertigo. The cause of this increase is likely multifactorial and related to a focus on time, the acceptance of lower diagnostic specificity, an evolving fear to harm patients by withholding IVT in ambiguous cases, by an uncertainty of the residents in the clinical evaluation of patients presenting with vertigo, and by the recognition that IVT in SMs is rarely associated with complications<sup>249,250</sup>. The overwhelming evidence of the benefit from early treatment in AIS<sup>7,246,247</sup> clearly contributes to shaping a culture

where IVT treatment of SMs is more accepted than avoiding giving IVT to true stroke patients that could have been treated. Several large RCTs during the study period have further established the safety and efficacy of reperfusion treatment in AIS<sup>96,113,123,202,251</sup>, contributing to change the culture of treatment towards fewer restrictions. Simulation training is a central tool helping to adapt in this cultural change.

MRI in the initial management of patients suspected to suffer from AIS reduces the proportion of IVT-treated SMs<sup>50,237</sup>. Patients diagnosed with peripheral vertigo was the only subgroup that increased significantly in our study. While most patients presenting with vertigo suffer from benign disorders, up to 27% can end up with serious diagnoses and cerebral stroke is the underlying cause in 4–15%<sup>252,253</sup>. The clinical differentiation between peripheral and central causes of vertigo is challenging. In addition, a small but significant percentage of patients with AIS initially have negative MRI scans, especially in strokes located in the posterior fossa<sup>254</sup>. No significant increase in bleeding complications was found in our study. Only two patients were diagnosed with an asymptomatic ICH during the four-year study period, this finding is similar to what is found in other studies<sup>250</sup>.

To firmly establish a cause-effect relationship, is a general challenge in simulation training. During the study period, in a part of medicine where research and development evolves so fast, guidelines and recommendations change, and influence the treatment decisions even in the relatively short time span of this study. Therefore, there are probably

also additional factors influencing the stroke mimics rate, that are not directly coupled to the simulation training.

Other limitations in our study, is a relatively small sample size, as well as significantly less frequent atrial fibrillation found after introduction of simulation training, which could lower the number of true strokes in our study group.

As for paper I and II, this is also a single center study, with potential unintended, unknown factors that could constrain its generalizability. Yet, we present data gathered over several years from the sole stroke-treating hospital in the geographic area for the study, which allows us to present population-based data and avoid biases related to patient selection and transfer.

In summary, the implementation of in situ simulation-based team-training for the acute stroke treatment team seems to be safe but was associated with a significant increase in the proportion of patients treated with IVT that were later diagnosed as SMs. The increase consisted mainly of patients with peripheral vertigo. This emphasizes the need of implementing patients presenting with dizziness and vertigo in the weekly simulation-based team-training. Simulation-based team-training has the potential to improve team performance, with improvement observed in both simulated, and to some extent clinical performance, across various emergencies, including AIS<sup>7,19-21</sup>. Our quality improvement project, aimed at reducing treatment times, led to a significant increase in the proportion of IVT-treated patients that were



later diagnosed as SMs. Our findings highlight the importance of additional focus on unintended, potentially negative effects in quality improvement endeavors<sup>18,244</sup>.

### Future perspectives

The use of computer-based analysis in medicine has increased dramatically in recent years and is continuously evolving<sup>258</sup>. Several of these computer-based techniques use AI and combine clinical data, patient characteristics, and imaging results. This holds the potential for no less than revolutionizing patient care in the future, with advanced technology used to tailor treatment to every patient, and the possibility for making this technology, with subsequent advanced patient care, more easily available also to smaller stroke units in near future. AI certainly has drawbacks, like inadequate diversity of data used for training, such as limited engagement of resource-poor health institutions in the development and validation of AI algorithms, the lack of transparency, and the often high costs associated with the implementation of AI-based algorithms in clinical practice<sup>257</sup>. Still, the time where the validity of AI in medicine was questioned has passed. Today, the challenge is how to use this technology reasonable and safe. AI-based methods already play a large role in radiology and is expected to have even larger impact in the future, as well as in more clinical disciplines of medicine<sup>151,255</sup>. It is expected that AI has the potential to improve radiology and patients care and decrease costs<sup>259</sup>. Large amount of data used for learning is

fundamental for this development, where open access and sharing plays a key role. To complement technical and medical expertise combined is of vital importance in the development and implementation of good and clinically meaningful AI-based technology in medicine, as experienced with the work of this thesis as part of a technical and medical twin project. It is essential to provide high quality clinical data, including high quality imaging for training the models, to produce good and meaningful outputs for clinical use. Including additional parameters, such as CoV explored in this thesis, with the potential for a more reliable delineation of the ischemic lesion in the acute phase, offers significant promise for further advancing these techniques.

In a global perspective, the development of smaller, less fragile, and cheaper CT- and MRI scanners, compared to currently commonly used scanners, along with making AI-based technology available at lower costs<sup>257</sup>, also holds the potential that this technology can be more accessible for patients in lower- and middle-income countries. This development will also have the potential to give patients with AIS therapy earlier in high income countries even before the patients arrive in the hospitals, as it will be more available, easier to use and can be placed in remote locations.

Although CT is the preferred imaging modality in the initial assessment of patients with a suspected AIS in many stroke centers, MRI is superior to CT in many aspects, and initial assessment with MRI has demonstrated feasibility within guideline-based frames for treatment

times<sup>108</sup> and results comparable to in patients initially assessed with CT<sup>107</sup>. Increasing the use of MRI in the acute setting, along with computer-based analysis using AI, will probably provide improved diagnostic accuracy.

Especially in recent years, there has been an increased emphasis on the importance of open access for scientific publications. Open access ensures that research findings are open and freely available to everyone, has the potential of increasing its impact as openly accessible research is more likely to be read and cited, and facilitates the exchange of both findings and ideas among researchers globally, having the potential to accelerate the scientific progress<sup>260,261</sup>. Open access also has drawbacks, like the often high open-access charges set by the publisher, and the emerging number of medical journals, including journals of lower quality, for which high open-access charges has made it easier to establish profit for journals with low/lacking peer review standards<sup>260</sup>. In Norway, several institutions and research funders have adopted guidelines and requirements to promote open access to research publications<sup>261</sup>. Among these are the University of Stavanger, which shall be an open university, with its research output being openly available to everyone<sup>262</sup>. The two published papers in this thesis, paper I and II, are both open access papers. For paper II and III, we state that the data that support the findings are available from the corresponding author upon reasonable request. For paper I, the code used is publicly available online in a GitHub repository. Despite its drawbacks, sharing data and

ensuring open access publications hold significant potential for advancing and speeding up research.

If systems for simulation training, that enable continuous monitoring of health care providers, can provide real-time feedback customized for each participant, and additionally is coupled to clinical results from the patients that every participant is involved with, a more effective real time feedback will lead to learning without delay. In the future, we believe that automatic analyses and reporting will be an integrated part of every patient pathway in the hospital and other institutions, and that learning and feedback is a more continuous integrated part of working with humans compared to today's measures. To technically solve these issues is probably not a major challenge. Issues on privacy and surveillance, on the other hand, will probably pose a bigger challenge.

## 6 References

1. WHO. Optimizing brain health across the life course: WHO position paper. 2022.
2. Collaborators GS. Global, regional, and national burden of stroke and its risk factors, 1990-2019: a systematic analysis for the Global Burden of Disease Study 2019. *Lancet Neurol* 2021;20(10):795-820. (In eng). DOI: 10.1016/s1474-4422(21)00252-0.
3. Zerna C, Thomalla G, Campbell BCV, Rha J-H, Hill MD. Current practice and future directions in the diagnosis and acute treatment of ischaemic stroke. *The Lancet* 2018;392(10154):1247-1256. DOI: 10.1016/s0140-6736(18)31874-9.
4. Berge E, Whiteley W, Audebert H, et al. European Stroke Organisation (ESO) guidelines on intravenous thrombolysis for acute ischaemic stroke. *Eur Stroke J* 2021;6(1):I-lxii. (In eng). DOI: 10.1177/2396987321989865.
5. Powers WJ, Rabinstein AA, Ackerson T, et.al. Guidelines for the early management of patients with acute ischemic stroke: 2019 update to the 2018 guidelines for the early management of acute ischemic stroke a guideline for healthcare professionals from the American Heart Association/American Stroke Association. *Stroke* 2019;50(12):e344-e418. DOI: 10.1161/STR.0000000000000211.
6. Turc G, Bhogal P, Fischer U, et al. European Stroke Organisation (ESO) - European Society for Minimally Invasive Neurological Therapy (ESMINT) Guidelines on Mechanical Thrombectomy in Acute Ischaemic Stroke Endorsed by Stroke Alliance for Europe (SAFE). *Eur Stroke J* 2019;4(1):6-12. (In eng). DOI: 10.1177/2396987319832140.
7. Ajmi SC, Advani R, Fjetland L, et al. Reducing door-to-needle times in stroke thrombolysis to 13 min through protocol revision and simulation training: A quality improvement project in a Norwegian stroke centre. *BMJ Qual Saf*: 2019;28(11):939-948. DOI: 10.1136/bmjqs-2018-009117.

## References

---

8. Emberson J, Lees KR, Lyden P, et al. Effect of treatment delay, age, and stroke severity on the effects of intravenous thrombolysis with alteplase for acute ischaemic stroke: a meta-analysis of individual patient data from randomised trials. *Lancet* 2014;384(9958):1929-35. (In eng). DOI: 10.1016/s0140-6736(14)60584-5.
9. Astrup J, Siesjö BK, Symon L. Thresholds in cerebral ischemia - the ischemic penumbra. *Stroke* 1981;12(6):723-5. (In eng). DOI: 10.1161/01.str.12.6.723.
10. Goyal M, Ospel JM, Menon B, et al. Challenging the Ischemic Core Concept in Acute Ischemic Stroke Imaging. *Stroke* 2020;51(10):3147-3155. (In eng). DOI: 10.1161/strokeaha.120.030620.
11. Biesbroek JM, Niesten JM, Dankbaar JW, Biessels GJ, Velthuis BK, Reitsma JB, van der Schaaf IC. Diagnostic accuracy of CT perfusion imaging for detecting acute ischemic stroke: a systematic review and meta-analysis. *Cerebrovasc Dis* 2013;35(6):493-501. (In eng). DOI: 10.1159/000350200.
12. Martins N, Aires A, Mendez B, et al. Ghost Infarct Core and Admission Computed Tomography Perfusion: Redefining the Role of Neuroimaging in Acute Ischemic Stroke. *Interv Neurol* 2018;7(6):513-521. (In eng). DOI: 10.1159/000490117.
13. Engedal TS, Hjort N, Hougaard KD, et al. Transit time homogenization in ischemic stroke - A novel biomarker of penumbral microvascular failure? *J Cereb Blood Flow Metab* 2018;38(11):2006-2020. (In eng). DOI: 10.1177/0271678x17721666.
14. Ostergaard L, Jespersen SN, Mouridsen K, et al. The role of the cerebral capillaries in acute ischemic stroke: the extended penumbra model. *J Cereb Blood Flow Metab* 2013;33(5):635-48. DOI: 10.1038/jcbfm.2013.18.
15. Ostergaard L, Sorensen AG, Chesler DA, et al. Combined diffusion-weighted and perfusion-weighted flow heterogeneity magnetic resonance imaging in acute stroke. *Stroke* 2000;31(5):1097-103. (In eng). DOI: 10.1161/01.str.31.5.1097.
16. Livne M, Kossen T, Madai VI, et al. Multiparametric Model for Penumbral Flow Prediction in Acute Stroke. *Stroke*

## References

---

- 2017;48(7):1849-1854. DOI: 10.1161/STROKEAHA.117.016631.
17. Dalkara T, Arsava EM. Can restoring incomplete microcirculatory reperfusion improve stroke outcome after thrombolysis? *J Cereb Blood Flow Metab* 2012;32(12):2091-9. DOI: 10.1038/jcbfm.2012.139.
  18. Høllesli LJ, Ajmi SC, Kurz MW, et al. Simulation-based team-training in acute stroke: Is it safe to speed up? *Brain Behav* 2022;12(12):e2814. (In eng). DOI: 10.1002/brb3.2814.
  19. Murphy M, Curtis K, McCloughen A. What is the impact of multidisciplinary team simulation training on team performance and efficiency of patient care? An integrative review. *Australas Emerg Nurs J* 2016;19(1):44-53. (In eng). DOI: 10.1016/j.aenj.2015.10.001.
  20. Tahtali D, Bohmann F, Rostek P, et al. Crew resource management and simulator training in acute stroke therapy. *Nervenarzt* 2016;87(12):1322-1331. (In ger). DOI: 10.1007/s00115-016-0162-5.
  21. Mundell WC, Kennedy CC, Szostek JH, Cook DA. Simulation technology for resuscitation training: a systematic review and meta-analysis. *Resuscitation* 2013;84(9):1174-83. (In eng). DOI: 10.1016/j.resuscitation.2013.04.016.
  22. Sacco RL, Kasner SE, Broderick JP, et al. An updated definition of stroke for the 21st century: a statement for healthcare professionals from the American Heart Association/American Stroke Association. *Stroke* 2013;44(7):2064-89. (In eng). DOI: 10.1161/STR.0b013e318296aeca.
  23. Adams HP, Jr., Bendixen BH, Kappelle LJ, Biller J, Love BB, Gordon DL, Marsh EE, 3rd. Classification of subtype of acute ischemic stroke. Definitions for use in a multicenter clinical trial. TOAST. Trial of Org 10172 in Acute Stroke Treatment. *Stroke* 1993;24(1):35-41. (In eng). DOI: 10.1161/01.str.24.1.35.
  24. Ay H, Furie KL, Singhal A, Smith WS, Sorensen AG, Koroshetz WJ. An evidence-based causative classification system for acute ischemic stroke. *Ann Neurol* 2005;58(5):688-97. (In eng). DOI: 10.1002/ana.20617.

## References

---

25. Kunz A, Iadecola C. Cerebral vascular dysregulation in the ischemic brain. *Handb Clin Neurol* 2009;92:283-305. (In eng). DOI: 10.1016/s0072-9752(08)01914-3.
26. Schaafsma JD, Rawal S, Coutinho JM, et al. Diagnostic Impact of Intracranial Vessel Wall MRI in 205 Patients with Ischemic Stroke or TIA. *AJNR Am J Neuroradiol* 2019;40(10):1701-1706. (In eng). DOI: 10.3174/ajnr.A6202.
27. Lakomkin N, Dhamoon M, Carroll K, et al. Prevalence of large vessel occlusion in patients presenting with acute ischemic stroke: a 10-year systematic review of the literature. *J Neurointerv Surg* 2019;11(3):241-245. (In eng). DOI: 10.1136/neurintsurg-2018-014239.
28. Tomasetti L, Hølleli LJ, Engan K, Kurz KD, Kurz MW, Khanmohammadi M. Machine learning algorithms vs. thresholding to segment ischemic regions in patients with acute ischemic stroke. *IEEE J Biomed Health Inform* 2021;Pp (In eng). DOI: 10.1109/jbhi.2021.3097591.
29. Waqas M, Mokin M, Primiani CT, et al. Large Vessel Occlusion in Acute Ischemic Stroke Patients: A Dual-Center Estimate Based on a Broad Definition of Occlusion Site. *J Stroke Cerebrovasc Dis* 2020;29(2):104504. (In eng). DOI: 10.1016/j.jstrokecerebrovasdis.2019.104504.
30. Mokin M, Pendurthi A, Ljubimov V, Burgin WS, Siddiqui AH, Levy EI, Primiani CT. ASPECTS, Large Vessel Occlusion, and Time of Symptom Onset: Estimation of Eligibility for Endovascular Therapy. *Neurosurgery* 2018;83(1):122-127. (In eng). DOI: 10.1093/neuros/nyx352.
31. Rai AT, Seldon AE, Boo S, et al. A population-based incidence of acute large vessel occlusions and thrombectomy eligible patients indicates significant potential for growth of endovascular stroke therapy in the USA. *J Neurointerv Surg* 2017;9(8):722-726. (In eng). DOI: 10.1136/neurintsurg-2016-012515.
32. Rocha M, Desai SM, Jadhav AP, Jovin TG. Prevalence and Temporal Distribution of Fast and Slow Progressors of Infarct Growth in Large Vessel Occlusion Stroke. *Stroke* 2019;50(8):2238-2240. (In eng). DOI: 10.1161/strokeaha.118.024035.



## References

---

33. Malhotra K, Gornbein J, Saver JL. Ischemic Strokes Due to Large-Vessel Occlusions Contribute Disproportionately to Stroke-Related Dependence and Death: A Review. *Front Neurol* 2017;8:651. (In eng). DOI: 10.3389/fneur.2017.00651.
34. Ojaghiahghi S, Vahdati SS, Mikaeilpour A, Ramouz A. Comparison of neurological clinical manifestation in patients with hemorrhagic and ischemic stroke. *World J Emerg Med* 2017;8(1):34-38. DOI: 10.5847/wjem.j.1920-8642.2017.01.006.
35. Stevens E, Emmett E, Wang Y, McKeivitt C, Wolfe C. The Burden of Stroke in Europe - Challenges for Policy Makers. *EU Parliament in May 2017*: 2017.
36. Wafa HA, Wolfe CDA, Emmett E, Roth GA, Johnson CO, Wang Y. Burden of Stroke in Europe: Thirty-Year Projections of Incidence, Prevalence, Deaths, and Disability-Adjusted Life Years. *Stroke* 2020;51(8):2418-2427. DOI: 10.1161/STROKEAHA.120.029606.
37. Lindsay MP, Norrving B, Sacco RL, et al. World Stroke Organization (WSO): Global Stroke Fact Sheet 2019. *Int J Stroke* 2019;14(8):806-817. DOI: 10.1177/1747493019881353.
38. Boehme AK, Esenwa C, Elkind MSV. Stroke Risk Factors, Genetics, and Prevention. *Circ Res* 2017;120(3):472-495. (In eng). DOI: 10.1161/CIRCRESAHA.116.308398.
39. Yuh WT, Alexander MD, Ueda T, Maeda M, Taoka T, Yamada K, Beauchamp NJ. Revisiting Current Golden Rules in Managing Acute Ischemic Stroke: Evaluation of New Strategies to Further Improve Treatment Selection and Outcome. *AJR Am J Roentgenol* 2017;208(1):32-41. (In eng). DOI: 10.2214/ajr.16.16557.
40. Symon L. The relationship between CBF, evoked potentials and the clinical features in cerebral ischaemia. *Acta Neurol Scand Suppl* 1980;78:175-90. (In eng).
41. del Zoppo GJ, Sharp FR, Heiss WD, Albers GW. Heterogeneity in the penumbra. *J Cereb Blood Flow Metab* 2011;31(9):1836-51. (In eng). DOI: 10.1038/jcbfm.2011.93.
42. Markus HS. Cerebral perfusion and stroke. *J Neurol Neurosurg Psychiatry* 2004;75(3):353. DOI: 10.1136/jnnp.2003.025825.
43. Dawson SL, Panerai RB, Potter JF. Serial changes in static and dynamic cerebral autoregulation after acute ischaemic stroke.

## References

---

- Cerebrovasc Dis 2003;16(1):69-75. (In eng). DOI: 10.1159/000070118.
44. Sharbrough FW, Messick JM, Jr., Sundt TM, Jr. Correlation of continuous electroencephalograms with cerebral blood flow measurements during carotid endarterectomy. *Stroke* 1973;4(4):674-83. (In eng). DOI: 10.1161/01.str.4.4.674.
45. Grewer C, Gameiro A, Zhang Z, Tao Z, Braams S, Rauen T. Glutamate forward and reverse transport: from molecular mechanism to transporter-mediated release after ischemia. *IUBMB Life* 2008;60(9):609-19. (In eng). DOI: 10.1002/iub.98.
46. Doyle KP, Simon RP, Stenzel-Poore MP. Mechanisms of ischemic brain damage. *Neuropharmacology* 2008;55(3):310-8. (In eng). DOI: 10.1016/j.neuropharm.2008.01.005.
47. Deb P, Sharma S, Hassan KM. Pathophysiologic mechanisms of acute ischemic stroke: An overview with emphasis on therapeutic significance beyond thrombolysis. *Pathophysiology* 2010;17(3):197-218. (In eng). DOI: 10.1016/j.pathophys.2009.12.001.
48. European Stroke Organisation (ESO) Executive Committee; ESO Writing Committee. Guidelines for Management of Ischaemic Stroke and Transient Ischaemic Attack 2008. *Cerebrovasc Dis* 2008;25(5):457-507. DOI: 10.1159/000131083.
49. Moreau F, Asdaghi N, Modi J, Goyal M, Coutts SB. Magnetic Resonance Imaging versus Computed Tomography in Transient Ischemic Attack and Minor Stroke: The More You See the More You Know. *Cerebrovasc Dis Extra* 2013;3(1):130-6. (In eng). DOI: 10.1159/000355024.
50. Bhattacharya P, Nagaraja N, Rajamani K, Madhavan R, Santhakumar S, Chaturvedi S. Early use of MRI improves diagnostic accuracy in young adults with stroke. *J Neurol Sci* 2013;324(1-2):62-4. (In eng). DOI: 10.1016/j.jns.2012.10.002.
51. McDonough R, Ospel J, Goyal M. State of the Art Stroke Imaging: A Current Perspective. *Can Assoc Radiol J* 2021;8465371211028823. (In eng). DOI: 10.1177/08465371211028823.

## References

---

52. Goldman LW. Principles of CT: multislice CT. *J Nucl Med Technol* 2008;36(2):57-68; quiz 75-6. (In eng). DOI: 10.2967/jnmt.107.044826.
53. Rydberg J, Liang Y, Teague SD. Fundamentals of multichannel CT. *Semin Musculoskelet Radiol* 2004;8(2):137-46. (In eng). DOI: 10.1055/s-2004-829485.
54. Nakano S, Iseda T, Kawano H, Yoneyama T, Ikeda T, Wakisaka S. Correlation of early CT signs in the deep middle cerebral artery territories with angiographically confirmed site of arterial occlusion. *AJNR Am J Neuroradiol* 2001;22(4):654-9. (In eng).
55. Barber PA, Demchuk AM, Zhang J, Buchan AM. Validity and reliability of a quantitative computed tomography score in predicting outcome of hyperacute stroke before thrombolytic therapy. ASPECTS Study Group. Alberta Stroke Programme Early CT Score. *Lancet* 2000;355(9216):1670-4. (In eng). DOI: 10.1016/s0140-6736(00)02237-6.
56. von Kummer R, Dzialowski I. Imaging of cerebral ischemic edema and neuronal death. *Neuroradiology* 2017;59(6):545-553. DOI: 10.1007/s00234-017-1847-6.
57. Wardlaw JM, Mielke O. Early signs of brain infarction at CT: observer reliability and outcome after thrombolytic treatment--systematic review. *Radiology* 2005;235(2):444-53. (In eng). DOI: 10.1148/radiol.2352040262.
58. Hacke W, Kaste M, Fieschi C, et al. Intravenous thrombolysis with recombinant tissue plasminogen activator for acute hemispheric stroke. The European Cooperative Acute Stroke Study (ECASS). *JAMA* 1995;274(13):1017-25. (In eng).
59. Broocks G, McDonough R, Meyer L, et al. Reversible Ischemic Lesion Hypodensity in Acute Stroke CT Following Endovascular Reperfusion. *Neurology* 2021;97(11):e1075-e1084. (In eng). DOI: 10.1212/wnl.00000000000012484.
60. Naruto N, Itoh T, Noguchi K. Dual energy computed tomography for the head. *Jpn J Radiol* 2018;36(2):69-80. (In eng). DOI: 10.1007/s11604-017-0701-4.
61. Shinohara Y, Ohmura T, Ibaraki M, et al. Non-contrast dual-energy CT using X-map for acute ischemic stroke: region-specific comparison with simulated 120-kVp CT and diffusion-

## References

---

- weighted MR images. *Jpn J Radiol* 2024;42(2):165-173. (In eng). DOI: 10.1007/s11604-023-01490-3.
62. Pressman BD, Tourje EJ, Thompson JR. An early CT sign of ischemic infarction: increased density in a cerebral artery. *AJR Am J Roentgenol* 1987;149(3):583-6. (In eng). DOI: 10.2214/ajr.149.3.583.
63. Camargo EC, Furie KL, Singhal AB, et al. Acute brain infarct: detection and delineation with CT angiographic source images versus nonenhanced CT scans. *Radiology* 2007;244(2):541-8. (In eng). DOI: 10.1148/radiol.2442061028.
64. Menon BK, d'Esteire CD, Qazi EM, Almekhlafi M, Hahn L, Demchuk AM, Goyal M. Multiphase CT Angiography: A New Tool for the Imaging Triage of Patients with Acute Ischemic Stroke. *Radiology* 2015;275(2):510-20. (In eng). DOI: 10.1148/radiol.15142256.
65. García-Tornel A, Carvalho V, Boned S, et al. Improving the Evaluation of Collateral Circulation by Multiphase Computed Tomography Angiography in Acute Stroke Patients Treated with Endovascular Reperfusion Therapies. *Interv Neurol* 2016;5(3-4):209-217. (In eng). DOI: 10.1159/000448525.
66. Volny O, Cimflova P, Kadlecova P, Vanek P, Vanicek J, Menon BK, Mikulik R. Single-Phase Versus Multiphase CT Angiography in Middle Cerebral Artery Clot Detection-Benefits for Less Experienced Radiologists and Neurologists. *J Stroke Cerebrovasc Dis* 2017;26(1):19-24. (In eng). DOI: 10.1016/j.jstrokecerebrovasdis.2016.08.023.
67. Fasen B, Heijboer RJJ, Hulsmans FH, Kwee RM. CT Angiography in Evaluating Large-Vessel Occlusion in Acute Anterior Circulation Ischemic Stroke: Factors Associated with Diagnostic Error in Clinical Practice. *AJNR Am J Neuroradiol* 2020;41(4):607-611. (In eng). DOI: 10.3174/ajnr.A6469.
68. Volders D, Shewchuk JR, Marangoni M, Ni Mhurchu E, Heran M. Beyond the collaterals: Additional value of multiphase CTA in acute ischemic stroke evaluation. *Neuroradiol J* 2019;32(4):309-314. (In eng). DOI: 10.1177/1971400919845361.
69. Polito V, La Piana R, Del Pilar Cortes M, Tampieri D. Assessment of clot length with multiphase CT angiography in

## References

---

- patients with acute ischemic stroke. *Neuroradiol J* 2017;30(6):593-599. (In eng). DOI: 10.1177/1971400917736928.
70. Dundamadappa S, Iyer K, Agrawal A, Choi DJ. Multiphase CT Angiography: A Useful Technique in Acute Stroke Imaging-Collaterals and Beyond. *AJNR Am J Neuroradiol* 2021;42(2):221-227. (In eng). DOI: 10.3174/ajnr.A6889.
71. Biesbroek JM, Niesten JM, Dankbaar JW, et al. Diagnostic Accuracy of CT Perfusion Imaging for Detecting Acute Ischemic Stroke: A Systematic Review and Meta-Analysis. *Cerebrovasc Dis* 2013;35(6):493-501. DOI: 10.1159/000350200.
72. Kawiorski MM, Vicente A, Lourido D, et al. Good Clinical and Radiological Correlation from Standard Perfusion Computed Tomography Accurately Identifies Salvageable Tissue in Ischemic Stroke. *J Stroke Cerebrovasc Dis* 2016;25(5):1062-69. (In eng). DOI: 10.1016/j.jstrokecerebrovasdis.2016.01.009.
73. Zhu G, Michel P, Aghaebrahim A, et al. Computed tomography workup of patients suspected of acute ischemic stroke: perfusion computed tomography adds value compared with clinical evaluation, noncontrast computed tomography, and computed tomography angiogram in terms of predicting outcome. *Stroke* 2013;44(4):1049-55. (In eng). DOI: 10.1161/strokeaha.111.674705.
74. Becks MJ, Manniesing R, Vister J, et al. Brain CT perfusion improves intracranial vessel occlusion detection on CT angiography. *J Neuroradiol* 2019;46(2):124-129. (In eng). DOI: 10.1016/j.neurad.2018.03.003.
75. Amukotuwa SA, Wu A, Zhou K, Page I, Brotchie P, Bammer R. Distal Medium Vessel Occlusions Can Be Accurately and Rapidly Detected Using Tmax Maps. *Stroke* 2021;52(10):3308-3317. (In eng). DOI: 10.1161/strokeaha.120.032941.
76. Siegler JE, Rosenberg J, Cristancho D, et al. Computed tomography perfusion in stroke mimics. *Int J Stroke* 2020;15(3):299-307. (In eng). DOI: 10.1177/1747493019869702.

## References

---

77. Kurz KD, Ringstad G, Odland A, Advani R, Farbu E, Kurz MW. Radiological imaging in acute ischaemic stroke. *Eur J Neurol* 2016;23 Suppl 1:8-17. DOI: 10.1111/ene.12849.
78. Tomasetti L, Engan K, Khanmohammadi M, Kurz KD. CNN Based Segmentation of Infarcted Regions in Acute Cerebral Stroke Patients From Computed Tomography Perfusion Imaging. Proceedings of the 11th ACM International Conference on Bioinformatics, Computational Biology and Health Informatics. Virtual Event, USA: Association for Computing Machinery; 2020:Article 59.
79. Nicolas-Jilwan M, Wintermark M. Automated Brain Perfusion Imaging in Acute Ischemic Stroke: Interpretation Pearls and Pitfalls. *Stroke* (1970) 2021;52(11):3728-3738. DOI: 10.1161/STROKEAHA.121.035049.
80. Calamante F, Christensen S, Desmond PM, Ostergaard L, Davis SM, Connelly A. The physiological significance of the time-to-maximum (Tmax) parameter in perfusion MRI. *Stroke* 2010;41(6):1169-74. (In eng). DOI: 10.1161/strokeaha.110.580670.
81. Wouters A, Christensen S, Straka M, et al. A Comparison of Relative Time to Peak and Tmax for Mismatch-Based Patient Selection. *Front Neurol* 2017;8:539. (In eng). DOI: 10.3389/fneur.2017.00539.
82. Straka M, Albers GW, Bammer R. Real-time diffusion-perfusion mismatch analysis in acute stroke. *J Magn Reson Imaging* 2010;32(5):1024-37. (In eng). DOI: 10.1002/jmri.22338.
83. Fieselmann A, Kowarschik M, Ganguly A, Hornegger J, Fahrig R. Deconvolution-Based CT and MR Brain Perfusion Measurement: Theoretical Model Revisited and Practical Implementation Details. *Int J Biomed Imaging* 2011;2011:467563. (In eng). DOI: 10.1155/2011/467563.
84. Olivot JM, Mlynash M, Thijs VN, et al. Optimal Tmax threshold for predicting penumbral tissue in acute stroke. *Stroke* 2009;40(2):469-75. DOI: 10.1161/STROKEAHA.108.526954.
85. Austein F, Riedel C, Kerby T, et al. Comparison of Perfusion CT Software to Predict the Final Infarct Volume After

## References

---

- Thrombectomy. *Stroke* 2016;47(9):2311-7. (In eng). DOI: 10.1161/strokeaha.116.013147.
86. Lum C, Ahmed ME, Patro S, et al. Computed tomographic angiography and cerebral blood volume can predict final infarct volume and outcome after recanalization. *Stroke* 2014;45(9):2683-8. (In eng). DOI: 10.1161/strokeaha.114.006163.
87. Schramm P, Schellinger PD, Klotz E, et al. Comparison of perfusion computed tomography and computed tomography angiography source images with perfusion-weighted imaging and diffusion-weighted imaging in patients with acute stroke of less than 6 hours' duration. *Stroke* 2004;35(7):1652-8. DOI: 10.1161/01.STR.0000131271.54098.22.
88. Wintermark M, Flanders AE, Velthuis B, et al. Perfusion-CT assessment of infarct core and penumbra: receiver operating characteristic curve analysis in 130 patients suspected of acute hemispheric stroke. *Stroke* 2006;37(4):979-85. (In eng). DOI: 10.1161/01.Str.0000209238.61459.39.
89. Campbell BC, Christensen S, Levi CR, Desmond PM, Donnan GA, Davis SM, Parsons MW. Comparison of computed tomography perfusion and magnetic resonance imaging perfusion-diffusion mismatch in ischemic stroke. *Stroke* 2012;43(10):2648-53. (In eng). DOI: 10.1161/strokeaha.112.660548.
90. Cereda CW, Christensen S, Campbell BCV, et al. A benchmarking tool to evaluate computer tomography perfusion infarct core predictions against a DWI standard. *J Cereb Blood Flow Metab* 2016;36(10):1780-1789. DOI: 10.1177/0271678X15610586.
91. Lin L, Bivard A, Levi CR, Parsons MW. Comparison of computed tomographic and magnetic resonance perfusion measurements in acute ischemic stroke: back-to-back quantitative analysis. *Stroke* 2014;45(6):1727-32. (In eng). DOI: 10.1161/strokeaha.114.005419.
92. Murphy BD, Fox AJ, Lee DH, et al. Identification of penumbra and infarct in acute ischemic stroke using computed tomography perfusion-derived blood flow and blood volume

## References

---

- measurements. *Stroke* 2006;37(7):1771-7. (In eng). DOI: 10.1161/01.Str.0000227243.96808.53.
93. Dani KA, Thomas RG, Chappell FM, Shuler K, MacLeod MJ, Muir KW, Wardlaw JM. Computed tomography and magnetic resonance perfusion imaging in ischemic stroke: definitions and thresholds. *Ann Neurol* 2011;70(3):384-401. (In eng). DOI: 10.1002/ana.22500.
94. Koopman MS, Berkhemer OA, Geuskens R, et al. Comparison of three commonly used CT perfusion software packages in patients with acute ischemic stroke. *J Neurointerv Surg* 2019;11(12):1249-1256. DOI: 10.1136/neurintsurg-2019-014822.
95. Campbell BC, Christensen S, Levi CR, Desmond PM, Donnan GA, Davis SM, Parsons MW. Cerebral blood flow is the optimal CT perfusion parameter for assessing infarct core. *Stroke* 2011;42(12):3435-40. DOI: 10.1161/STROKEAHA.111.618355.
96. Ma H, Campbell BCV, Parsons MW, et al. Thrombolysis Guided by Perfusion Imaging up to 9 Hours after Onset of Stroke. *N Engl J Med* 2019;380(19):1795-1803. DOI: 10.1056/NEJMoa1813046.
97. Bhatia R, Bal SS, Shobha N, et al. CT angiographic source images predict outcome and final infarct volume better than noncontrast CT in proximal vascular occlusions. *Stroke* 2011;42(6):1575-80. (In eng). DOI: 10.1161/strokeaha.110.603936.
98. Kidwell CS, Chalela JA, Saver JL, et al. Comparison of MRI and CT for detection of acute intracerebral hemorrhage. *JAMA* 2004;292(15):1823-30. (In eng). DOI: 10.1001/jama.292.15.1823.
99. Schellinger PD, Bryan RN, Caplan LR, et al. Evidence-based guideline: The role of diffusion and perfusion MRI for the diagnosis of acute ischemic stroke: report of the Therapeutics and Technology Assessment Subcommittee of the American Academy of Neurology. *Neurology* 2010;75(2):177-85. (In eng). DOI: 10.1212/WNL.0b013e3181e7c9dd.
100. González RG, Schaefer PW, Buonanno FS, et al. Diffusion-weighted MR imaging: diagnostic accuracy in patients imaged



## References

---

- within 6 hours of stroke symptom onset. *Radiology* 1999;210(1):155-62. (In eng). DOI: 10.1148/radiology.210.1.r99ja02155.
101. Srinivasan A, Goyal M, Al Azri F, Lum C. State-of-the-art imaging of acute stroke. *Radiographics* 2006;26 Suppl 1:S75-95. (In eng). DOI: 10.1148/rg.26si065501.
102. Lövblad KO, Laubach HJ, Baird AE, Curtin F, Schlaug G, Edelman RR, Warach S. Clinical experience with diffusion-weighted MR in patients with acute stroke. *AJNR Am J Neuroradiol* 1998;19(6):1061-6. (In eng)
103. Burke JF, Gelb DJ, Quint DJ, Morgenstern LB, Kerber KA. The impact of MRI on stroke management and outcomes: a systematic review. *J Eval Clin Pract* 2013;19(6):987-93. (In eng). DOI: 10.1111/jep.12011.
104. Paolini S, Burdine J, Verenes M, Webster J, Faber T, Graham CB, Sen S. Rapid Short MRI Sequence Useful in Eliminating Stroke Mimics Among Acute Stroke Patients Considered for Intravenous Thrombolysis. *J Neurol Disord* 2013;1:137. (In eng). DOI: 10.4172/2329-6895.1000137.
105. Fiebich JB, Schellinger PD, Jansen O, et al. CT and diffusion-weighted MR imaging in randomized order: diffusion-weighted imaging results in higher accuracy and lower interrater variability in the diagnosis of hyperacute ischemic stroke. *Stroke* 2002;33(9):2206-10. (In eng). DOI: 10.1161/01.str.0000026864.20339.cb.
106. Atchaneeyasakul K, Shang T, Haussen D, Ortiz G, Yavagal D. Impact of MRI Selection on Triage of Endovascular Therapy in Acute Ischemic Stroke: The MRI in Acute Management of Ischemic Stroke (MIAMIS) Registry. *Interv Neurol* 2020;8(2-6):135-143. (In eng). DOI: 10.1159/000490580.
107. Kang DW, Chalela JA, Dunn W, Warach S. MRI screening before standard tissue plasminogen activator therapy is feasible and safe. *Stroke* 2005;36(9):1939-43. (In eng). DOI: 10.1161/01.STR.0000177539.72071.f0.
108. Atchaneeyasakul K, Liebeskind DS, Jahan R, et al. Efficient Multimodal MRI Evaluation for Endovascular Thrombectomy of Anterior Circulation Large Vessel Occlusion. *J Stroke*

## References

---

- Cerebrovasc Dis 2020;29(12):105271. (In eng). DOI: 10.1016/j.jstrokecerebrovasdis.2020.105271.
109. JM UK-I, Trivedi RA, Graves MJ, et al. Utility of an ultrafast magnetic resonance imaging protocol in recent and semi-recent strokes. *J Neurol Neurosurg Psychiatry* 2005;76(7):1002-5. (In eng). DOI: 10.1136/jnnp.2004.046201.
110. Simonsen CZ, Madsen MH, Schmitz ML, Mikkelsen IK, Fisher M, Andersen G. Sensitivity of diffusion- and perfusion-weighted imaging for diagnosing acute ischemic stroke is 97.5%. *Stroke* 2015;46(1):98-101. (In eng). DOI: 10.1161/strokeaha.114.007107.
111. Huisman TA. Diffusion-weighted and diffusion tensor imaging of the brain, made easy. *Cancer Imaging* 2010;10 Spec no A(1a):S163-71. (In eng). DOI: 10.1102/1470-7330.2010.9023.
112. Thomalla G, Cheng B, Ebinger M, et al. DWI-FLAIR mismatch for the identification of patients with acute ischaemic stroke within 4-5 h of symptom onset (PRE-FLAIR): a multicentre observational study. *Lancet Neurol* 2011;10(11):978-86. (In eng). DOI: 10.1016/s1474-4422(11)70192-2.
113. Thomalla G, Simonsen CZ, Boutitie F, et al. MRI-Guided Thrombolysis for Stroke with Unknown Time of Onset. *N Engl J Med* 2018;379(7):611-622. DOI: 10.1056/NEJMoa1804355.
114. Naik D, Viswamitra S, Kumar AA, Srinath MG. Susceptibility weighted magnetic resonance imaging of brain: A multifaceted powerful sequence that adds to understanding of acute stroke. *Annals of Indian Academy of Neurology* 2014;17(1):58-61. (In eng). DOI: 10.4103/0972-2327.128555.
115. Flacke S, Urbach H, Keller E, et al. Middle cerebral artery (MCA) susceptibility sign at susceptibility-based perfusion MR imaging: clinical importance and comparison with hyperdense MCA sign at CT. *Radiology* 2000;215(2):476-82. (In eng). DOI: 10.1148/radiology.215.2.r00ma09476.
116. Rovira A, Orellana P, Alvarez-Sabín J, et al. Hyperacute ischemic stroke: middle cerebral artery susceptibility sign at echo-planar gradient-echo MR imaging. *Radiology* 2004;232(2):466-73. (In eng). DOI: 10.1148/radiol.2322030273.

## References

---

117. Chalela JA, Alsop DC, Gonzalez-Atavales JB, Maldjian JA, Kasner SE, Detre JA. Magnetic resonance perfusion imaging in acute ischemic stroke using continuous arterial spin labeling. *Stroke* 2000;31(3):680-7. (In eng). DOI: 10.1161/01.str.31.3.680.
118. Campbell BCV, Ma H, Ringleb PA, et al. Extending thrombolysis to 4.5-9 h and wake-up stroke using perfusion imaging: a systematic review and meta-analysis of individual patient data. *Lancet* 2019;394(10193):139-147. DOI: 10.1016/S0140-6736(19)31053-0.
119. Albers GW, Marks MP, Kemp S, et al. Thrombectomy for Stroke at 6 to 16 Hours with Selection by Perfusion Imaging. *N Engl J Med* 2018;378(8):708-718. DOI: 10.1056/NEJMoa1713973.
120. Thomalla G, Gerloff C. Acute imaging for evidence-based treatment of ischemic stroke. *Curr Opin Neurol* 2019;32(4):521-529. (In eng). DOI: 10.1097/wco.0000000000000716.
121. Thomalla G, Boutitie F, Ma H, et al. Intravenous alteplase for stroke with unknown time of onset guided by advanced imaging: systematic review and meta-analysis of individual patient data. *Lancet* 2020;396(10262):1574-1584. DOI: 10.1016/S0140-6736(20)32163-2.
122. Belani P, Kihira S, Pacheco F, Pawha P, Cruciata G, Nael K. Addition of arterial spin-labelled MR perfusion to conventional brain MRI: clinical experience in a retrospective cohort study. *BMJ Open* 2020;10(6):e036785. (In eng). DOI: 10.1136/bmjopen-2020-036785.
123. Nogueira RG, Jadhav AP, Haussen DC, et al. Thrombectomy 6 to 24 Hours after Stroke with a Mismatch between Deficit and Infarct. *N Engl J Med* 2018;378(1):11-21. DOI: 10.1056/NEJMoa1706442.
124. Ostergaard L, Jespersen SN, Engedahl T, et al. Capillary dysfunction: its detection and causative role in dementias and stroke. *Curr Neurol Neurosci Rep* 2015;15(6):37. DOI: 10.1007/s11910-015-0557-x.
125. Nielsen A, Hansen MB, Tietze A, Mouridsen K. Prediction of Tissue Outcome and Assessment of Treatment Effect in Acute

## References

---

- Ischemic Stroke Using Deep Learning. *Stroke* 2018;49(6):1394-1401. DOI: 10.1161/STROKEAHA.117.019740.
126. Angleys H, Østergaard L, Jespersen SN. The effects of capillary transit time heterogeneity (CTH) on brain oxygenation. *J Cereb Blood Flow Metab* 2015;35(5):806-17. (In eng). DOI: 10.1038/jcbfm.2014.254.
127. Jespersen SN, Ostergaard L. The roles of cerebral blood flow, capillary transit time heterogeneity, and oxygen tension in brain oxygenation and metabolism. *J Cereb Blood Flow Metab* 2012;32(2):264-77. DOI: 10.1038/jcbfm.2011.153.
128. Villringer A, Them A, Lindauer U, Einhüpl K, Dirnagl U. Capillary perfusion of the rat brain cortex. An in vivo confocal microscopy study. *Circ Res* 1994;75(1):55-62. (In eng). DOI: 10.1161/01.res.75.1.55.
129. Østergaard L. Blood flow, capillary transit times, and tissue oxygenation: the centennial of capillary recruitment. *J Appl Physiol (1985)* 2020;129(6):1413-1421. (In eng). DOI: 10.1152/jappphysiol.00537.2020.
130. Lassen NA. The luxury-perfusion syndrome and its possible relation to acute metabolic acidosis localised within the brain. *Lancet* 1966;2(7473):1113-5. (In eng). DOI: 10.1016/s0140-6736(66)92199-4.
131. Rasmussen PM, Jespersen SN, Østergaard L. The effects of transit time heterogeneity on brain oxygenation during rest and functional activation. *J Cereb Blood Flow Metab* 2015;35(3):432-42. (In eng). DOI: 10.1038/jcbfm.2014.213.
132. Iadecola C. Neurovascular regulation in the normal brain and in Alzheimer's disease. *Nat Rev Neurosci* 2004;5(5):347-60. (In eng). DOI: 10.1038/nrn1387.
133. Livne M, Boldsen JK, Mikkelsen IK, Fiebach JB, Sobesky J, Mouridsen K. Boosted Tree Model Reforms Multimodal Magnetic Resonance Imaging Infarct Prediction in Acute Stroke. *Stroke* 2018;49(4):912-918. DOI: 10.1161/STROKEAHA.117.019440.
134. Baron JC. Perfusion thresholds in human cerebral ischemia: historical perspective and therapeutic implications. *Cerebrovasc Dis* 2001;11 Suppl 1:2-8. (In eng). DOI: 10.1159/000049119.

## References

---

135. Lee J, GURSOY-OZDEMIR Y, FU B, BOAS DA, DALKARA T. Optical coherence tomography imaging of capillary reperfusion after ischemic stroke. *Appl Opt* 2016;55(33):9526-9531. (In eng). DOI: 10.1364/ao.55.009526.
136. Mouridsen K, Hansen MB, Ostergaard L, Jespersen SN. Reliable estimation of capillary transit time distributions using DSC-MRI. *J Cereb Blood Flow Metab* 2014;34(9):1511-21. DOI: 10.1038/jcbfm.2014.111.
137. Rorick MB, Nichols FT, Adams RJ. Transcranial Doppler correlation with angiography in detection of intracranial stenosis. *Stroke* 1994;25(10):1931-4. (In eng). DOI: 10.1161/01.str.25.10.1931.
138. Baron JC. Stroke research in the modern era: images versus dogmas. *Cerebrovasc Dis* 2005;20(3):154-63. (In eng). DOI: 10.1159/000087199.
139. Mountz JM. Nuclear medicine in the rehabilitative treatment evaluation in stroke recovery. Role of diaschisis resolution and cerebral reorganization. *Eura Medicophys* 2007;43(2):221-39. (In eng).
140. White P, Nanapragasam A. What is new in stroke imaging and intervention? *Clin Med (Lond)* 2018;18(Suppl 2):s13-s16. (In eng). DOI: 10.7861/clinmedicine.18-2-s13.
141. Scalzo F, Liebeskind DS. Perfusion Angiography in Acute Ischemic Stroke. *Comput Math Methods Med* 2016;2016:2478324. (In eng). DOI: 10.1155/2016/2478324.
142. Nguyen-Huynh MN, Wintermark M, English J, Lam J, Vittinghoff E, Smith WS, Johnston SC. How accurate is CT angiography in evaluating intracranial atherosclerotic disease? *Stroke* 2008;39(4):1184-8. (In eng). DOI: 10.1161/strokeaha.107.502906.
143. Kaufmann TJ, Huston J, 3rd, Mandrekar JN, Schleck CD, Thielen KR, Kallmes DF. Complications of diagnostic cerebral angiography: evaluation of 19,826 consecutive patients. *Radiology* 2007;243(3):812-9. (In eng). DOI: 10.1148/radiol.2433060536.
144. Lansberg MG, Lee J, Christensen S, et al. RAPID automated patient selection for reperfusion therapy: a pooled analysis of the Echoplanar Imaging Thrombolytic Evaluation Trial

## References

---

- (EPITHET) and the Diffusion and Perfusion Imaging Evaluation for Understanding Stroke Evolution (DEFUSE) Study. *Stroke* 2011;42(6):1608-1614. (In eng). DOI: 10.1161/STROKEAHA.110.609008.
145. Kasasbeh AS, Christensen S, Parsons MW, Campbell B, Albers GW, Lansberg MG. Artificial Neural Network Computer Tomography Perfusion Prediction of Ischemic Core. *Stroke* 2019;50(6):1578-1581. (In eng). DOI: 10.1161/strokeaha.118.022649.
146. Hamet P, Tremblay J. Artificial intelligence in medicine. *Metabolism* 2017;69s:S36-s40. (In eng). DOI: 10.1016/j.metabol.2017.01.011.
147. Copeland BJ. Artificial intelligence. *Britannica* 2021.
148. Hosch WL. Machine learning. *Britannica* 2021.
149. Zwass V. Neural Network. *Encyclopedia* 2020.
150. Anwar SM, Majid M, Qayyum A, Awais M, Alnowami M, Khan MK. Medical Image Analysis using Convolutional Neural Networks: A Review. *J Med Syst* 2018;42(11):226. (In eng). DOI: 10.1007/s10916-018-1088-1.
151. Singh SP, Wang L, Gupta S, Goli H, Padmanabhan P, Gulyás B. 3D Deep Learning on Medical Images: A Review. *Sensors (Basel)* 2020;20(18):5097. (In eng). DOI: 10.3390/s20185097.
152. Kemmling A, Flottmann F, Forkert ND, et al. Multivariate dynamic prediction of ischemic infarction and tissue salvage as a function of time and degree of recanalization. *J Cereb Blood Flow Metab* 2015;35(9):1397-405. (In eng). DOI: 10.1038/jcbfm.2015.144.
153. Qiu W, Kuang H, Ospel JM, Hill MD, Demchuk AM, Goyal M, Menon BK. Automated Prediction of Ischemic Brain Tissue Fate from Multiphase Computed Tomographic Angiography in Patients with Acute Ischemic Stroke Using Machine Learning. *J Stroke* 2021;23(2):234-243. (In eng). DOI: 10.5853/jos.2020.05064.
154. Schaefer PW, Grant PE, Gonzalez RG. Diffusion-weighted MR imaging of the brain. *Radiology* 2000;217(2):331-45. (In eng). DOI: 10.1148/radiology.217.2.r00nv24331.
155. Labeyrie MA, Turc G, Hess A, et al. Diffusion lesion reversal after thrombolysis: a MR correlate of early neurological

## References

---

- improvement. *Stroke* 2012;43(11):2986-91. (In eng). DOI: 10.1161/strokeaha.112.661009.
156. Lakomkin N, Pan J, Stein L, Malkani B, Dhamoon M, Mocco J. Diffusion MRI Reversibility in Ischemic Stroke Following Thrombolysis: A Meta-Analysis. *J Neuroimaging* 2020;30(4):471-476. (In eng). DOI: 10.1111/jon.12703.
157. Román LS, Menon BK, Blasco J, et al. Imaging features and safety and efficacy of endovascular stroke treatment: a meta-analysis of individual patient-level data. *Lancet Neurol* 2018;17(10):895-904. (In eng). DOI: 10.1016/s1474-4422(18)30242-4.
158. Cagnazzo F, Derraz I, Dargazanli C, et al. Mechanical thrombectomy in patients with acute ischemic stroke and ASPECTS  $\leq 6$ : a meta-analysis. *J Neurointerv Surg* 2020;12(4):350-355. (In eng). DOI: 10.1136/neurintsurg-2019-015237.
159. Bendszus M, Fiehler J, Subtil F, et al. Endovascular thrombectomy for acute ischaemic stroke with established large infarct: multicentre, open-label, randomised trial. *Lancet* 2023;402(10414):1753-1763. (In eng). DOI: 10.1016/s0140-6736(23)02032-9.
160. Sarraj A, Hassan AE, Abraham MG, et al. Trial of Endovascular Thrombectomy for Large Ischemic Strokes. *N Engl J Med* 2023;388(14):1259-1271. (In eng). DOI: 10.1056/NEJMoa2214403.
161. Boned S, Padroni M, Rubiera M, et al. Admission CT perfusion may overestimate initial infarct core: the ghost infarct core concept. *J Neurointerv Surg* 2017;9(1):66-69. (In eng). DOI: 10.1136/neurintsurg-2016-012494.
162. Lui YW, Tang ER, Allmendinger AM, Spektor V. Evaluation of CT perfusion in the setting of cerebral ischemia: patterns and pitfalls. *AJNR Am J Neuroradiol* 2010;31(9):1552-63. (In eng). DOI: 10.3174/ajnr.A2026.
163. Pulli B, Heit JJ, Wintermark M. Computed Tomography-Based Imaging Algorithms for Patient Selection in Acute Ischemic Stroke. *Neuroimaging Clin N Am* 2021;31(2):235-250. (In eng). DOI: 10.1016/j.nic.2020.12.002.

## References

---

164. Kuang H, Qiu W, Boers AM, et al. Computed Tomography Perfusion-Based Machine Learning Model Better Predicts Follow-Up Infarction in Patients With Acute Ischemic Stroke. *Stroke* 2021;52(1):223-231. (In eng). DOI: 10.1161/strokeaha.120.030092.
165. Alkadhi H, Euler A. The Future of Computed Tomography: Personalized, Functional, and Precise. *Invest Radiol* 2020;55(9):545-555. (In eng). DOI: 10.1097/rli.0000000000000668.
166. Soares BP, Tong E, Hom J, et al. Reperfusion is a more accurate predictor of follow-up infarct volume than recanalization: a proof of concept using CT in acute ischemic stroke patients. *Stroke* 2010;41(1):e34-40. (In eng). DOI: 10.1161/strokeaha.109.568766.
167. De Silva DA, Fink JN, Christensen S, et al. Assessing reperfusion and recanalization as markers of clinical outcomes after intravenous thrombolysis in the echoplanar imaging thrombolytic evaluation trial (EPITHET). *Stroke* 2009;40(8):2872-4. (In eng). DOI: 10.1161/strokeaha.108.543595.
168. del Zoppo GJ, Schmid-Schönbein GW, Mori E, Copeland BR, Chang CM. Polymorphonuclear leukocytes occlude capillaries following middle cerebral artery occlusion and reperfusion in baboons. *Stroke* 1991;22(10):1276-83. (In eng). DOI: 10.1161/01.str.22.10.1276.
169. Mujanovic A, Ng F, Meinel TR, et al. No-reflow phenomenon in stroke patients: A systematic literature review and meta-analysis of clinical data. *Int J Stroke* 2023:17474930231180434. (In eng). DOI: 10.1177/17474930231180434.
170. Ng FC, Churilov L, Yassi N, et al. Prevalence and Significance of Impaired Microvascular Tissue Reperfusion Despite Macrovascular Angiographic Reperfusion (No-Reflow). *Neurology* 2022;98(8):e790-e801. (In eng). DOI: 10.1212/wnl.00000000000013210.
171. Alexandrov AV, Hall CE, Labiche LA, Wojner AW, Grotta JC. Ischemic stunning of the brain: early recanalization without immediate clinical improvement in acute ischemic stroke.



## References

---

- Stroke 2004;35(2):449-52. DOI: 10.1161/01.STR.0000113737.58014.B4.
172. Albers GW, Thijs VN, Wechsler L, et al. Magnetic resonance imaging profiles predict clinical response to early reperfusion: the diffusion and perfusion imaging evaluation for understanding stroke evolution (DEFUSE) study. *Ann Neurol* 2006;60(5):508-17. (In eng). DOI: 10.1002/ana.20976.
173. Yemisci M, GURSOY-OZDEMIR Y, VURAL A, CAN A, TOPALKARA K, DALKARA T. Pericyte contraction induced by oxidative-nitrative stress impairs capillary reflow despite successful opening of an occluded cerebral artery. *Nat Med* 2009;15(9):1031-7. (In eng). DOI: 10.1038/nm.2022.
174. Hougaard KD, Hjort N, Zeidler D, et al. Remote ischemic preconditioning as an adjunct therapy to thrombolysis in patients with acute ischemic stroke: a randomized trial. *Stroke* 2014;45(1):159-67. DOI: 10.1161/STROKEAHA.113.001346.
175. Mollet I, Marto JP, Mendonça M, Baptista MV, Vieira HLA. Remote but not Distant: a Review on Experimental Models and Clinical Trials in Remote Ischemic Conditioning as Potential Therapy in Ischemic Stroke. *Mol Neurobiol* 2021:1-32. (In eng). DOI: 10.1007/s12035-021-02585-6.
176. National Institute for Health and Care Excellence (NICE). Stroke and transient ischaemic attack in over 16s: Diagnosis and initial management. NICE guideline. National Institute for Health and Care Excellence (UK). Copyright © NICE 2019.
177. Delgado Almandoz JE, Schaefer PW, Goldstein JN, Rosand J, Lev MH, González RG, Romero JM. Practical scoring system for the identification of patients with intracerebral hemorrhage at highest risk of harboring an underlying vascular etiology: the Secondary Intracerebral Hemorrhage Score. *AJNR Am J Neuroradiol* 2010;31(9):1653-60. (In eng). DOI: 10.3174/ajnr.A2156.
178. Röther J, Ford GA, Thijs VNS. Thrombolytics in Acute Ischaemic Stroke: Historical Perspective and Future Opportunities. *Cerebrovasc Dis* 2013;35(4):313-319. DOI: 10.1159/000348705.

## References

---

179. Group NIOndaSr-PSS. Tissue plasminogen activator for acute ischemic stroke. *N Engl J Med* 1995;333(24):1581-7. (In eng). DOI: 10.1056/nejm199512143332401.
180. Hacke W, Donnan G, Fieschi C, et al. Association of outcome with early stroke treatment: pooled analysis of ATLANTIS, ECASS, and NINDS rt-PA stroke trials. *Lancet* 2004;363(9411):768-74. DOI: 10.1016/S0140-6736(04)15692-4.
181. Campbell BC, Meretoja A, Donnan GA, Davis SM. Twenty-Year History of the Evolution of Stroke Thrombolysis With Intravenous Alteplase to Reduce Long-Term Disability. *Stroke* 2015;46(8):2341-6. (In eng). DOI: 10.1161/strokeaha.114.007564.
182. Wardlaw JM, Murray V, Berge E, del Zoppo GJ. Thrombolysis for acute ischaemic stroke. *Cochrane Database Syst Rev* 2014;2014(7):Cd000213. (In eng). DOI: 10.1002/14651858.CD000213.pub3.
183. Roth JM. Recombinant tissue plasminogen activator for the treatment of acute ischemic stroke. *Proc (Bayl Univ Med Cent)* 2011;24(3):257-9. (In eng). DOI: 10.1080/08998280.2011.11928729.
184. Hacke W, Kaste M, Bluhmki E, et al. Thrombolysis with Alteplase 3 to 4.5 Hours after Acute Ischemic Stroke. *N Engl J Med* 2008;359(13):1317-29. DOI: 10.1056/NEJMoa0804656.
185. Keyt BA, Paoni NF, Refino CJ, et al. A faster-acting and more potent form of tissue plasminogen activator. *Proc Natl Acad Sci U S A* 1994;91(9):3670-4. (In eng). DOI: 10.1073/pnas.91.9.3670.
186. Alamowitch S, Turc G, Palaiodimou L, et al. European Stroke Organisation (ESO) expedited recommendation on tenecteplase for acute ischaemic stroke. *Eur Stroke J* 2023;8(1):8-54. (In eng). DOI: 10.1177/23969873221150022.
187. Saqqur M, Uchino K, Demchuk AM, et al. Site of arterial occlusion identified by transcranial Doppler predicts the response to intravenous thrombolysis for stroke. *Stroke* 2007;38(3):948-54. (In eng). DOI: 10.1161/01.STR.0000257304.21967.ba.

## References

---

188. Lee KY, Han SW, Kim SH, et al. Early recanalization after intravenous administration of recombinant tissue plasminogen activator as assessed by pre- and post-thrombolytic angiography in acute ischemic stroke patients. *Stroke* 2007;38(1):192-3. (In eng). DOI: 10.1161/01.Str.0000251788.03914.00.
189. Marks MP, Olivot JM, Kemp S, et al. Patients with acute stroke treated with intravenous tPA 3-6 hours after stroke onset: correlations between MR angiography findings and perfusion- and diffusion-weighted imaging in the DEFUSE study. *Radiology* 2008;249(2):614-23. (In eng). DOI: 10.1148/radiol.2492071751.
190. Campbell BCV, Mitchell PJ, Churilov L, et al. Tenecteplase versus Alteplase before Thrombectomy for Ischemic Stroke. *N Engl J Med* 2018;378(17):1573-1582. (In eng). DOI: 10.1056/NEJMoa1716405.
191. Investigators PPST. The penumbra pivotal stroke trial: safety and effectiveness of a new generation of mechanical devices for clot removal in intracranial large vessel occlusive disease. *Stroke* 2009;40(8):2761-8. (In eng). DOI: 10.1161/strokeaha.108.544957.
192. Tarr R, Hsu D, Kulcsar Z, et al. The POST trial: initial post-market experience of the Penumbra system: revascularization of large vessel occlusion in acute ischemic stroke in the United States and Europe. *J Neurointerv Surg* 2018;10(Suppl 1):i35-i38. (In eng). DOI: 10.1136/jnis.2010.002600.rep.
193. Costalat V, Machi P, Lobotesis K, et al. Rescue, combined, and stand-alone thrombectomy in the management of large vessel occlusion stroke using the solitaire device: a prospective 50-patient single-center study: timing, safety, and efficacy. *Stroke* 2011;42(7):1929-35. (In eng). DOI: 10.1161/strokeaha.110.608976.
194. Menon BK, Goyal M. Thrombus aspiration or retrieval in acute ischaemic stroke. *Lancet* 2019;393(10175):962-963. (In eng). DOI: 10.1016/s0140-6736(19)30476-3.
195. Turk AS, 3rd, Siddiqui A, Fifi JT, et al. Aspiration thrombectomy versus stent retriever thrombectomy as first-line approach for large vessel occlusion (COMPASS): a multicentre, randomised, open label, blinded outcome, non-inferiority trial.

## References

---

- Lancet 2019;393(10175):998-1008. (In eng). DOI: 10.1016/s0140-6736(19)30297-1.
196. Martinez-Gutierrez JC, Leslie-Mazwi T, Chandra RV, et al. Number needed to treat: A primer for neurointerventionalists. *Interv Neuroradiol* 2019;25(6):613-618. (In eng). DOI: 10.1177/1591019919858733.
197. Wintermark M, Albers GW, Broderick JP, et al. Acute Stroke Imaging Research Roadmap II. *Stroke* 2013;44(9):2628-39. (In eng). DOI: 10.1161/strokeaha.113.002015.
198. Goyal M, Menon BK, van Zwam WH, et al. Endovascular thrombectomy after large-vessel ischaemic stroke: a meta-analysis of individual patient data from five randomised trials. *Lancet* 2016;387(10029):1723-31. (In eng). DOI: 10.1016/s0140-6736(16)00163-x.
199. Campbell BC, Mitchell PJ, Kleinig TJ, et al. Endovascular therapy for ischemic stroke with perfusion-imaging selection. *N Engl J Med* 2015;372(11):1009-18. DOI: 10.1056/NEJMoa1414792.
200. Saver JL, Goyal M, Bonafe A, et al. Stent-retriever thrombectomy after intravenous t-PA vs. t-PA alone in stroke. *N Engl J Med* 2015;372(24):2285-95. (In eng). DOI: 10.1056/NEJMoa1415061.
201. Jovin TG, Chamorro A, Cobo E, et al. Thrombectomy within 8 hours after symptom onset in ischemic stroke. *N Engl J Med* 2015;372(24):2296-306. (In eng). DOI: 10.1056/NEJMoa1503780.
202. Berkhemer OA, Fransen PS, Beumer D, et al. A randomized trial of intraarterial treatment for acute ischemic stroke. *N Engl J Med* 2015;372(1):11-20. (In eng). DOI: 10.1056/NEJMoa1411587.
203. Goyal M, Demchuk AM, Menon BK, et al. Randomized assessment of rapid endovascular treatment of ischemic stroke. *N Engl J Med* 2015;372(11):1019-30. (In eng). DOI: 10.1056/NEJMoa1414905.
204. Albers GW, Lansberg MG, Brown S, et al. Assessment of Optimal Patient Selection for Endovascular Thrombectomy Beyond 6 Hours After Symptom Onset: A Pooled Analysis of

## References

---

- the AURORA Database. *JAMA Neurol* 2021;78(9):1064-1071. (In eng). DOI: 10.1001/jamaneurol.2021.2319.
205. Langezaal LCM, van der Hoeven E, Mont'Alverne FJA, et al. Endovascular Therapy for Stroke Due to Basilar-Artery Occlusion. *N Engl J Med* 2021;384(20):1910-1920. (In eng). DOI: 10.1056/NEJMoa2030297.
206. Liu X, Dai Q, Ye R, et al. Endovascular treatment versus standard medical treatment for vertebrobasilar artery occlusion (BEST): an open-label, randomised controlled trial. *Lancet Neurol* 2020;19(2):115-122. (In eng). DOI: 10.1016/s1474-4422(19)30395-3.
207. Purushotham A, Campbell BC, Straka M, et al. Apparent diffusion coefficient threshold for delineation of ischemic core. *Int J Stroke* 2015;10(3):348-53. DOI: 10.1111/ij.s.12068.
208. Turc G, Tsivgoulis G, Audebert HJ, et al. European Stroke Organisation – European Society for Minimally Invasive Neurological Therapy expedited recommendation on indication for intravenous thrombolysis before mechanical thrombectomy in patients with acute ischaemic stroke and anterior circulation large vessel occlusion. *European Stroke Journal* 2022;7(1):I-XXVI. DOI: 10.1177/23969873221076968.
209. Sporns PB, Fiehler J, Ospel J, et al. Expanding indications for endovascular thrombectomy-how to leave no patient behind. *Ther Adv Neurol Disord* 2021;14:1756286421998905. (In eng). DOI: 10.1177/1756286421998905.
210. Findakly S, Maingard J, Phan K, et al. Endovascular clot retrieval for M2 segment middle cerebral artery occlusion: a systematic review and meta-analysis. *Intern Med J* 2020;50(5):530-541. (In eng). DOI: 10.1111/imj.14333.
211. Fifi JT, Yaeger K, Matsoukas S, Hassan AE, Yoo A, Sheth S, Zaidat OO. Aspiration thrombectomy of M2 middle cerebral artery occlusion to treat acute ischemic stroke: A core lab-adjudicated subset analysis from the COMPLETE registry and literature review. *Front Neurol* 2023;14:1076754. (In eng). DOI: 10.3389/fneur.2023.1076754.
212. Altenbernd J, Kuhnt O, Hennigs S, Hilker R, Loehr C. Frontline ADAPT therapy to treat patients with symptomatic M2 and M3 occlusions in acute ischemic stroke: initial experience with the

## References

---

- Penumbra ACE and 3MAX reperfusion system. *J Neurointerv Surg* 2018;10(5):434-439. (In eng). DOI: 10.1136/neurintsurg-2017-013233.
213. Millán M, Ramos-Pachón A, Dorado L, et al. Predictors of Functional Outcome After Thrombectomy in Patients With Prestroke Disability in Clinical Practice. *Stroke* 2022;53(3):845-854. (In eng). DOI: 10.1161/strokeaha.121.034960.
214. Goyal N, Tsivgoulis G, Malhotra K, et al. Medical Management vs Mechanical Thrombectomy for Mild Strokes: An International Multicenter Study and Systematic Review and Meta-analysis. *JAMA Neurol* 2020;77(1):16-24. (In eng). DOI: 10.1001/jamaneurol.2019.3112.
215. Sporns PB, Sträter R, Minnerup J, et al. Feasibility, Safety, and Outcome of Endovascular Recanalization in Childhood Stroke: The Save ChildS Study. *JAMA Neurol* 2020;77(1):25-34. (In eng). DOI: 10.1001/jamaneurol.2019.3403.
216. Sporns PB, Psychogios MN, Straeter R, et al. Clinical Diffusion Mismatch to Select Pediatric Patients for Embolectomy 6 to 24 Hours After Stroke: An Analysis of the Save ChildS Study. *Neurology* 2021;96(3):e343-e351. (In eng). DOI: 10.1212/wnl.00000000000011107.
217. Kwah LK, Diong J. National Institutes of Health Stroke Scale (NIHSS). *J Physiother* 2014;60(1):61. (In eng). DOI: 10.1016/j.jphys.2013.12.012.
218. Brott T, Adams HP, Jr., Olinger CP, et al. Measurements of acute cerebral infarction: a clinical examination scale. *Stroke* 1989;20(7):864-70. (In eng). DOI: 10.1161/01.str.20.7.864.
219. Goldstein LB, Samsa GP. Reliability of the National Institutes of Health Stroke Scale. Extension to non-neurologists in the context of a clinical trial. *Stroke* 1997;28(2):307-10. (In eng). DOI: 10.1161/01.str.28.2.307.
220. Meyer BC, Hemmen TM, Jackson CM, Lyden PD. Modified National Institutes of Health Stroke Scale for use in stroke clinical trials: prospective reliability and validity. *Stroke* 2002;33(5):1261-6. (In eng). DOI: 10.1161/01.str.0000015625.87603.a7.

## References

---

221. Harrison JK, McArthur KS, Quinn TJ. Assessment scales in stroke: clinimetric and clinical considerations. *Clin Interv Aging* 2013;8:201-11. (In eng). DOI: 10.2147/cia.S32405.
222. Yakhkind A, McTaggart RA, Jayaraman MV, Siket MS, Silver B, Yaghi S. Minor Stroke and Transient Ischemic Attack: Research and Practice. *Front Neurol* 2016;7:86-86. (In eng). DOI: 10.3389/fneur.2016.00086.
223. Lindsell CJ, Alwell K, Moomaw CJ, et al. Validity of a retrospective National Institutes of Health Stroke Scale scoring methodology in patients with severe stroke. *J Stroke Cerebrovasc Dis* 2005;14(6):281-3. (In eng). DOI: 10.1016/j.jstrokecerebrovasdis.2005.08.004.
224. Goldstein LB, Bertels C, Davis JN. Interrater reliability of the NIH stroke scale. *Arch Neurol* 1989;46(6):660-2. (In eng). DOI: 10.1001/archneur.1989.00520420080026.
225. Johnston KC, Wagner DP. Relationship between 3-month National Institutes of Health Stroke Scale score and dependence in ischemic stroke patients. *Neuroepidemiology* 2006;27(2):96-100. (In eng). DOI: 10.1159/000095245.
226. Boone M, Chillon JM, Garcia PY, Canaple S, Lamy C, Godefroy O, Bugnicourt JM. NIHSS and acute complications after anterior and posterior circulation strokes. *Ther Clin Risk Manag* 2012;8:87-93. (In eng). DOI: 10.2147/tcrm.S28569.
227. Martin-Schild S, Albright KC, Tanksley J, Pandav V, Jones EB, Grotta JC, Savitz SI. Zero on the NIHSS does not equal the absence of stroke. *Ann Emerg Med* 2011;57(1):42-5. (In eng). DOI: 10.1016/j.annemergmed.2010.06.564.
228. Woo D, Broderick JP, Kothari RU, et al. Does the National Institutes of Health Stroke Scale favor left hemisphere strokes? NINDS t-PA Stroke Study Group. *Stroke* 1999;30(11):2355-9. (In eng). DOI: 10.1161/01.str.30.11.2355.
229. Quinn TJ, Dawson J, Walters M. Dr John Rankin; his life, legacy and the 50th anniversary of the Rankin Stroke Scale. *Scott Med J* 2008;53(1):44-7. (In eng). DOI: 10.1258/rsmsmj.53.1.44.
230. Broderick JP, Adeoye O, Elm J. Evolution of the Modified Rankin Scale and Its Use in Future Stroke Trials. *Stroke*

## References

---

- 2017;48(7):2007-2012. (In eng). DOI: 10.1161/strokeaha.117.017866.
231. Farrell B, Godwin J, Richards S, Warlow C. The United Kingdom transient ischaemic attack (UK-TIA) aspirin trial: final results. *J Neurol Neurosurg Psychiatry* 1991;54(12):1044-54. (In eng). DOI: 10.1136/jnnp.54.12.1044.
232. van Swieten JC, Koudstaal PJ, Visser MC, Schouten HJ, van Gijn J. Interobserver agreement for the assessment of handicap in stroke patients. *Stroke* 1988;19(5):604-7. (In eng). DOI: 10.1161/01.str.19.5.604.
233. Leifer D, Bravata DM, Connors JJ, 3rd, et al. Metrics for measuring quality of care in comprehensive stroke centers: detailed follow-up to Brain Attack Coalition comprehensive stroke center recommendations: a statement for healthcare professionals from the American Heart Association/American Stroke Association. *Stroke* 2011;42(3):849-77. (In eng). DOI: 10.1161/STR.0b013e318208eb99.
234. Quinn TJ, Dawson J, Walters MR, Lees KR. Reliability of the modified Rankin Scale: a systematic review. *Stroke* 2009;40(10):3393-5. (In eng). DOI: 10.1161/strokeaha.109.557256.
235. de Haan R, Limburg M, Bossuyt P, van der Meulen J, Aaronson N. The clinical meaning of Rankin 'handicap' grades after stroke. *Stroke* 1995;26(11):2027-30. (In eng). DOI: 10.1161/01.str.26.11.2027.
236. McClelland G, Rodgers H, Flynn D, Price CI. The frequency, characteristics and aetiology of stroke mimic presentations: a narrative review. *Eur J Emerg Med* 2019;26(1):2-8. (In eng). DOI: 10.1097/mej.0000000000000550.
237. Burton TM, Luby M, Nadareishvili Z, Benson RT, Lynch JK, Latour LL, Hsia AW. Effects of increasing IV tPA-treated stroke mimic rates at CT-based centers on clinical outcomes. *Neurology* 2017;89(4):343-348. (In eng). DOI: 10.1212/wnl.00000000000004149.
238. Liberman AL, Liotta EM, Caprio FZ, Ruff I, Maas MB, Bernstein RA, Khare R, Bergman D, Prabhakaran S. Do efforts to decrease door-to-needle time risk increasing stroke mimic



## References

---

- treatment rates? *Neurol Clin Pract* 2015;5(3):247-252. DOI: 10.1212/CPJ.0000000000000122.
239. Goyal N, Male S, Al Wafai A, Bellamkonda S, Zand R. Cost burden of stroke mimics and transient ischemic attack after intravenous tissue plasminogen activator treatment. *J Stroke Cerebrovasc Dis* 2015;24(4):828-33. (In eng). DOI: 10.1016/j.jstrokecerebrovasdis.2014.11.023.
240. Willems LM, Kurka N, Bohmann F, Rostek P, Pfeilschifter W. Tools for your stroke team: adapting crew-resource management for acute stroke care. *Pract Neurol* 2019;19(1):36-42. (In eng). DOI: 10.1136/practneurol-2018-001966.
241. Brazil V. Translational simulation: not 'where?' but 'why?' A functional view of in situ simulation. *Adv Simul (Lond)* 2017;2:20. (In eng). DOI: 10.1186/s41077-017-0052-3.
242. Psychogios K, Tsiygoulis G. Intravenous thrombolysis for acute ischemic stroke: why not? *Curr Opin Neurol* 2022;35(1):10-17. (In eng). DOI: 10.1097/wco.0000000000001004.
243. Hacke W, Kaste M, Bluhmki E, et al. Thrombolysis with alteplase 3 to 4.5 hours after acute ischemic stroke. *N Engl J Med* 2008;359(13):1317-29. DOI: 10.1056/NEJMoa0804656.
244. Nickson CP, Petrosniak A, Barwick S, Brazil V. Translational simulation: from description to action. *Adv Simul (Lond)* 2021;6(1):6. (In eng). DOI: 10.1186/s41077-021-00160-6.
245. Zaidat OO, Yoo AJ, Khatri P, et al. Recommendations on angiographic revascularization grading standards for acute ischemic stroke: a consensus statement. *Stroke* 2013;44(9):2650-63. (In eng). DOI: 10.1161/strokeaha.113.001972.
246. Advani R, Naess H, Kurz MW. The golden hour of acute ischemic stroke. *Scand J Trauma Resusc Emerg Med* 2017;25(1):54. (In eng). DOI: 10.1186/s13049-017-0398-5.
247. Meretoja A, Keshtkaran M, Saver JL, et al. Stroke thrombolysis: save a minute, save a day. *Stroke* 2014;45(4):1053-8. (In eng). DOI: 10.1161/strokeaha.113.002910.
248. Mundiyanapurath S, Ringleb PA, Diatschuk S, et al. Capillary Transit Time Heterogeneity Is Associated with Modified Rankin Scale Score at Discharge in Patients with Bilateral High

## References

---

- Grade Internal Carotid Artery Stenosis. PLoS One 2016;11(6):e0158148. DOI: 10.1371/journal.pone.0158148.
249. Moulin S, Leys D. Stroke mimics and chameleons. *Curr Opin Neurol* 2019;32(1):54-59. DOI: 10.1097/WCO.0000000000000620.
250. Kvistad CE, Novotny V, Næss H, H, Hagberg G, Ihle-Hansen H, Waje-Andreassen U, Thomassen L, Logallo N. Safety and predictors of stroke mimics in The Norwegian Tenecteplase Stroke Trial (NOR-TEST). *Int J Stroke* 2019;14(5):508-16. DOI: 10.1177/1747493018790015.
251. Campbell BC, Mitchell PJ, Kleinig TJ, et al. Endovascular therapy for ischemic stroke with perfusion-imaging selection. *N Engl J Med* 2015;372(11):1009-18. (In eng). DOI: 10.1056/NEJMoa1414792.
252. Newman-Toker DE, Hsieh YH, Camargo CA, Jr., Pelletier AJ, Butchy GT, Edlow JA. Spectrum of dizziness visits to US emergency departments: cross-sectional analysis from a nationally representative sample. *Mayo Clin Proc* 2008;83(7):765-75. (In eng). DOI: 10.4065/83.7.765.
253. Royl G, Ploner CJ, Leithner C. Dizziness in the emergency room: diagnoses and misdiagnoses. *Eur Neurol* 2011;66(5):256-63. (In eng). DOI: 10.1159/000331046.
254. Edlow BL, Hurwitz S, Edlow JA. Diagnosis of DWI-negative acute ischemic stroke. *Neurology* 2017;89(3):256-62. DOI: 10.1212/wnl.00000000000004120.
255. Sarker IH. Deep Learning: A Comprehensive Overview on Techniques, Taxonomy, Applications and Research Directions. *SN Comput Sci.* 2021;2(6):420. DOI: 10.1007/s42979-021-00815-1.
256. Joskowicz L, Cohen D, Caplan N, Sosna J. Inter-observer variability of manual contour delineation of structures in CT. *Eur Radiol.* 2019;29(3):1391-1399. DOI: 10.1007/s00330-018-5695-5.
257. Mollura DJ, Culp MP, Pollack E, Battino G, Scheel JR, Mango VL, Elahi A, Schweitzer A, Dako F. Artificial Intelligence in Low- and Middle-Income Countries: Innovating Global Health Radiology. *Radiology.* 2020;297(3):513-520. DOI: 10.1148/radiol.2020201434.

### References

---

258. Bindra S, Jain R. Artificial intelligence in medical science: a review. *Ir J Med Sci.* 2023 Nov 12. doi: 10.1007/s11845-023-03570-9. Epub ahead of print. PMID: 37952245.
259. Geis JR, Brady AP, Wu CC, et al. Ethics of Artificial Intelligence in Radiology: Summary of the Joint European and North American Multisociety Statement. *J Am Coll Radiol.* 2019;16(11):1516-1521. DOI: 10.1016/j.jacr.2019.07.028.
260. Wang JZ, Pourang A, Burrall B. Open access medical journals: Benefits and challenges. *Clin Dermatol.* 2019;37(1):52-55. DOI: 10.1016/j.clindermatol.2018.09.010.
261. <https://www.forskningsradet.no/forskningspolitikk-strategi/apen-forskning/publikasjoner/>
262. <https://www.uis.no/sites/default/files/2023-11/Open%20access%20policy%20for%20the%20University%20of%20Stavanger.pdf>

## **Appendices**

***Paper I:*** Machine Learning Algorithms Versus Thresholding to Segment Ischemic Regions in Patients With Acute Ischemic Stroke.

***Paper II:*** Is the parametric calculation “transit time coefficient variation” capable of predicting tissue outcome in patients with acute ischemic stroke?

***Paper III:*** Simulation-based team-training in acute stroke: Is it safe to speed up?

# Machine Learning Algorithms Versus Thresholding to Segment Ischemic Regions in Patients With Acute Ischemic Stroke

Luca Tomasetti , Liv Jorunn Høllesli, Kjersti Engan , Senior Member, IEEE, Kathinka Dæhli Kurz , Martin Wilhelm Kurz, and Mahdiah Khanmohammadi

**Abstract**—Objective: Computed tomography (CT) scan is a fast and widely used modality for early assessment in patients with symptoms of a cerebral ischemic stroke. CT perfusion (CTP) is often added to the protocol and is used by radiologists for assessing the severity of the stroke. Standard parametric maps are calculated from the CTP datasets. Based on parametric value combinations, ischemic regions are separated into presumed infarct core (irreversibly damaged tissue) and penumbra (tissue-at-risk). Different thresholding approaches have been suggested to segment the parametric maps into these areas. The purpose of this study is to compare fully-automated methods based on machine learning and thresholding approaches to segment the hypoperfused regions in patients with ischemic stroke. **Methods:** We test two different architectures with three mainstream machine learning algorithms. We use parametric maps as input features, and manual annotations made by two expert neuroradiologists as ground truth. **Results:** The best results are produced with random forest (RF) and *Single-Step* approach; we achieve an average Dice coefficient of 0.68 and 0.26, respectively for penumbra and core, for the three groups analysed. We also achieve an average in volume difference of 25.1 ml for penumbra and 7.8 ml for core. **Conclusions:** Our best RF-based method outperforms the classical thresholding approaches, to segment both the ischemic regions in a group of patients regardless of the severity of vessel occlusion. **Significance:**

A correct visualization of the ischemic regions will guide treatment decisions better.

**Index Terms**—Computed tomography perfusion, Ischemic stroke, Machine learning, Thresholding.

## NOMENCLATURE

BT	Brain Tissue.
CBF	Cerebral blood flow.
CBV	Cerebral blood volume.
CNN	Convolutional Neural Network.
CT	Computed Tomography.
CTA	Computed Tomography Angiography.
CTP	Computed Tomography Perfusion.
DT	Decision Tree.
DWI	Diffusion-weighted Imaging.
LVO	Large Vessel Occlusion
MIP	Maximum Intensity Projection.
ML	Machine Learning.
MRI	Magnetic Resonance Imaging.
MTT	Mean transfer time.
NCCT	Non-contrast Computed Tomography.
NIHSS	National Institutes of Health Stroke Scale.
RF	Random Forest.
SLIC	Simple Linear Iterative Clustering.
SMOTE	Synthetic Minority Over-sampling Technique
SVM	Support Vector Machine
Non-LVO	Non-Large Vessel Occlusion.
T <sub>Max</sub>	Time-to-maximum
TTP	Time-to-peak.
WIS	Without Ischemic Stroke.

## I. INTRODUCTION

CEREBRAL stroke is the second leading cause of death and the third leading cause of disability worldwide [1]. Despite significantly reduced incidence over the past years in the entire world, the worldwide prevalence of cerebral stroke is estimated to be 17 million strokes causing 6.5 million deaths per year [1], [2]. In Norway, acute cerebral stroke is the third leading cause of death in adults and the leading cause of disability and admission to nursing homes [3], [4]. Changes in demography will result in a predicted 34% increase in stroke incidence in Europe between

Manuscript received February 25, 2021; revised June 17, 2021; accepted July 9, 2021. Date of publication July 16, 2021; date of current version February 4, 2022. This work was supported by the Regional Ethic Committee Project 2012/1499. (Luca Tomasetti, and Liv Jorunn Høllesli contributed equally to this work.) (Corresponding author: Luca Tomasetti.)

Luca Tomasetti, Kjersti Engan, and Mahdiah Khanmohammadi are with the Department of Electrical Engineering and Computer Science, University of Stavanger, 4021 Stavanger, Norway (e-mail: luca.tomasetti@uis.no; kjersti.engan@uis.no; mahdiah.khanmohammadi@uis.no).

Liv Jorunn Høllesli and Kathinka Dæhli Kurz are with the Department of Electrical Engineering and Computer Science, University of Stavanger, 4021 Stavanger, Norway, and also with the Stavanger Medical Imaging Laboratory (SMIL), Department of Radiology, Stavanger University Hospital, 4019 Stavanger, Norway (e-mail: liv.jorunn.hollesli@sus.no; kathinka.dehli.kurz@sus.no).

Martin Wilhelm Kurz is with the Neuroscience Research Group, Stavanger University Hospital, 4019 Stavanger, Norway and with the Department of Neurology, Stavanger University Hospital, 4019 Stavanger, Norway, and also with the Department of Clinical Medicine, University of Bergen, 5007 Bergen, Norway (e-mail: friedrich.martin.wilhelm.kurz@sus.no).

Digital Object Identifier 10.1109/JBHI.2021.3097591

2015 and 2035, which is likely to be mirrored in other parts of the world [2]. Thus, cerebral stroke has a huge socio-economic impact on society and a tremendous impact on the quality of life for every single patient [5].

There are two broad categories of cerebral stroke; hemorrhagic and ischemic stroke. Approximately 20% of all strokes are due to hemorrhage, while approximately 80% are due to ischemia [6]. Both groups can further be divided into different subtypes. Ischemic stroke may be caused by arteriosclerosis, thrombi, emboli, dissections, or systemic hypoperfusion, all of them leading to ischemia due to reduced blood flow in regions of the brain.

The severity of ischemia usually varies within the area of reduced blood flow, and for clinical use, the area is divided into two distinct regions: ischemic core and penumbra. The ischemic core is defined as irreversibly damaged brain tissue [7]. The tissue within the penumbra is critically hypoperfused and is located around and adjacent to the infarct core. If blood flow is restored timely, this tissue may regain neurological function [7]. If the blood flow remains low, however, the area of penumbra will transfer into an irreversibly damaged infarct core. The ischemic penumbra was introduced by Astrup *et al.* as “a region of hypoperfused, electrically silent, and functionally impaired but viable tissue” [8]. Restoring blood flow and thereby preventing the penumbra from proceeding to irreversibly damaged infarct core, is the main treatment goal in patients with acute ischemic stroke (AIS). Penumbra may change into infarct core rapidly in AIS patients. Therefore, rapid recognition of stroke symptoms and acute treatment in a stroke center are of vital importance.

According to the European Stroke Organization guidelines, Computed Tomography (CT) or Magnetic Resonance Imaging (MRI) are the two modalities recommended for diagnostic imaging in acute stroke patients [9]. MRI with diffusion-weighted imaging (DWI) is superior to Computed Tomography (CT) scans for detection of small acute infarctions and identification of some stroke mimics. Nevertheless, CT is the preferred imaging modality in many centers for acute stroke patients due to its widespread availability, rapid scan times, and its high sensitivity for detecting hemorrhage. DWI has been considered the gold standard for ischemic core estimation [10]–[14]; however, there are very few hospitals where MRI is used as the first imaging tool in acute stroke patients, since it is not always timely available on a 24/7 basis, plus, some patients have contraindications for this type of modality. MRI is usually performed within the first days after an AIS. Treatment, timing of treatment, and other variables will affect further development of the penumbra. Hence, any core of follow-up MRI might have developed after the acute imaging and might not be comparable with the imaging results in the acute setting. In the last years, DWI has been contested as the de-facto gold standard since it cannot accurately differentiate irreversibly ischemic tissue from salvageable tissue [15], [16], and it has been shown that the detected ischemic regions can be partially reverse, especially if DWI is performed in the early window time [16]–[18].

At Stavanger University Hospital (SUS), patients with suspected acute stroke are routinely investigated with non-contrast computed tomography (NCCT) of the head, CT angiography

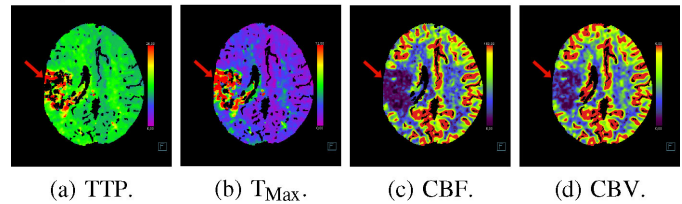


**Fig. 1.** Parametric maps of a single slice of a patient's brain. In this patient there is an ischemic area on the right side in the vascular territory of the middle cerebral artery (pointed by a red arrow). Time-to-peak (TTP) = time-to-peak; time-to-maximum ( $T_{Max}$ ) = time-to-maximum; Cerebral blood flow (CBF) = relative cerebral blood flow; Cerebral blood volume (CBV) = relative cerebral blood volume.

(CTA) of the precerebral and cerebral arteries, i.e. arch to vertex angiogram, and CT Perfusion (CTP) immediately after hospital admission. In most cases MRI including DWI is performed during the next days. In patients with suspected stroke with unknown time of symptom onset, MRI with DWI is used as a first-line diagnostic tool upon hospital admission.

Whether treatment is applied depends on time from symptom onset to hospital admission, but also largely depends on imaging results with CT Perfusion being the key-modality for patient selection. In CTP a time series of three-dimensional (3D) datasets are acquired during contrast agent injection. Based on the changes in the tissue density over time, color-coded parametric maps are calculated. The different parametric maps highlight spatio-temporal information from the passage of the contrast agent within the brain tissue. Generally, parametric maps based on CTP are generated in two steps: the first step acquires a time-density curve for each pixel based on the track of the contrast agent. The second step consists of extracting specific information from the generated time-density curves. Cerebral blood flow (CBF), cerebral blood volume (CBV), time-to-peak (TTP), mean transit time (MTT) and time-to-maximum ( $T_{Max}$ ) are all examples of parametric maps [7]. Radiologists use parametric maps for diagnosis and treatment planning and are indirectly assessing penumbra and core by evaluating such parametric maps. An example of the parametric maps of a single brain slice, involved in this study, is given in Fig. 1.

Time is a fundamental factor for patients affected by an ischemic stroke. Automation of the recognition process for the ischemic regions, penumbra and core, can be immensely helpful for medical doctors for treatment decisions. Over the last decades, different methods and parameters were tested to find the most suitable approach to segment the ischemic regions using parametric maps as input.

Region growing is a technique to extract connected areas in an image based on pixel information; this method is defined as semi-automatic because the user manually selects a seed for the growing region algorithm. This technique was used by Matesin *et al.* [19] in relation with CT head images of stroke lesions, and by Dastidar *et al.* [20], for measuring the volumetric infarction using 3D T2 Fast Spin Echo MRI in patients affected by stroke. Their goal was to delineate ischemic areas, and not to distinct the core from the penumbra. The first delineation of both areas, using a region growing technique in combination with the parametric

maps acquired by CTP analyses, was implemented by Contin *et al.* [21].

A series of studies have proposed experiments with threshold values on the derived parametric maps to improve the results achieved by the region's growing approaches. Different thresholds have been proposed for different parametric maps, generated from different vendors, and applied to various datasets [10]–[12], [22] to estimate both the ischemic regions, or the infarct core, or penumbra. These studies have used follow-up images (such as DWI or NCCT), acquired hours later after the stroke onset, to delineate the ground truth of the infarct regions and used them as a comparison for their predictions. For this reason, studies using DWI as follow-up imaging present some limitations: they only included patients who were later identified with infarct lesions in follow-up images, excluding the ones who underwent the same routine at the time of hospital admission but did not show any lesion in the follow-up DWI; they also excluded patients with contraindication for MRI. Moreover, since the threshold values were compared with final infarctions, assessed after the patient's treatment, they do not present a perfect estimation of the infarctions before treatment decision; thus, they are not the best candidates to help medical doctors during the treatment making decision. Furthermore, the studies have proposed quite distinct thresholding values due to the different vendors used for post-processing evaluation and the distinct window of time ( $\leq 1$  hour to 7 days) used for follow-up images to evaluate the ground truth for the ischemic regions. Thus, there is no real consensus to properly define the ischemic regions based on threshold values on the parametric maps derived from CTP.

In recent years, Machine Learning (ML) and neural network algorithms have achieved promising results in a large number of medical image analysis applications, and have also made their way into the stroke application [23]–[27]. Kemmling *et al.* proposed a generalized linear model using the parametric maps as input and clinical data to quantify changes of tissue infarction [23]. Qiu *et al.* implemented a ML-based algorithm to detect early infarction in patients with AIS using NCCT as input and follow-up DWI as ground truth [24]. Kasasbeh *et al.* used a semi-automatic approach based on a convolutional neural network (CNN) with the entire set of parametric maps as input to classify the infarct core using follow-up DWI as ground truth [26]. However, these ML and CNN based methods were only trained to classify the infarct core regions and did not find the penumbra areas. Differently, Qiu *et al.* developed two distinct ML models, using a multiphase CTA as input and DWI/NCCT follow-up images as ground truth, to predict core and penumbra [25]. Their primary goal was to demonstrate the validity of using multiphase CTA in comparison to CTP imaging for evaluating ischemic regions, but they stated limitations in their data material. Nevertheless, using follow-up images for delineating the ischemic regions limits the usability for medical doctors since they might not be helpful for treatment decisions but just for comparison with the clinical outcome. Our research group was, to the best of our knowledge, the first using the entire 4D CTP data as input to a neural network to segment both penumbra and core simultaneously. A modified U-Net model was used in a small pilot study to segment both penumbra and

core regions using the entire 4D CTP volume as input and with ground truth generated with manual expert assessment directly from the parametric maps [27]. The results were promising, but they were based on a very small pilot study and need to be validated on a larger sample size.

Before continuing to use the entire 4D dataset as input, we wish to study the utility of automatically segmenting the penumbra and core based on the parametric maps that are already calculated in the standard software used in clinical practice. Based on the ideas and the shortcomings of the published methods, we propose in this paper a ML-based method using the parametric maps as input and both core and penumbra regions as output, in addition to healthy tissue. One can argue that CNN naturally fits this type of problem; nevertheless, several examples of classical ML methods with this application can be found in the literature [23]–[25] using follow-up images as ground truth, bearing with them the same issues mentioned earlier. Moreover, learning good CNN models usually require large datasets, and/or transfer-learning, and we have a limited dataset to work with. Thus, we aim to properly understand if well-established ML models, less data-hungry and complex than CNN models, can help to predict both the ischemic regions and have the potential to assist medical doctors during treatment decisions. We give a comparison of the proposed method with different parameters and with thresholding methods from the literature. This paper contributes with the following:

- Proposing a fully-automatic ML-based algorithm to segment both penumbra *and* infarct core regions in patients affected by AIS, since a correct visualization of the salvageable tissue will guide treatment decision better,
- Using the parametric maps as input, due to their wide usage by medical doctors for early assessment of ischemic strokes,
- Training the models using a dataset with different groups of patients based on their level of vessel occlusion, generalizing the models and the training data and not restricting the type of patients that can be tested,
- Adopting as ground truth, images annotated by expert neuroradiologists directly from the parametric maps based on CTP,
- And finally, testing different ML algorithms and parameters to find the most suitable approach. Both a single-step approach, segmenting normal brain, penumbra, and core in one go; and a two-step approach, segmenting penumbra and core individually before combining them, were tested. This was further compared to thresholding approaches.

## II. DATA MATERIAL

### A. Dataset and Ground Truth

1) *Context:* Stavanger University Hospital (SUS) serves a population of 365.000. Close to 450 patients with AIS are annually admitted to the hospital. All consecutive patients with suspected AIS having received intravenous thrombolytic therapy are prospectively listed in a population-based database. Information about clinical severity measured by the National Institutes of

**TABLE I**  
PATIENT CHARACTERISTICS

		LVO	Non-LVO	WIS
Age (average/range)		72 (39-94) years	75 (41-94) years	60 (27-85) years
Gender	Male	49 (64%)	37 (62%)	8 (53%)
	Female	28 (36%)	23 (38%)	7 (47%)
NIHSS score (maximum /minimum /average)	On hospital admission	38/0/13	19/0/6	14/1/3
	On hospital discharge	25/0/5	10/0/2	1/0/0

Health Stroke Scale (NIHSS, scoring scale assessing neurological deficit) on admission, and at discharge are available. Long term functional outcome measured by the modified Rankin scale (mRS, scoring scale assessing long term functional outcome) at 90 days are also registered, in addition to mRS on hospital admission.

2) *Dataset*: The dataset in this study comprises CTP scans from 152 patients between January 2014 and August 2020. 137 of these patients had an AIS with visible perfusion deficit. Patients with AIS were divided into the following groups: 77 patients with large vessel occlusion (LVO), and 60 patients with non-large vessel occlusion (Non-LVO). Additionally, 15 patients without ischemic stroke (WIS) who were admitted with suspicion of stroke, but turned out not to have a stroke in the diagnostic workup, were included in the dataset. Age, gender, and NIHSS score for the groups are shown in [Table I](#).

LVO was defined using CT angiography; occlusion of the internal carotid artery, M1 and proximal M2 segment of the middle cerebral artery, A1 segment of the anterior cerebral artery, P1 segment of the posterior cerebral artery, basilar artery, and vertebral artery occlusion were regarded LVO. Non-LVO was defined as patients with perfusion deficits and affection of more distal arteries or with perfusion deficits without visible proximal artery occlusion.

3) *Ground Truth*: Ground truth images are manually annotated by two expert neuroradiologists. The manual annotations are done using the entire set of the CT examination including the parametric maps from the CTP (CBV, CBF, TTP,  $T_{Max}$ ), the maximum intensity projection (MIP) images, calculated as the maximum Hounsfield unit value over the time sequence of the CTP, providing a 3D volume from the 4D acquisition of CTP. Furthermore, the MRI examination performed within 1 to 3 days after the CT examination was used in assistance to generate the ground truth images. In-house developed software was used for the annotations.

## B. Imaging Protocol and Analysis

The CT scanners used for image acquisition were Siemens Somatom Definition Flash (installed in 2012) and a Siemens Somatom Definition Edge (installed in 2014), Erlangen, Germany.

Patients with suspected acute cerebral stroke with symptom onset within 4,5 hours prior to hospital admission were routinely investigated by NCCT of the head. If contraindications were excluded, intravenous thrombolysis bolus-dose was administered

**TABLE II**  
COMPUTED TOMOGRAPHY TECHNICAL PROTOCOL FOR ACUTE ISCHEMIC STROKE

	NCCT of the head	CTA of the cerebral arteries	CT perfusion
Patient position	Head first, supine	Head first, supine	Head first, supine
Spiral/sequence	Spiral	Spiral	Spiral
kV	120	100	80
mAs	280	160	200
Rotation time (s)	1	0.28	0.28
Slice collimation	3 mm c 20 x 0.6 mm	0.6 mm c 128 x 0.6 mm	5 mm c 32 x 1.2 mm
Pitch	0.55	1.0	-
X-care	Yes	No	No
IV contrast	No	60 ml Omnipaque 350 mg I/ml + 40 ml NaCl	40 ml Omnipaque 350 mg I/ml + 40 ml NaCl
Flow rate	-	5 ml/second	6 ml/second
Start delay	-	4 seconds	4 seconds, ≥60 seconds after CTA
Scan direction	Caudocranial		

**TABLE III**  
INFORMATION ABOUT THE DATASET AND THE THRESHOLD VALUE(S) OF THE VARIOUS RESEARCH METHOD ANALYZED

Article	Patients	NIHSS (mean)	Vendor	Stroke onset	Follow-up Images	Threshold	
						Penumbra	Core
Bathla <i>et al.</i> [28]	39	7	Siemens	N.A.	≤ 24h	$T_{Max} > 6s$	CBF < 20%
Wintermark <i>et al.</i> [11]	130	15.3	Philips	≤ 12h	≤ 7d	MTT > 145s	CBV ≤ 2.0ml/100g
Campbell <i>et al.</i> [12]	49	16.5	Philips	≤ 6h	≤ 1h	$T_{Max} > 6s$	CBF < 31% (with TTP > 4s)
Cereda <i>et al.</i> [10]	103	16	In-house	≤ 8h	≤ 3h	N.A.	CBF < 38% (with $T_{Max} > 4s$ )
Bivard <i>et al.</i> [13]	180	12	Toshiba	≤ 6h	≤ 24h	TTP > +5s	CBF < 30%
Murphy <i>et al.</i> [22]	25	15.1	General Electric	≤ 7h	N.A.	CBF ≤ 25ml/100g CBV ≤ 2.15ml/100g	CBF ≤ 13.3ml/100g CBV ≤ 1.12ml/100g
Schaefer <i>et al.</i> [14]	55	14	General Electric	≤ 9h	≤ 3h	N.A.	CBF ≤ 15% + CBV ≤ 30%

in the CT lab. Then CTA and CTP were performed. Technical details about the protocols are shown in [Table II](#). Further, the CTP images were analyzed using the software “syngo.via” from Siemens Healthineers with manufacturer default settings to generate color-coded parametric maps (CBF, CBV, TTP, MTT, and  $T_{Max}$ ).

## III. ISCHEMIC SEGMENTATION BY THRESHOLDING

Several studies define threshold values on some of the parametric calculations or on a combination of them to segment the ischemic stroke regions. The variability in the chosen thresholding value(s) is mainly due to the various vendors used for post-processing the parametric maps, the different definitions of the ground truth for the ischemic regions. It also lies in the decision of using the entire brain or just the ipsilesional hemisphere in statistical evaluations. [Table III](#) lists some of them in addition to information about their dataset, the number of patients, NIHSS score, time of stroke onset, vendor used, and their defined threshold values on different parametric maps. It also shows the different optimal thresholds that are proposed in each of these studies to segment either core, penumbra, or both.

Most of the listed studies evaluated their method by testing the mismatch between values from parametric maps derived from CTP images and the corresponding follow-up DWI, as the gold standard. The only study which did not use DWI as ground truth for the ischemic regions is Murphy *et al.* [22]. They defined the core region 5 to 7 days after the onset of stroke in the NCCT images, while the penumbra was the difference between the infarct and ischemic region. Nevertheless, they state that this difference “could lead to an underestimation of the final infarct size”. All the approaches displayed in [Table III](#), with differences in their



chosen parametric maps and the optimal values, demonstrate the lack of a consensus to define the ischemic regions based on thresholds.

Only the default setting used by “syngo.via” to define the ischemic regions after the parametric maps generation ( $CBF < 27$  ml/100 ml/min to define tissue at risk and  $CBV < 1.2$  ml/100 ml for non-viable tissue) and the thresholds proposed by Bathla *et al.* [28] were implemented for comparison with our best method due to the usage of the same vendor and software system as our input. We compare with a gold standard based on expert assessment of the parametric maps and manual delineation of the regions since these expert assessments are used normally for treatment decisions and are clinically relevant.

#### IV. MACHINE LEARNING APPROACHES

Applying ML algorithms in the field of medical image analysis is rapidly growing [29]. To train state-of-the-art ML models, patient data sets that have the necessary size and quality of samples are needed. Given that the patient data is protected by strict privacy and security rules this can be a challenge, however, if the necessary training set is available to train appropriate ML algorithms, good prediction models can be obtained. The ML models tested in this study include Support Vector Machine, Decision Tree learning, and Random Forest. Each ML algorithm uses in input a training set  $T = \{(x_1, y_1), \dots, (x_T, y_T)\}$ , composed of  $x_i$  features vectors and the relative  $y_i$  class label.

**Support Vector Machine (SVM)** is an algorithm used for binary classification that creates a line or a hyperplane, which separates the features from the input data into classes. In 1992, Boser *et al.* [30] proposed a supervised classification algorithm that has evolved into SVM as we know it today.

**Decision Tree learning (DT)**, firstly introduced by Breiman *et al.* [31], is an efficient classification technique that creates a tree-like structure by computing the relationship between independent features and a target. DT covers both binary and multi-class classification. The tree splits into branches by using conditions at each internal node and the end of the branch that does not split anymore is the decision (leaf).

**Random Forest (RF)** is a supervised learning algorithm and the “forest” consists of an ensemble of decision trees. To classify a new object from an input vector, the input vector is fed to each tree in the forest and each tree casts a unit vote for the most popular class at the input vector. Finally, the forest chooses the classification having the most votes. [32] proposed this algorithm to minimize a possible overfitting problem generated by the usage of a single DT [32].

#### V. PROPOSED METHOD

In this paper, we test a single and a two-step method for segmenting core and penumbra in patients suspected of AIS using machine learning based on the parametric maps (CBF, CBV, TTP, and  $T_{Max}$ ), derived from CTP datasets acquired at admission, the MIP map, and the NIHSS score. Various stages are performed during the proposed methods: (1) *Brain extraction and data imbalance*: extracting the brain tissue from

the parametric maps to use only the pixel values inside the brain as input features, (2) *SLIC*: obtaining the 3D superpixel version of the parametric maps (CBF, CBV,  $T_{Max}$ , and TTP), (3) *Machine Learning algorithm*: Feeding the features from the parametric maps and their generated superpixel to our implemented machine learning algorithms to predict the ischemic regions.

Fig. 2 shows the flowchart of our proposed methods. In the remainder of the paper, we call them **Single-Step** and **Two-Step** approaches. The features used for the proposed methods are the four parametric maps, the MIP map, and the NIHSS score. The input to the *Single-Step* method is all the aforementioned features (top part of Fig. 2) and it classifies both core and penumbra simultaneously. The *Single-Step* approach was tested with the DT and RF algorithms, but not with the SVM model since our implemented SVM model performs only binary classifications. In addition to the *Single-Step* method, we test another multi-stage classification method, which is simply adapted from the way neuroradiologists at SUS perform during the treatment decision process. The *Two-Step* approach is based on:

- Step1:** Takes as input the MIP, TTP, and  $T_{Max}$  maps, plus the NIHSS score; it performs a prediction of the penumbra region and outputs a binary image showing the predicted penumbra.
- Step2:** CBV and CBF parametric maps are used as input; it predicts the ischemic core resulting in a binary image.

#### A. Brain Extraction and Data Imbalance

We introduce a preprocessing step to extract the brain tissue from the whole image and work with pixels within the brain tissue (BT). In the remainder of the paper, the set of pixels belonging to the brain tissue for all patients  $p$  is called  $BT = \bigcup BT^p$ , while the various parametric maps are called  $CBF^p$ ,  $CBV^p$ ,  $TTP^p$ , and  $T_{Max}^p$ . This step helps to balance the classes inside the dataset. Moreover, we convert the pixel values into a [0,1] interval for each input feature based on the color bar on the right of each corresponding parametric map. Each input feature is mapped with the corresponding color in the bar and transformed into a value in the [0,1] interval, where the value 0 corresponds to the bottom value in the bar, while the value 1 indicates the top value. This was performed to reduce each input feature into a single value instead of keeping all three color channels.

#### B. Superpixel (SLIC)

A modified version of the Simple Linear Iterative Clustering (SLIC) algorithm [33] is employed to generate superpixel regions in the parametric maps. The regions are based on the initial segmentation of the intensity values of the maps. Using SLIC, we stacked each slice to obtain a 3D superpixel version for each parametric map and used it as extra features as input to the model. These new features should help the models to consider the adjacent pixels along the third dimension (z-axis). In the remainder of the paper, the superpixel version of the parametric maps for a patient  $p$  are called:  $CBF_{SLIC}^p$ ,  $CBV_{SLIC}^p$ ,  $TTP_{SLIC}^p$ , and  $T_{Max}_{SLIC}^p$ . SLIC generates superpixel regions by clustering pixels utilizing their proximity and similarity in the image plane. An example of a normalized TTP map from one of the

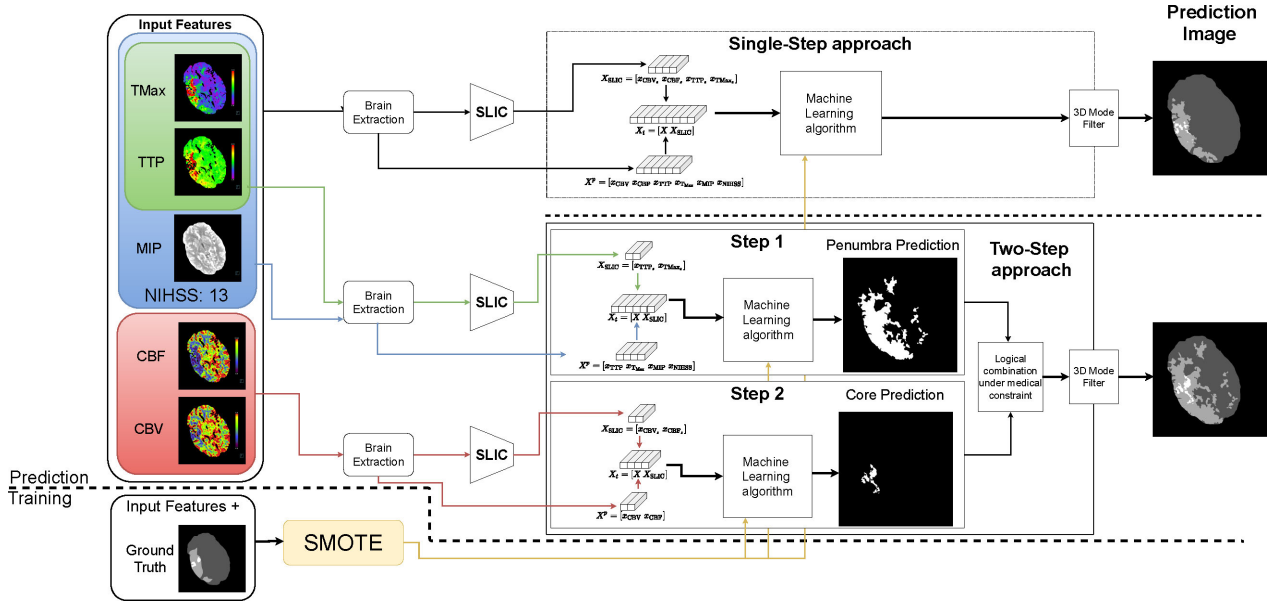


**Fig. 2.** Visual description of the proposed multi-classification methods: for the *Single-Step* approach, all the parametric maps are adopted as input features for the Machine Learning (ML) algorithm to generate a final prediction image. The *Two-Step* approach works in a different way: Step1 takes in input six features for each pixel inside the brain and generates a binary map to classify the penumbra region(s) in a brain slice; Step2 takes in input 4 features, for each pixel, from different parametric maps and returns as output a binary map containing the predicted core region(s) if any. The final prediction combines the two binary maps only including the core regions that are inside the penumbra regions. A final post-processing step using a 3D mode filter is implemented. Simple Linear Iterative Clustering (SLIC) refers to the algorithm to extract superpixel regions.

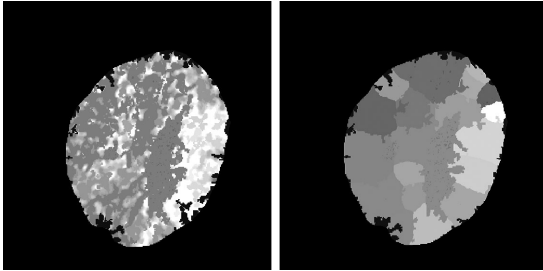


**Fig. 3.** Visual comparison of a TTP map in grayscale (left) and the generated superpixel image (right) after the brain extraction.

patients analyzed and the generated superpixel image is given in **Fig. 3**.

### C. Machine Learning for Core and Penumbra

We implement three mainstream classical ML methods including, support vector machines, decision tree, and random forest. To the best of our knowledge, there exists no defined convention on which of the parametric maps should be used to detect core and which shows penumbra better. Let  $L^p$  be the number of pixels in  $BT^p$ . In the training phase, the totality of input features to these ML approaches are defined as a matrix. For a patient  $p$ , let the input features vector for CBV be:

$$x_{CBV}^p = \text{stack}(\text{CBV}^p(i, j))_{\forall(i, j) \in BT^p}$$

where  $x_{CBV}^p$  is a vector of size  $L^p$ . The stack function concatenates all the pixels in an image, row-by-row, into a vector. The

input features totality of the parametric maps for a patient  $p$  is given by the matrix  $X^p$ . For simplicity we omit the  $p$  in the following notation where all definition are on a single patient:

$$X = [x_{CBV} \ x_{CBF} \ x_{TTP} \ x_{T_{Max}} \ x_{MIP} \ x_{NIHSS}]$$

Defining  $[1]$  as a all-ones vector of length  $L^p$ ,  $x_{NIHSS}$  is defined as  $x_{NIHSS} = \text{NIHSS} \cdot [1]$ . In the same way, the input features totality for the superpixel version of the parametric maps is given by the matrix  $X_{SLIC}^p$ , defined as:

$$X_{SLIC} = [x_{CBV_s} \ x_{CBF_s} \ x_{TTP_s} \ x_{T_{Max_s}}]$$

where  $x_{CBV_s}$  is represented as a vector:

$$x_{CBV_s} = \text{stack}(\text{CBV}_{SLIC}^p(i, j))_{\forall(i, j) \in BT^p}$$

The total matrix  $X_T$  is given by the combination of the two input features matrices depending on the model trained:  $X_T = [X \ X_{SLIC}]$ .

In the prediction phase, as shown in **Fig. 2**, the input features matrix  $X^p$  used for Step1 has 6 columns since the CBV and CBF parametric maps are excluded. Then, the model generates a binary map for the penumbra region over the entire image. Subsequently, the input feature matrix for the second step is derived only from CBV and CBF parametric maps plus their corresponding superpixel versions. This matrix has 4 columns as illustrated in **Fig. 2**. The selection of parametric maps is also in line with proposed methods in the literature [12]–[14] since TTP and  $T_{Max}$  are often used for detecting penumbra, while the other parametric maps are used for segmenting core regions.

**TABLE IV**  
DIVISION IN TRAINING, VALIDATION, AND HOLDOUT DATASET

	Training (#; %)	Validation (#; %)	Holdout (#; %)	Tot. (#; %)
LVO	29; 37.7	29; 37.7	19; 24.6	77; 50.6
Non-LVO	24; 40	25; 41.7	11; 18.3	60; 30.5
WIS	6; 40	6; 40	3; 20	15; 9.8
<b>Total</b>	<b>59; 38.8</b>	<b>60; 39.5</b>	<b>33; 21.7</b>	<b>152; 100</b>

To create the final prediction image, in the *Two-Step* approach, the binary predictions of core and penumbra are logically combined so the common white areas in both predictions indicate ischemic core in the final result. The logical AND combination simulate the medical constraint, where the ischemic core is limited to be inside the penumbra since the hypoperfused tissue always contains the dead tissue. For both the approaches (*Single-Step* and *Two-Step*), the patient's predictions pass through a 3D mode filter. This post-processing step helps to reduce unwanted noise and it also allows the predictions from a ML method to rely on the adjacent voxels in the z-axis, i.e. between adjacent slices.

## VI. EXPERIMENTS AND RESULTS

### A. Dataset Division

In this paper data from 152 patients were used, 137 from AIS patients divided into two groups (LVO and Non-LVO) and 15 patients WIS but who were admitted with suspicion of stroke. The dataset was randomly split into a training, validation, and holdout set, as described in [Table IV](#), carefully dividing the LVO, Non-LVO, and WIS patients over the sets. The idea behind this division is to create a model that generalizes the classification of the ischemic regions working for all.

As many have reported, DWI is a questionable measure to describe the ischemic core [10], [15]–[18], thus we propose to use manual annotations made by two expert neuroradiologists as the golden ground truth to assess both the ischemic regions during early stages and with different level of severity.

Even with removing the background and only considering the pixels inside the BT, the core and penumbra classes are still undersampled, leading to a class imbalance problem in the dataset. To overcome this problem, during the training phase we implement the Synthetic Minority Over-sampling Technique (SMOTE) algorithm [34] to over-sample the classes with a minor number of occurrences. SMOTE relies on the generation of synthetic examples on the difference between the feature vector under construction and its nearest neighbor. We over-sample the penumbra by a maximum of 5 times its standard amount and the core by a maximum of 20 times. These maximum values were chosen for their class importance and amounts. Before applying the SMOTE algorithm, the core and penumbra classes represent only 0.5% and 9.4% of the entire set respectively. After the application of the algorithm, they represent 7.6% and 36.5% of the dataset respectively.

### B. Evaluation Metrics

In all the experiments the predictions are compared with the ground truth and multi-class confusion matrices are

**TABLE V**  
EXAMPLE OF MULTI-CLASS CONFUSION MATRIX FOR THE CORE CLASS.  
TP = TRUE POSITIVE, FP = FALSE POSITIVE, FN = FALSE NEGATIVE, AND  
TN = TRUE NEGATIVE

		Predicted class		
		Core	Penumbra	Healthy Brain
Actual class	Core	TP <sub>c</sub>	FN <sub>c</sub>	FN <sub>c</sub>
	Penumbra	FP <sub>c</sub>	TN <sub>c</sub>	TN <sub>c</sub>
	Healthy Brain	FP <sub>c</sub>	TN <sub>c</sub>	TN <sub>c</sub>

generated. Our dataset is composed of three classes  $\mathbf{C} \in \{\text{core, penumbra, healthy brain}\}$ .

[Table V](#) presents a multi-class confusion matrix example for the core class: TP<sub>c</sub> (True Positive) indicates the number of pixels predicted correctly as the core; FP<sub>c</sub> (False Positive) represents the number of pixels classified as core class but belonging to a different class; FN<sub>c</sub> (False Negative) is the number of pixels predicted as a different class but labeled as the core in a ground truth image; TN<sub>c</sub> (True Negative) displays the number of pixels that are classified as not core and belonging to one of the other classes. All the values in each multi-class confusion matrix are calculated based only on the number of voxels inside the BT, excluding all non-brain tissue voxels as the binary mask of brain vs background is found during pre-processing. From each confusion matrix of class  $c \in \mathbf{C}$ , we calculate the recall  $\text{rec}_c = \frac{\text{TP}_c}{\text{TP}_c + \text{FN}_c}$ , the precision  $\text{prec}_c = \frac{\text{TP}_c}{\text{TP}_c + \text{FP}_c}$ , and the Dice coefficient (equivalent to the F1-score)  $\text{Dice}_c = \frac{2 \cdot \text{prec}_c \cdot \text{rec}_c}{\text{prec}_c + \text{rec}_c} = \frac{2 \cdot \text{TP}_c}{2 \cdot \text{TP}_c + \text{FP}_c + \text{FN}_c}$ . The range for these values is [0,1]. We also consider the Hausdorff distance between predictions and ground truth regions [35], and the absolute difference in the volume among the predictions ( $V_p$  [ml]) and the ground truth ( $V_g$  [ml]):  $\Delta V = |V_g - V_p|$ . The range value for the Hausdorff distance and  $\Delta V$  is  $[0, \infty]$  Bland-Altman plots were used to illustrate mean differences and limit of agreement between predicted volume and volume calculated from ground truth images.

### C. Hyper-Parameter Optimization of ML Algorithms

Before evaluating our methods, a series of hyper-parameter optimizations on the ML algorithms were performed using a Bayesian optimization. The input features for these optimizations, for a patient  $p$ , were solely based on  $X^p$ , without the usage of SLIC nor SMOTE algorithms. For DT and RF models, the hyper-parameters taken into consideration during the optimization were:

- the minimum number of leaf, with a range  $[1, L^p/2]$ ,
- the maximum number of decision splits, in the range  $[1, L^p - 1]$ ,
- Gini's diversity index, Twoing rule, and Cross-entropy for the split criterion to use,
- the number of decision trees in the model (1 for the DT algorithm, a range of  $[1, 500]$  for the RF).

Differently, for the SVM model, we considered the following:

- Gaussian, Linear, and Polynomial kernel functions,
- the maximum penalty on the observations with a range of  $[0.001, 1000]$ ,
- standardized vs not standardized features.

TABLE VI

OPTIMAL HYPER-PARAMETERS FOR THE DECISION TREE (DT) AND RANDOM FOREST (RF) ALGORITHMS DIVIDED BY *SINGLE-STEP* AND *TWO-STEP* APPROACHES

Method		# DT	Split criterion	Min # Leaf	Max # Split	
DT	<i>Single-Step</i>	1	Cross-entropy	138	22489	
	<i>Two-Step</i>		Step1	Cross-entropy	153	358000
			Step2	Cross-entropy	10	34427
RF	<i>Single-Step</i>	4	Gini	345	5535	
	<i>Two-Step</i>	Step1	Cross-entropy	384	1400500	
		Step2	10	Gini	2	20979

TABLE VII

OPTIMAL HYPER-PARAMETERS FOR THE SUPPORT VECTOR MACHINE (SVM) MODEL WITH THE *TWO-STEP* APPROACH

Method		Kernel Function	Max penalty	Standardize
SVM	<i>Two-Step</i>	Step1	Gaussian	993.73
		Step2	Gaussian	0.487

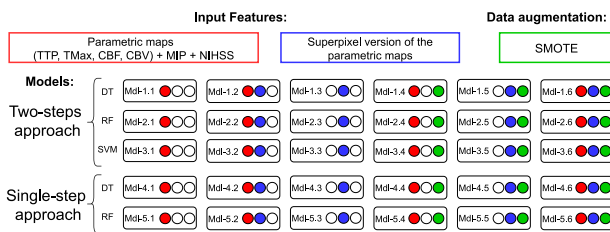


Fig. 4. Description of the models implemented to test the two approaches, the input features used (the parametric maps with or without the superpixel regions), the usage of data augmentation (SMOTE). Filled circle corresponds to including the corresponding input/augmentation box. Experiments' names are included in the reminder of the paper. DT = Decision Tree; RF = Random Forest; SVM = Support Vector Machine.

The values display in Table VI show the best hyper-parameters for the DT and RF algorithms divided by *Single-Step* and *Two-Step* approaches, after an exhaustive set of experiments. Table VII presents the optimal hyper-parameters for the SVM model. All the experiments described in the next sections use the same set of hyper-parameters defined in Table VI and Table VII.

#### D. Experiment 1 - ML Algorithms and Feature Combination

For both the *Two-Step* and the *Single-Step* approaches, a series of six experiments were conducted to determine whether the inclusion of superpixels as extra features is beneficial and to see if using SMOTE to balance the classes during training gives better models. These six experiments were repeated for the different ML algorithms except SVM for *Single-Step* approach, due to our implementation of the approach which performs only binary classification.

Fig. 4 illustrates the 30 conducted experiments: (*Two-Step* × 3 ML algorithms) × 6 + (*Single-Step* × 2 ML algorithms) × 6. The number of superpixel regions used for this set of experiments is 10. Fig. 5 shows the results for all models during the first experiment set taking into account all the various groups (LVO, Non-LVO, and WIS) together. The best model was selected mainly based on the averaging metrics in Fig. 5 for both the

classes. Looking at Fig. 5, *Mdl-5.1* shows the best performances both for core and penumbra regardless of the group. Nevertheless, *Mdl-5.2* offers comparable results to *Mdl-5.1* in the majority of the metrics. Moreover, *Mdl-5.2* uses the superpixel regions as input features, on the contrary of *Mdl-5.1*, and the best number of superpixel regions should be investigated further.

#### E. Experiment 2 - Number of Superpixels

After the first experiment set, we performed a series of empirical analyses on *Mdl-5.2* to choose the most adequate number of superpixel regions for the SLIC algorithm that produces the best results. We repeat a series of experiments using the *Mdl-5.2* starting with 25 total number of 3D superpixel regions and continue by increasing the number until 600. The increment is 25 for each iteration. Fig. 6 presents the results obtained with different numbers of superpixel regions including 10 and also the total number of pixels in the image for *Mdl-5.2*. Fig. 6 shows the average metrics for the LVO and Non-LVO groups, and the average for the entire validation set (LVO, Non-LVO, and WIS). The combination of statistical metrics for both penumbra and core classes shows a clear difference when superpixel is used as shown in Fig. 6. As highlighted in the figure, 100 superpixel regions give slightly better results compared to the others. It is noticeable that 100 superpixel regions yield the lowest volume difference for the penumbra class, which highly influenced the selection decision, the highest Dice coefficient for the core class on average, and significant results for the other metrics, and as such we propose to use 100 in further experiments.

#### F. Experiment 3 - Validate the Superpixel Result

The chosen number of superpixels, 100, was validated by repeating all the thirty experiments described in Fig. 4 and using 100 superpixel regions instead of 10 regions, which was used during the first evaluation round. Due to ineffective performance, SVM has been exempt from this validation step. Results are depicted in Fig. 7 showing the overall metrics for both the two ischemic regions. The model *Mdl-5.2* still shows the most promising results even compared with *Mdl-5.1*. It achieves the highest Dice coefficient and precision values for both the classes, and excellent  $\Delta V$  results.

#### G. Hyper-Parameter Optimization on the Best Model

The selected *Mdl-5.2* model went under a final step of performing optimization of its hyper-parameters with the current setting (100 superpixel regions) validated in the previous experiment set. We have taken into consideration the same hyper-parameters defined in Sec. VI-C for RF. The new optimal hyper-parameters for *Mdl-5.2* are 48 number of DT, cross-entropy as the selected split criterion, 68982 as the maximum number of decision splits, and 315 as the minimum number of leaves.

#### H. Final Test of the Best Model

We test the holdout set proposing *Mdl-5.2* as the best model, 100 as the most efficient number of superpixel regions, with the hyper-parameters defined in Sec. VI-G. A visual result of

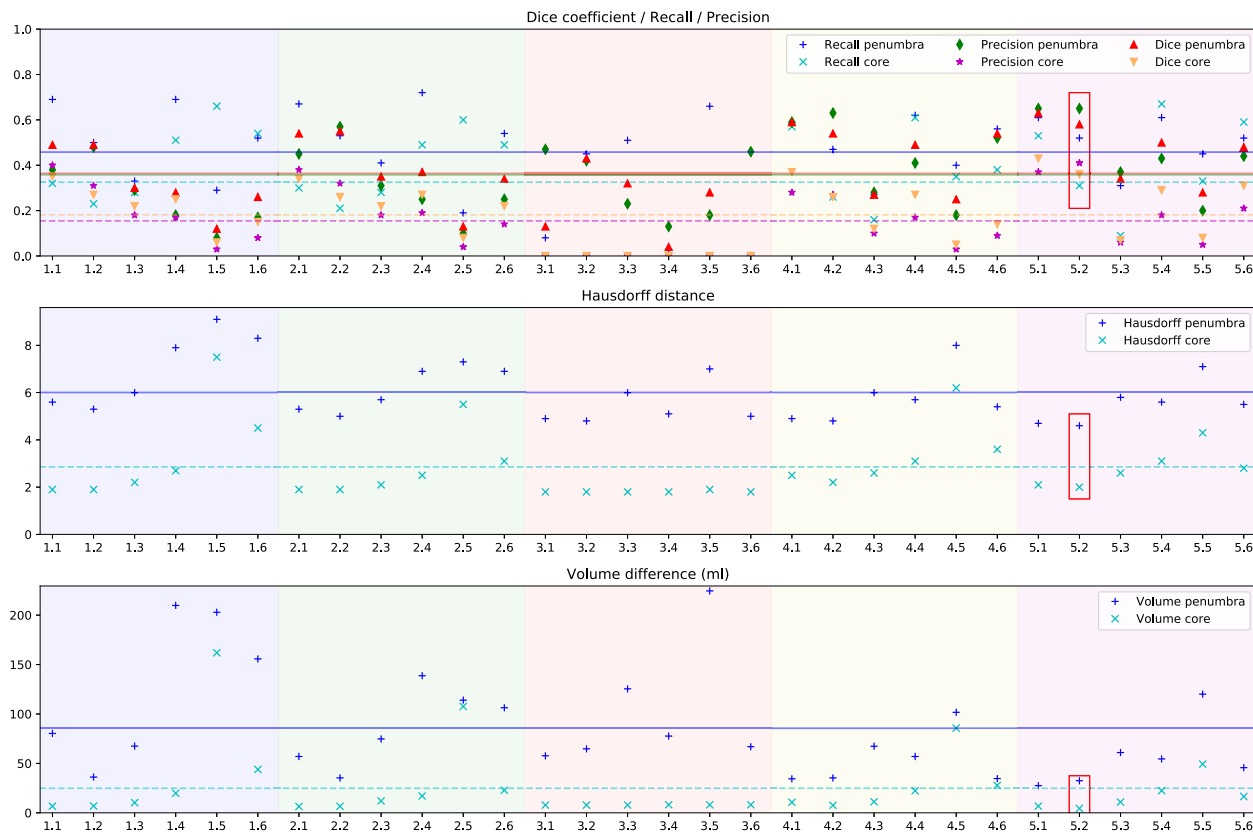


**Fig. 5.** Results generated with the validation set on the 30 experiments described in Fig. 4. The  $x$ -axis contains the experiment IDs, while the  $y$ -axis refers to the statistic values. Each value represents the average of the patients in the validation set, including all the different severities. Note that for the top subplot we want high values, but for the mid and bottom subplots we want low values. All the experiments were tested with a number of superpixel regions equal to 10. The colored regions in the plot represent the division of the various experiments: blue, green, and red contain the experiments with the two steps approach using DT, RF, and SVM models respectively; yellow and purple have the experiments for DT and RF with the *Single-Step* approach. The colored horizontal lines display the average for the corresponding statistical measures. Solid lines are used for penumbra and dashed for core average measures, top image in order (solid) recall, Dice, precision; (dashed) recall, Dice, precision. With the only exception of *Mdl-5.1*, *Mdl-5.2* (inside a red rectangle) is the one that presents the best tradeoff for all the evaluation metrics among the set of experiments.

two sample predicted images along with ground truth and their corresponding parametric maps are shown in Fig. 8.

Furthermore, we remove the post-processing step (3D mode filter) and predict the regions to understand how the results are influenced by this step. Table VIII presents the results of the proposed best model, i.e. the *Single-Step* method with RF, *Mdl-5.2*, and 100 as the number of superpixels, in comparison with the same model without any post-processing step, the “syngo.via” default setting to define the ischemic regions, and the thresholding values proposed by Bathla *et al.* [28], since it is, to the best of our knowledge, the only research using “syngo.via” as vendor. Table VIII also depicts reported results from other thresholding methods ([11]–[13], [22]) which used other vendors for parametric maps acquisition and post-processing steps, thus a direct comparison with our model is not possible. Bland-Altman plots are used to visualize the predicted volume in comparison with the ground truth volume between the four methods compared in Table VIII, shown in Fig. 9. For all rows, the statistical results are based solely on our holdout set to establish fair comparability with the other approaches. The results for two subsets of the data (LVO, Non-LVO) are presented separately, while for the WIS subset only  $\Delta V$  is displayed.

### Inter-observer variability

33 randomly selected patients (19 from the LVO subset, 11 from the Non-LVO subset, and 3 from the WIS group) were manually annotated by two different neuroradiologists, using the same criteria adopted for the creation of the ground truth images. The aim is to understand the inter-observer variability between two neuroradiologists. We investigate the inter-observer variability and compare it with the metrics of the automated method. Table VIII shows the inter-observer variability in the measurements of the ischemic regions for the two subsets of the data, LVO and Non-LVO, in comparison with the results achieved with our best method *Mdl-5.2*.

## VII. DISCUSSION

We have proposed a multi-stage algorithm based on ML that automatically classifies ischemic core and penumbra regions in parametric maps generated from CTP images. The CTP scans were acquired from patients with AIS and WIS. In a real-life situation, medical doctors need to decide the treatment for a patient in a small time window; thus, an automatic approach can be valuable. Expert assessments used as ground truth are

TABLE VIII

PATIENTS INCLUDED IN THIS TABLE ARE ALL PART OF THE HOLDOUT SET. THE RESULTS ARE PRESENTED FOR PENUMBRA (CORE) REGIONS. COMPARISON BETWEEN VARIOUS RESEARCHES USING THRESHOLDING VALUES WITH THE SAME VENDOR "SYNGO.VIA" (DEFAULT SETTING AND [28]) AND OUR BEST MODEL (*Mdl-5.2*). PREDICTIONS FROM [11]–[13], [22] ARE PRESENTED BUT THEY ARE NOT FOR COMPARISON DUE TO THE USAGE OF DIFFERENT VENDOR AND/OR POST-PROCESSING STEPS FOR GENERATING PARAMETRIC MAPS. ‡ MARKS THE RESULTS FOR THE *Mdl-5.2* METHOD WITHOUT USING ANY POST-PROCESSING STEP. INTER-OBSERVER VARIABILITY FOR TWO EXPERT NEURORADIOLOGISTS ( $NR_1$ ,  $NR_2$ ) AND THE SELECTED MODEL *Mdl-5.2* IS ALSO PRESENTED. NOTE THAT FOR THE DICE COEFFICIENT HIGHER VALUES ARE BETTER ( $\uparrow$ ), WHILE FOR HAUSDORFF DISTANCE AND  $\Delta V$  LOWER VALUES ARE PREFERABLE ( $\downarrow$ )

Method	Vendor	Dice Coefficient $\uparrow$			Hausdorff Distance $\downarrow$			$\Delta V$ (ml) $\downarrow$			
		LVO	Non-LVO	All	LVO	Non-LVO	All	LVO	Non-LVO	WIS	All
Penumbra (Core)											
Best Method ( <i>Mdl-5.2</i> ) ‡	Siemens "syngo.via"	0.66 (0.26)	0.51 (0.03)	0.66 (0.26)	6.9 (4.8)	3.5 (0.9)	5.2 (3.1)	44.2 (16.2)	6.9 (0.8)	1.4 (0.0)	27.9 (9.6)
Best Method ( <i>Mdl-5.2</i> )		<b>0.69 (0.27)</b>	<b>0.56 (0.03)</b>	<b>0.68 (0.26)</b>	<b>6.5 (4.3)</b>	<b>4.8 (2.7)</b>	<b>4.8 (2.7)</b>	<b>40.7 (12.9)</b>	<b>4.9 (1.0)</b>	<b>0.9 (0.0)</b>	<b>25.1 (7.8)</b>
Default Setting		0.31 (0.25)	0.11 (0.04)	0.27 (0.20)	7.8 (6.2)	5.6 (4.4)	6.6 (5.2)	67.5 (48.2)	51.8 (37.4)	3.7 (12.1)	58.2 (40.8)
Bathia et al. [28]		0.47 (0.17)	0.22 (0.03)	0.45 (0.14)	6.9 (6.9)	4.5 (4.7)	5.6 (5.7)	65.2 (63.3)	16.5 (44.3)	22.5 (6.6)	43.3 (53.5)
Other thresholding methods presented but not used for comparison											
Bivard et al. [13]	Toshiba	0.42 (0.19)	0.16 (0.03)	0.39 (0.15)	7.3 (6.5)	4.6 (4.4)	5.8 (5.4)	70.6 (52.9)	30.2 (36.0)	1.5 (9.1)	50.8 (43.3)
Cambell et al. [12]	Philips	N.A. (0.22)	N.A. (0.04)	N.A. (0.18)	N.A. (5.9)	N.A. (3.9)	N.A. (4.9)	N.A. (35.2)	N.A. (24.9)	N.A. (5.6)	N.A. (29.1)
Murphy et al. [22]	General Electric	0.17 (0.27)	0.08 (0.05)	0.16 (0.23)	7.5 (5.0)	4.8 (3.1)	6.1 (4.0)	96.7 (13.4)	21.1 (13.3)	8.6 (2.1)	63.5 (12.3)
Wintermark et al. [11]	Philips	N.A. (0.19)	N.A. (0.02)	N.A. (0.14)	N.A. (7.5)	N.A. (5.5)	N.A. (6.4)	N.A. (90.8)	N.A. (71.4)	N.A. (20.1)	N.A. (77.9)
Inter-observer variability											
$NR_1$ vs $NR_2$	Siemens "syngo.via"	0.80 (0.55)	0.67 (0.33)	0.79 (0.54)	5.1 (3.2)	1.9 (0.5)	3.6 (2.0)	33.3 (5.6)	5.5 (0.7)	0.0 (0.0)	21.0 (3.5)
<i>Mdl-5.2</i> vs $NR_1$		0.69 (0.25)	0.51 (0.01)	0.68 (0.25)	6.6 (4.2)	3.3 (0.5)	5.0 (2.6)	53.6 (12.4)	8.7 (0.3)	0.9 (0.0)	33.8 (7.2)
<i>Mdl-5.2</i> vs $NR_2$		0.71 (0.30)	0.56 (0.03)	0.70 (0.30)	6.4 (4.2)	3.0 (0.7)	4.8 (2.9)	38.6 (12.2)	4.9 (1.0)	0.9 (0.0)	23.9 (7.3)

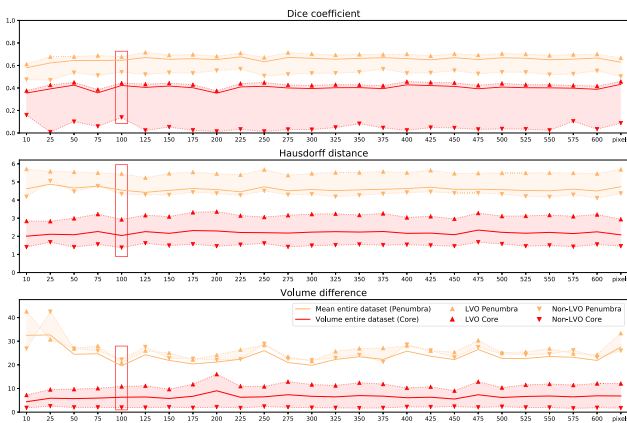


Fig. 6. Various plots (Dice coeff., Hausdorff dist.,  $\Delta V$ ) achieved with the validation set for selecting the best number of superpixel regions for *Mdl-5.2*. The  $x$ -axis indicates the number of superpixel regions. Results achieved by the best-performed model are highlighted with a red rectangle. Solid lines represent the average of the patients in the validation set, including all the different severities. Three top lines in all plots corresponds to penumbra, lower corresponds to core.

commonly implemented in clinical use in many applications. We consider it to be a good method to interpret the ischemic regions, due to the lack of consensus on thresholding methods and the recent oppositions over the de-facto DWI as the gold standard [15]–[18]. Nevertheless, these assessments present some variability among the experts (Table VIII), thus an automatic approach might present some advantages during analysis and can aid medical doctors in rapid recognition of ischemic regions. We have trained our method with ground truth images directly acquired from the CTP parametric maps, MIP, and follow-up images. This results in better and more precise visualization of the two ischemic regions in the brain: the salvageable (penumbra) and the irreversibly damaged tissue (infarct core). Fast and correct visualization of the penumbra will guide the treatment better since it is fundamental to treat patients where relevant tissue can be saved, and not invest a lot of resources and time in trying to save tissue that is already irreversibly damaged and

where the treatment might even harm the patient due to the risk of hemorrhage.

The criteria to select the best method was based on a study of various implemented experiments and their relative statistical results. First, we performed a set of thirty experiments described in Sec. VI-D and in Fig. 4, to select the right features and model. From the relative outcomes in Fig. 5, the results provided by *Mdl-5.2* (RF with *Single-Step* approach using all parametric maps at once) produces considerable statistical measures in the majority of the metrics, regardless of the severity group or class. It is interesting to notice that the *Single-Step* approach generates better results on all metrics but the *Two-Step* approach with RF produces slightly better results in the Hausdorff distance for the core class. Results for irreversibly damaged tissue for SVM models were not taken into consideration since these models fail to predict the mentioned class.

Subsequently, we applied a different number of superpixel regions to *Mdl-5.2* to find one that gives the best prediction results (Sec. VI-E, and in Fig. 6). It is clear that the results are not the best without applying superpixel, however, there is not a clear difference between different numbers of superpixel regions; Dice coefficient and Hausdorff distance outcomes do not present large discrepancies during the increment of superpixel regions; the metric influencing the final decision was the volume difference due to its drastic drop for the selected number of superpixels for the penumbra class and a significantly low value for the core class. Another important factor that helped to select the best number of superpixel regions was how the performances of the models differ with the various stroke severity groups. From Fig. 6 it is clear to notice that, among all the experiments in this set, *Mdl-5.2* presented the best tradeoff between the difference in volume and Dice coefficient for both the classes. One can argue that 125 superpixel regions give more or less similar results as 100 regions, however,  $\Delta V$  is higher especially for penumbra regions, meaning that 125 superpixel regions provide an overestimation of the tissue at risk, especially for the LVO group.

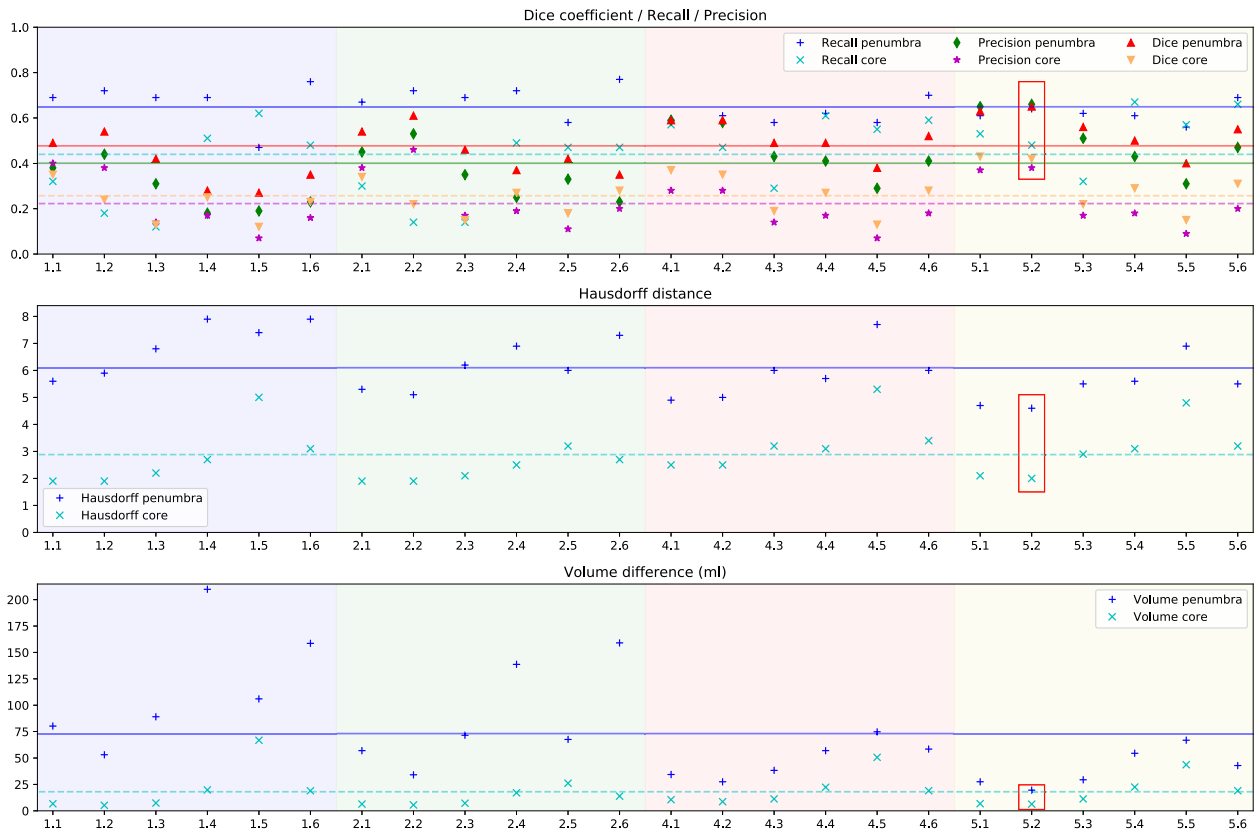


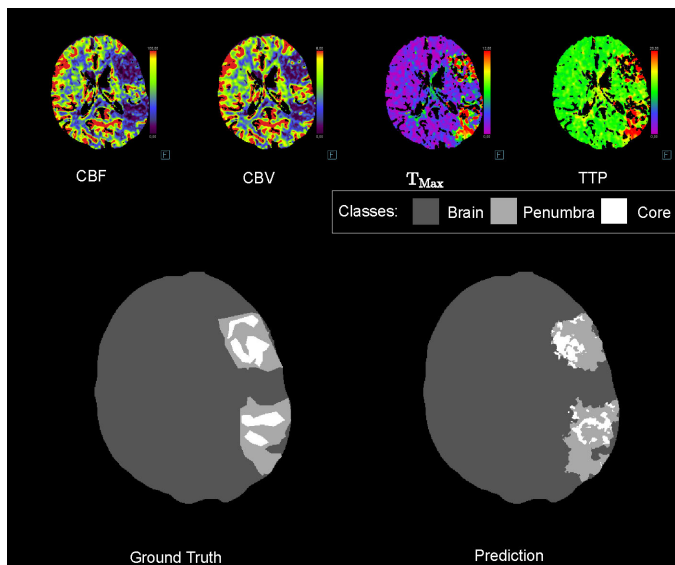
Fig. 7. Statistical measures to select the best input data combination to use. All the methods were tested with the best number of superpixel regions (100). Solid lines are used for penumbra and dashed for core average measures; top image in order (solid) recall, Dice, precision; (dashed) recall, Dice, precision. The best model (Mdl-5.2) is highlighted inside a red rectangle.

Finally, we validated the selected superpixel number by applying it to the other experiments (Sec. VI-F). SVM was excluded from this step as it performed poorly from the beginning (reference to Fig. 5). As shown in Fig. 7, increasing the number of superpixel regions slightly improved the statistical measures for both classes. Moreover, results achieved by *Mdl-5.2* present higher precision and lower  $\Delta V$  in comparison with the other models. The proposed method can classify correctly both penumbra and core in patients affected by a large vessel occlusion. The differences between the healthy and the ischemic tissue are more noticeable, in contrast with ischemic regions in patients with Non-LVO; an example is given in Fig. 8 for two brain slices of two patients affected by LVO (Fig. 8 (a)) and Non-LVO (Fig. 8 (b)). From the examples in Fig. 8 and the results in Table VIII, our best method is shown to predict penumbra regions more precisely than core areas. In patients with LVO, the prediction of core regions achieved promising results. However, the detection of core regions in patients with Non-LVO is more challenging; the small core area can be difficult to classify correctly. This issue might be related to the limited number of samples for that particular class, since patients in the Non-LVO group does not always have a core region. We compared the performance of the proposed RF-based method with approaches based on thresholding suggested in the literature and the results are presented in Table VIII; comparison is only performed with the default setting and values from Bathla *et al.* [28] due to the usage of

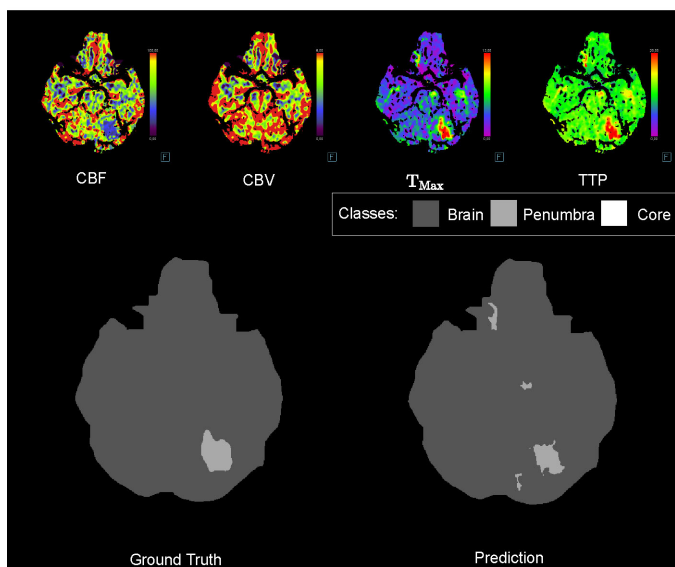
the same vendor. Predictions from the other methods [11]–[13], [22] are just presented for visualization purposes; a comparison does not apply to the utilization of different vendors to generate the parametric maps, but it illustrates an important limitation of thresholding.

The proposed method (*Mdl-5.2*) performs better than the thresholding approaches concerning the evaluation metrics. The use of a post-processing step slightly increment the performances of the best method, as it is possible to evince from Table VIII and Fig. 9. The *Mdl-5.2* method (using a 3D mode filter as a post-processing step) achieved the highest metrics for all the classes regardless of the stroke severity level. The sole exception where the model does not perform well is with the core class for Non-LVO group since, as it is possible to evince from Table VIII, it is the hardest class to predict correctly due to its limited number of samples and its narrow size in the BT.

Core predictions are slightly better than the one presented by the thresholding methods regardless of the group, while penumbra predictions are superior. This indicates a reliable understanding and agreement among ML predictions, threshold values, and neuroradiologists' annotations for the core regions. While, at the same time, it presents some uncertainties regarding the penumbra's definition. This might be related to the fact that the infarct core and penumbra are two dynamic regions inside the brain and highly dependent on the acquisition time of CTP and DWI. The perfusion examination shows the perfusion at that



(a) A 71-year-old man with LVO and a baseline NIHSS score of 8.



(b) A 60-year-old woman with Non-LVO and a baseline NIHSS score of 1.

**Fig. 8.** Visual comparison with four parametric maps (top), ground truth images (left), and the corresponding predicted image with the best method (right) of one slice for two patients included in the testset, one labeled as LVO (a), the other as Non-LVO (b). The dark grey area is healthy brain tissue, the light grey area represents the penumbra, and the white region indicates the ischemic core.

specific time, the penumbra and core size may change rapidly. In many studies, MRI is not performed immediately after CTP. DWI, often used as the gold standard for defining the ischemic core, cannot define penumbra. Our method, relying the ground truth on both CTP generated right after hospital admission (parametric maps derived from CTP, and MIP) and follow-up images, seems to provide a reliable method to predict both penumbra and core. Note that we propose to make predictions only based on data available right after hospital admission. The areas defined as ground truth from the DWI sequence can over- or underestimate the ischemic core in individual patients, making

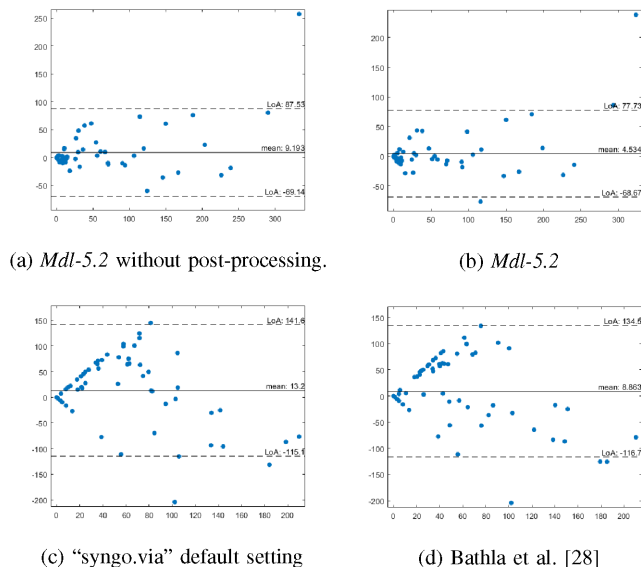


**Fig. 9.** Bland-Altman plots of the volume calculated between the predictions and the ground truth images for model *Mdl-5.2* with (b), without (a) post-processing step, the “syngo.via” default setting (c), and the values presented by Bathla *et al.* [28] (d).

it unrealistic to expect perfect concordance between ischemic core measurements on CTP and DWI [10], [16]–[18]. Other reasons are: first, they are not taking into consideration any spatial characteristics of an image; second, the values are very sensitive to image artifacts. Third, patients with contraindication to MRI, i.e. heart pacemaker, metal foreign body, might be excluded from studies where MRI and DWI images are used. Moreover, it is complicated to find an optimal threshold value for any group of patients. All the methods rely on selected thresholds, which might produce good results for a particular and predefined group, but it might not be the best for a single case study or the entire dataset studied. Their validation method relies on the comparison of the thresholding values with the clinical outcome of the patient; however, this is not perfect as the patient might have received treatment or the symptoms might have changed. Nevertheless, the delineation of the core should not be smaller due to treatment if the model delineates the core region correctly.

Table VIII shows the inter-observer variability in thirty patients divided by stroke severity into LVO and the Non-LVO subsets. There is a discrepancy between the results for the LVO and the Non-LVO subsets. Results for the LVO group have some similarities between the manual annotations and the *Mdl-5.2*. Nevertheless, manual annotations present better results in all the statistic measurements in comparison with the *Mdl-5.2* method in the Non-LVO subset. However, results in Table VIII illustrate the difficulties of achieving a consensus even among neuroradiologists.

## VIII. CONCLUSION

We proposed an automatic multi-classification approach for segmenting both ischemic core and penumbra based on random



forest using the parametric maps as input features, *Mdl-5.2*. We implemented other approaches based on thresholding, proposed in the literature, and compared them with our proposed method considering manual annotations as the ground truth generated from parametric maps. The method was trained with patients, both with AIS and WIS, grouped by different stroke severities. It shows good results for patients with large vessel occlusions, but not very good for patients with non-large vessel occlusions. Our method generates more precise results than the thresholding approaches for the two regions, but there is still room for improvement. We achieve an average Dice coefficient of 0.68 and 0.26, respectively for penumbra and core, for the three groups analyzed. We also achieve an average in volume difference of 25.1 ml for penumbra and 7.8 ml for core. Detecting ischemic core and penumbra regions in patients with non-large vessel occlusion can be very complicated, as shown in Fig. 8. Therefore, in the future, we plan to use approaches based on deep neural networks with 4D Computed Tomography Perfusion (CTP) volume as input instead of the parametric maps to work with the original acquired data.

## REFERENCES

- [1] V. L. Feigin, B. Norrving, and G. A. Mensah, "Global burden of stroke," *Circulation Res.*, vol. 120, no. 3, pp. 439–448, 2017.
- [2] E. Stevens, E. Emmett, Y. Wang, C. McKeivitt, and C. Wolfe, "The burden of stroke in Europe, report," King's College London Stroke Alliance Europe (SAFE), 2017.
- [3] B. Indredavik, R. Salvesen, H. Næss, and D. Thorsvik, "Nasjonalt retningslinje for behandling og rehabilitering ved hjerneslag," Helsedirektoratet: Oslo, 2010.
- [4] W. Johnson, O. Onuma, M. Owolabi, and S. Sachdev, "Stroke: A global response is needed," *Bull. World Health Org.*, vol. 94, no. 9, p. 634, 2016.
- [5] E. J. Benjamin *et al.*, "Heart disease and stroke statistics-2018 update: A report from the American heart association," *Circulation*, 2018.
- [6] S. Ojaghihaghghi, S. S. Vahdati, A. Mikaeilpour, and A. Ramouz, "Comparison of neurological clinical manifestation in patients with hemorrhagic and ischemic stroke," *World J. Emerg. Med.*, vol. 8, no. 1, p. 34, 2017.
- [7] K. Kurz, G. Ringstad, A. Odland, R. Advani, E. Farbu, and M. Kurz, "Radiological imaging in acute ischaemic stroke," *Eur. J. Neurol.*, vol. 23, pp. 8–17, 2016.
- [8] J. Astrup, B. K. Siesjö, and L. Symon, "Thresholds in cerebral ischemia-the ischemic penumbra," *Stroke*, vol. 12, no. 6, pp. 723–725, 1981.
- [9] E. S. O. E. E. Committee, *et al.*, "Guidelines for management of ischaemic stroke and transient ischaemic attack 2008," *Cerebrovascular Dis.*, vol. 25, no. 5, pp. 457–507, 2008.
- [10] C. W. Cereda *et al.*, "A benchmarking tool to evaluate computer tomography perfusion infarct core predictions against a DWI standard," *J. Cereb. Blood Flow Metab.*, vol. 36, no. 10, pp. 1780–1789, 2016.
- [11] M. Wintermark *et al.*, "Perfusion-ct assessment of infarct core and penumbra: Receiver operating characteristic curve analysis in 130 patients suspected of acute hemispheric stroke," *Stroke*, vol. 37, no. 4, pp. 979–985, 2006.
- [12] B. C. Campbell *et al.*, "Comparison of computed tomography perfusion and magnetic resonance imaging perfusion-diffusion mismatch in ischemic stroke," *Stroke*, vol. 43, no. 10, pp. 2648–2653, 2012.
- [13] A. Bivard *et al.*, "Defining acute ischemic stroke tissue pathophysiology with whole brain CT perfusion," *J. neuroradiol.*, vol. 41, no. 5, pp. 307–315, 2014.
- [14] P. W. Schaefer *et al.*, "Limited reliability of computed tomographic perfusion acute infarct volume measurements compared with diffusion-weighted imaging in anterior circulation stroke," *Stroke*, vol. 46, no. 2, pp. 419–424, 2015.
- [15] P. Schellinger *et al.*, "Evidence-based guideline: The role of diffusion and perfusion MRI for the diagnosis of acute ischemic stroke: Report of the Therapeutics and Technology Assessment Subcommittee of the American Academy of Neurology," *Neurol.*, vol. 75, no. 2, pp. 177–185, 2010.
- [16] M. Goyal *et al.*, "Challenging the ischemic core concept in acute ischemic stroke imaging," *Stroke*, vol. 51, no. 10, pp. 3147–3155, 2020.
- [17] C. S. Kidwell *et al.*, "Thrombolytic reversal of acute human cerebral ischemic injury shown by diffusion/perfusion magnetic resonance imaging," *Ann. Neurol.: Official J. Amer. Neurological Assoc. Child Neurol. Soc.*, vol. 47, no. 4, pp. 462–469, 2000.
- [18] M.-A. Labeyrie *et al.*, "Diffusion lesion reversal after thrombolysis: A mr correlate of early neurological improvement," *Stroke*, vol. 43, no. 11, pp. 2986–2991, 2012.
- [19] M. Matesin, S. Loncaric, and D. Petracic, "A rule-based approach to stroke lesion analysis from CT brain images," in *Proc. IEEE 2nd Int. Symp. Image Signal Process. Anal. Conjunction 23rd Int. Conf. Inf. Techno. Interfaces*, 2001, pp. 219–223.
- [20] P. Dastidar, T. Heinonen, J.-P. Ahonen, M. Jehkonen, and G. Molnár, "Volumetric measurements of right cerebral hemisphere infarction: Use of a semiautomatic MRI segmentation technique," *Comput. Biol. Med.*, vol. 30, no. 1, pp. 41–54, 2000.
- [21] L. Contin, C. Beer, M. Bynevelt, H. Wittsack, and G. Garrido, "Semi-automatic segmentation of core and penumbra regions in acute ischemic stroke: Preliminary results," in *Proc. IWSSIP Int. Conf.*, 2010.
- [22] B. Murphy *et al.*, "Identification of penumbra and infarct in acute ischemic stroke using computed tomography perfusion-derived blood flow and blood volume measurements," *Stroke*, vol. 37, no. 7, pp. 1771–1777, 2006.
- [23] A. Kemmling *et al.*, "Multivariate dynamic prediction of ischemic infarction and tissue salvage as a function of time and degree of recanalization," *J. Cereb. Blood Flow Metab.*, vol. 35, no. 9, pp. 1397–1405, 2015.
- [24] W. Qiu *et al.*, "Machine learning for detecting early infarction in acute stroke with non-contrast-enhanced CT," *Radiol.*, vol. 294, no. 3, pp. 638–644, 2020.
- [25] W. Qiu *et al.*, "Automated prediction of ischemic brain tissue fate from multiphase CT-Angiography in patients with acute ischemic stroke using machine learning," 2020, *medRxiv*.
- [26] A. S. Kasasbeh, S. Christensen, M. W. Parsons, B. Campbell, G. W. Albers, and M. G. Lansberg, "Artificial neural network computer tomography perfusion prediction of ischemic core," *Stroke*, vol. 50, no. 6, pp. 1578–1581, 2019.
- [27] L. Tomasetti, K. Egan, M. Khanmohammadi, and K. D. Kurz, "CNN based segmentation of infarcted regions in acute cerebral stroke patients from computed tomography perfusion imaging," in *Proc. 11th ACM Int. Conf. Bioinf., Comput. Biology Health Informat.*, 2020, pp. 1–8.
- [28] G. Bathla, K. Limaye, B. Policeni, E. Klotz, M. Juergens, and C. Derdeyn, "Achieving comparable perfusion results across vendors the next step in standardizing stroke care: A technical report," *J. Neurointerventional Surg.*, vol. 11, no. 12, pp. 1257–1260, 2019.
- [29] M. Fatima, *et al.*, "Survey of machine learning algorithms for disease diagnostic," *J. Intell. Learn. Syst. Appl.*, vol. 9, no. 1, p. 1, 2017.
- [30] B. E. Boser, I. M. Guyon, and V. N. Vapnik, "A training algorithm for optimal margin classifiers," in *Proc. 5th Annu. Workshop Comput. Learn. Theory*, 1992, pp. 144–152.
- [31] L. Breiman, J. Friedman, C. J. Stone, and R. A. Olshen, *Classification and Regression Trees*. Boca Raton, FL, USA: CRC Press, 1984.
- [32] L. Breiman, "Random forests," *Mach. Learn.*, vol. 45, no. 1, pp. 5–32, 2001.
- [33] R. Achanta, A. Shaji, K. Smith, A. Lucchi, P. Fua, and S. Süsstrunk, "Slic Superpixels compared to state-of-the-art superpixel methods," *IEEE Trans. Pattern Anal. Mach. Intell.*, vol. 34, no. 11, pp. 2274–2282, Nov. 2012.
- [34] N. V. Chawla, K. W. Bowyer, L. O. Hall, and W. P. Kegelmeyer, "Smote: Synthetic minority over-sampling technique," *J. Artif. Intell. Res.*, vol. 16, pp. 321–357, 2002.
- [35] T. Birsan and D. Tiba, "One hundred years since the introduction of the set distance by Dimitrie Pompeiu," in *Proc. IFIP Conf. Syst. Model. Optim.* Springer, 2005, pp. 35–39.

**Is the parametric calculation “transit time coefficient variation” capable of predicting tissue outcome in patients with acute ischemic stroke?**

<sup>1,2</sup>Liv Jorunn Høllesli, <sup>2</sup>Luca Tomasetti, <sup>3</sup>Kim Beuschau Mouridsen, <sup>4</sup>Jörn Schulz, <sup>2</sup>Kjersti Engan, <sup>2</sup>Mahdieh Khanmohammadi, <sup>5,6</sup>Martin W. Kurz, <sup>1,2</sup>Kathinka D. Kurz

1. Stavanger Medical Imaging Laboratory (SMIL), Department of Radiology, Stavanger University Hospital, Stavanger, Norway. 2. Department of Electrical Engineering and Computer Science, University of Stavanger, Stavanger, Norway. 3. Center of Functionally Integrative Neuroscience, Institute for Clinical Medicine, Aarhus University, Aarhus, Denmark. 4. Department of Mathematics and Physics, University of Stavanger, Stavanger, Norway. 5. Neuroscience research group, Department of Neurology, Stavanger University Hospital, Stavanger, Norway. 6. Department of Clinical Medicine, University of Bergen, Bergen, Norway.

Corresponding author: Liv Jorunn Høllesli, Department of Radiology, Stavanger University Hospital, Postboks 8100, 4068 Stavanger, Norway (e-mail: [liv.jorunn.hollesli@sus.no](mailto:liv.jorunn.hollesli@sus.no))

## **Abstract**

**Introduction:** Knowledge of tissue viability is crucial for acute ischemic stroke (AIS) treatment strategy. Current perfusion-based imaging struggles to accurately differentiate salvageable from non-salvageable ischemic tissue. This study evaluated if the parametric calculation transit time coefficient variation (CoV) adds value to the conventional parametric measures cerebral blood flow (CBF) and cerebral blood volume (CBV) in tissue outcome prediction in large vessel occlusion (LVO) AIS patients.

**Materials and Methods:** Perfusion computed tomography (CTP) scans from 61 LVO AIS patients were assessed. All had admission CTP and follow up magnetic resonance imaging including diffusion weighted imaging (DWI). Patients were grouped by recanalization status. CTP parametric maps defined hypoperfused regions, DWI defined final infarct. CoV, CBF and CBV were assessed voxel-wise according to DWI-based outcome.

**Results:** Infarct risk showed a clear association with CBF and CBV in recanalized patients, and with CoV in non-recanalized patients.

**Discussion:** Our findings indicate that certain voxel value combinations are destined to become infarcted regardless of recanalization and can enhance infarct core delineation in the event of treatment failure more precisely compared to conventional parameters. Research exploring supplementary parametric calculations consequently pave the path for improved future treatment decisions.

### **Key words:**

Ischemic stroke, perfusion computed tomography, parametric measures, diffusion weighted imaging, recanalization

## Introduction

Globally, neurological disorders are the leading cause of disability-adjusted life years (DALYs) and the second leading cause of death(1). Cerebral stroke is a major contributor to this burden, ranking as the second leading cause of death and the third leading cause of death and disability combined(2). The global incidence of stroke is increasing(2) and reached 12.2 million cases in 2019, with acute ischemic stroke (AIS) constituting 62.4% of the cases(2).

In AIS, ischemic brain tissue is often divided into ischemic core and penumbra. Ischemic core is defined as irreversibly damaged, while the penumbra as critically hypoperfused but still salvageable brain tissue(3). Diagnostic imaging in patients with AIS is typically performed using Computed Tomography (CT) and Magnetic Resonance Imaging (MRI)(4). CT is widely utilized in many centers due to its high sensitivity for detecting hemorrhage, widespread availability, and rapid scan times(5, 6). The decision to apply treatment depends on factors such as time from symptom onset to hospital admission, absence of contraindications for intravenous thrombolytic therapy (IVT) and/or endovascular therapy (EVT), and clinical variables. Especially in extended time windows, evaluating tissue viability is crucial for selecting treatment strategy(4, 7, 8). Both perfusion CT (CTP) and perfusion MRI (MRP) are used for this purpose in the acute setting(9). However, currently utilized perfusion-based imaging techniques struggle to accurately differentiate between salvageable and non-salvageable ischemic tissue(10). Despite being considered the foremost gold standard technique, even cytotoxic edema on DWI is not a perfectly reliable measurement for identifying the ischemic core(10-13), potentially being both initial false negative(14) and reversible(15, 16).

Autoregulation mechanisms maintain stable blood flow to the brain tissue under varying cardiovascular conditions. In a severe ischemic event, the autoregulation capacity for stable blood flow to the brain tissue is exceeded(17). Two perfusion calculations, the mean of capillary transit times (MTT) and the standard deviation of capillary transit times, i.e., the capillary transit time heterogeneity (CTH), are used to calculate the oxygen extraction efficacy of the tissue(18-20). CTH is an indicator of microvascular distribution of blood and changes in proportion to MTT in healthy anatomical microvascular networks. The ratio between CTH and MTT, the transit time coefficient variation (CoV), has been utilized to distinguish passive alterations caused by hypoperfusion from impairment in vascular autoregulation. In response to reduced cerebral perfusion pressure during an ischemic event in the brain, by still intact autoregulation, a passive increase in CTH in proportion to MTT is seen, while CoV remains constant(21). Conversely, impaired autoregulation affects both CTH and CoV(18, 19). Microvascular patency affects conventional perfusion parameters only in cases where plasma, and thereby contrast media, fails to reach large proportions of the microvasculature

within an image voxel(21). Accordingly, conventional parametric maps reflect the vascular volume perfused by plasma, which holds limited amounts of oxygen, and do not capture the microvascular distribution of blood, which can be obtained through the perfusion calculations CTH and CoV(19, 21).

It has been suggested that cerebral ischemia causes widespread capillary no-flow, that is, the complete cessation or significant reduction of blood flow, leading to impeded delivery of oxygen and nutrition to the affected area of the brain(21, 22). Transit time homogenization, i.e., regions with extreme flow homogenization identified by CoV, is believed to visualize capillary no-flow(21, 23). Accordingly, low CoV values are associated with reduced cerebral blood volume (CBV) and are considered to represent a biomarker of penumbral microvascular failure(21).

A more accurate description of penumbra and core in patients with AIS, would significantly enhance treatment decisions in the acute phase. Parametric tools based on the microvascular blood distribution have demonstrated greater accuracy in determining ischemic brain tissue compared to conventional parameters(21, 24). Therefore, we included the parametric calculation CoV in our analysis. Most prior imaging-based studies on the microvascular distribution of blood are based on MRP(21, 25-28). There are only a few published analyses of CTP datasets so far(29, 30). Considering the widespread use of CTP in evaluating AIS patients, there is a pressing need for increased understanding of CTP. Our study aimed to evaluate if CoV calculated from CTP adds value to the conventional parametric measures cerebral blood flow (CBF) and CBV in the prediction of DWI-based tissue outcome in patients with large vessel occlusion (LVO) AIS.

## **Materials and methods**

### **Patients**

#### Context

As the only stroke-treating hospital in the region, Stavanger university hospital serves a population of 369.000, with around 450 patients annually admitted with AIS. All consecutive patients with suspected AIS having received intravenous thrombolysis (IVT) are prospectively included in a population based local thrombolysis registry. The registry contains multiple variables, including patient demographics, cerebrovascular risk factors, clinical severity measured by the National Institutes of Health Stroke Scale (NIHSS) on admission and at discharge, in-hospital mortality and

modified Rankin Scale (mRS) at baseline and 3 months post stroke measuring long-term functional outcome(13, 31).

### Dataset

CTP scans acquired between January 2014 and August 2020 from 109 patients were extracted from the thrombolysis registry. Anonymized CTP scans from all adult patients who underwent CTP and were diagnosed with AIS during this period were assessed. Patients with visible perfusion abnormalities on CTP, meeting satisfactory technical standards, and having follow up MRI available, were included in our study. All patients were examined with non-contrast enhanced CT (NCCT) of the head, CT angiography (CTA) of precerebral and intracranial arteries, and CTP immediately after hospital admission. All patients underwent a follow up MRI scan, typically within 24 hours, including DWI. The patients were categorized into two groups based on level of vessel occlusion. Large vessel occlusion (LVO) was defined as occlusion of any of the following arteries: Internal carotid artery, M1 and proximal M2 segment of the middle cerebral artery, A1 segment of the anterior cerebral artery, P1 segment of the posterior cerebral artery, basilar artery, and the vertebral artery. Patients with perfusion deficits and more distal artery occlusions or without visible artery occlusions (48 patients), were defined as non-LVO, and were not included in this study. A total of 61 patients with LVO were included. All patients received IVT, and 41 patients were additionally treated with EVT. Recanalization status was evaluated based on digital subtraction angiography (DSA) and 3D arterial magnetic resonance (MR) angiography in time of flight technique (TOF angiography). Patients were grouped according to recanalization status using the modified treatment in cerebral ischemia (mTICI) scale (mTICI $\leq$ 2a not recanalized, mTICI >2a recanalized)(32).

### **Imaging protocol and analysis**

The CT scanners used for image acquisition were Siemens Somatom Definition Flash and Siemens Somatom Definition Edge, Erlangen, Germany. Technical protocol details are given in the appendix. Syngo.via (Siemens Healthineers, Erlangen, Germany), with manufacturer default settings, was used to generate the CTP deconvolution-based parametric maps Time to maximum (Tmax), time to peak (TTP), CBF and CBV. Cercare Medical Neurosuite (Cercare Medical, Aarhus, Denmark) was used to generate the CTP deconvolution-based parametric maps CTH, CoV and the singular value decomposition (SVD)-based parametric map MTT.

The MR scanners used were two 3 Tesla (T) (Siemens Skyra, Siemens Healthineers, Erlangen, Germany and Philips Ingenia, Philips Medical Systems International B.V., Best, the Netherlands) and two 1,5 T scanners (Philips Ingenia, Philips Medical Systems International B.V., Best, the Netherlands and GE Discovery, GE Healthcare, Chicago, Illinois, USA). The stroke protocol comprised transversal DWI Echo-Planar Imaging, B-value 1000, a T2-weighted Turbo Spin Echo sequence, a Fluid-Attenuating Inversion Recovery sequence (FLAIR, in patients with unknown time of onset), T2\* Turbo Field Echo or Susceptibility-weighted imaging (SWI), and 3D arterial MR angiography in time of flight technique (TOF angiography).

### **Image processing and region of interest**

Two experienced neuroradiologists evaluated ischemic lesions on conventional parametric maps derived from the CTP dataset, and the MR examination. The region of interest, i.e., ground truth ischemic regions, were outlined manually using an in-house developed software in MATLAB(13); the syngo.via-derived CTP conventional parametric maps were used to outline the entire hypoperfused region, while cytotoxic edema on DWI was used to define final infarct (i.e., the union between the hypoperfused region from a CTP scan and cytotoxic edema on a follow-up DWI scan).

To ensure that the regions we compared in the parametric maps and the DWI images were corresponding anatomical areas in the brain, the parametric maps and the DWI images were aligned by image registration. Several steps were performed, illustrated in Figure 1. Firstly, we ensured that only DWI slices matching the CTP hypoperfused region was included for further analyses. This was done by providing manual input from an experienced neuroradiologist giving the top (blue) and bottom (red) slice, i.e., the region in the z-direction of the DWI volume that corresponds to the section of the brain with hypoperfused regions on CTP, see part 1 of the figure. The possible slight skew in the CTP volume relative to the DWI volume was ignored. For most of the patients, the number of slices in the corresponding CTP and DWI sections was identical in the z-direction, except for approximately 10% exhibiting a small mismatch. In these cases, the DWI slices were linearly interpolated to fit the number of CTP slices. Thereafter, illustrated in step 2 in Figure 1, image co-registration was performed slice-by-slice using a similarity transformation, consisting of translation, rotation, and scaling.

To allow composite voxel-wise analyses of outcome measures across all patients, perfusion variables (CoV, CBF and CBV) were normalized to normal appearing white matter (NAWM)(21). NAWM was defined by manual delineation of the contralateral centrum semiovale in most patients with a

supratentorial ischemic lesion, except in 7 patients where the contralateral corona radiata was used for delineation due to alterations such as pronounced hypoattenuation resulting from small vessel disease in the centrum semiovale. Further, in patients with an ischemic event in the posterior fossa, NAWM was delineated in the cerebellum or pons (8 patients). Voxels with extreme values ( $CBF > 100$  mL/100 mL/min;  $CBV > 6$  mL/100 mL;  $CoV > 7$ ) were excluded from the analyses a priori due to constraints in the syngo-via software, and these voxels were set to zero. At a slice-by-slice level, the pixels corresponding to the voxels without any bolus were assigned CBF or CBV pixel values equal to zero. Any resulting holes were then filled iteratively by starting at the edges and proceeding until each hole was filled with the lowest value from the edge, using an 8-neighbourhood approach, based on MATLAB predefined functions(33).

Using the manually defined ischemic regions, CTP was assessed voxel-wise for the parametric maps CoV, CBF and CBV according to DWI-based tissue outcome (figure 1, step 3). The parameters' effect on infarct risk was evaluated, including whether CoV adds value to the conventional parameters CBF and CBV in the prediction of tissue outcome. This was accomplished by examining the probability,  $p$ , for a voxel in the hypoperfused region on CTP to match the final infarct region on DWI for different combinations of CBF and CoV values, and similarly for different combinations of CBV and CoV values, resulting in  $p(\text{Infarct} | \text{CBF}, \text{CoV})$  and  $p(\text{Infarct} | \text{CBV}, \text{CoV})$ . The probability values were used to create 2D plots where the axes represent voxel values (CBF vs. CoV and CBV vs. CoV) and the color represents the probability, weighted to lie between 0-1, for such a combination of voxel values from the hypoperfused region to end up in the final infarct region on DWI. Some combinations of parametric map values are much less frequent than others, thus, 3D plots were made to add a third axis showing the probability of a given voxel in the hypoperfused region to have certain combinations of CBV (or CBF) and CoV values (figure 1, step 3, and figure 2 + 3)(21). In addition to CBF, CBV and CoV, recanalization status was also taken into consideration when assessing infarct risk in the 2D and 3D plots (figure 1, step 3, and figure 2 + 3)(21).



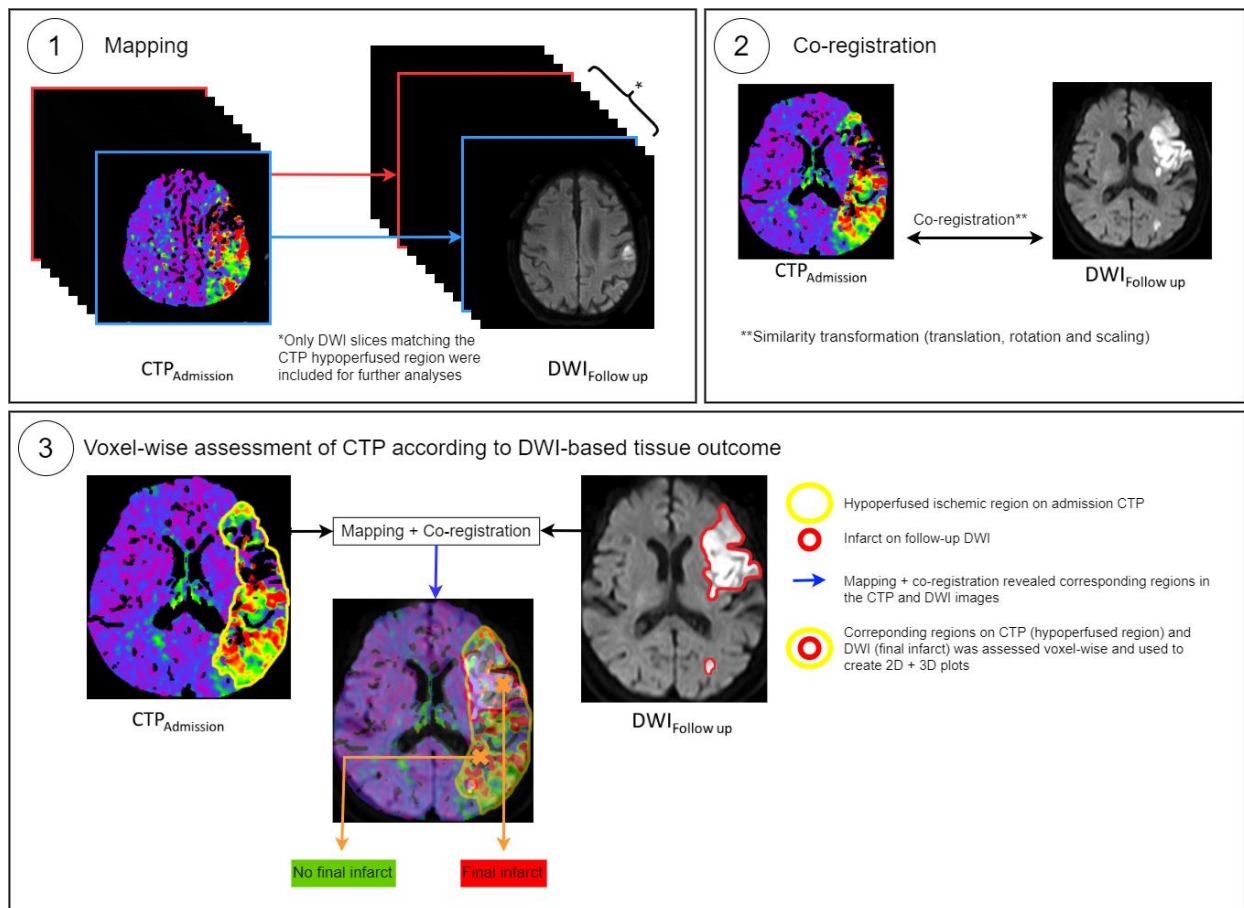


Figure 1: General overview of the processing steps involved: Step 1) maps the hyperperfused region on the CTP scans with the corresponding region on follow-up DWI scans. In step 2, image co-registration was performed slice-by-slice using a similarity transformation, consisting of translation, rotation and scaling. In step 3, voxel-wise assessment of CTP was done according to DWI-based tissue outcome.

## Statistics

Patients with LVO were grouped according to recanalization status. Statistical analyses were performed using SPSS Statistics version 24 (IBM Cooperation, Armonk, NY, USA) and MATLAB (R2020a, Update 1, The MathWorks, Inc., Natick, USA). Categorical variables are presented as count (percent, %) and continuous variables as median (interquartile range, IQR). Changes in ratios were evaluated using Fisher's exact test or Pearson Chi-Square, as appropriate. Changes in continuous variables were evaluated using Mann-Whitney test. Statistical significance was set at  $p < 0.05$  (two-sided).

## Ethical approval

The study is approved by the Regional ethic committee project 2012/1499, and by Sikt, the Norwegian Agency for Shared Services in Education and Research, reference number 953392. All procedures involving human participants were performed in accordance with the ethical standards of the institutional and/or national research committee and with the 1964 Helsinki Declaration and its later amendments or comparable ethical standards, including the ARRIVE guidelines.

## Results

Patient baseline characteristics, cerebrovascular risk factors and clinical outcome are shown in Table 1. The NIHSS score on admission was significantly lower in patients without recanalization compared to patients with recanalization. Additionally, there were significantly more EVT-treated patients among those with recanalization compared to non-recanalized patients. Otherwise, there were no statistical differences in baseline characteristics, cerebrovascular risk factors or patient outcomes between the two groups.

		Recanalization (n=48)	No recanalization (n=13)	p-value
Age, median (IQR)		72 (65, 80)	72 (55, 84)	0.74
Sex – female		12 (25)	5 (39)	0.49
NIHSS score Median, (IQR)	At admission	15 (7, 21)	3 (2, 17)	<b>0.02</b>
	At dismissal	2 (0, 6) (n=43)	1 (0, 12) (n=10)	0.67
mRS Median, (IQR)	Baseline	0 (0, 0)	0 (0, 0)	0.57
	At 3 months	2 (1, 4) (n=47)	2 (2, 5)	0.20
Atrial fibrillation		10 (21)	1 (8)	0.43
Hypertension		23 (48)	5 (39)	0.54*
Diabetes mellitus		4 (8)	3 (23)	0.16
Smoking		9 (19)	2 (15)	1.00

Anticoagulants	25 (52)	6 (46)	0.70*
Onset to CT (minutes) Median, (IQR)	61 (40, 105) (n=45)	93 (60, 175)	0.10
EVT	36 (75)	5 (39)	<b>0.02</b>

**Table 1:** Patient characteristics and clinical outcome in patients with LVO according to recanalization status.

Data presented as count (%) unless otherwise stated. P-values for changes in ratios from Fisher's exact test (except \*Pearson Chi-Square), p-values for changes in continuous variables from Mann-Whitney test. N = number of patients.

Smoking represents current smokers (non-smokers include non-smokers, previous smokers and patients with unknown smoking status).

Abbreviations: EVT, endovascular treatment; IQR, interquartile range; LVO, large vessel occlusion; mRS, modified Rankin Scale; NIHSS, National Institutes of Health Stroke Scale.

The combination of CoV versus CBF and CBV for the ischemic lesion on admission according to final outcome on follow-up DWI, is shown in the voxel-based 2D and 3D plots in figure 2 and 3. In patients with subsequent recanalization, both CBF and CBV showed a clear association with infarct risk. Low CBF and CBV were associated with high risk of infarction across a broad range of CoV values (figure 2). Conversely, in patients without recanalization, infarct risk was largely dependent on CoV. In these patients, there was a tendency towards lower CoV values, where a large proportion of tissue with reduced CoV developed into infarction, also in regions with higher CBF and CBV values (figure 3). In Figure 2 and 3, areas with red color on the 3D curves, represent combinations of voxel values associated with a high risk of infarction. These voxels were predominantly located beside the peaks for both CBF and CBV, most evident in recanalized patients.

Figure 2: Recanalized patients

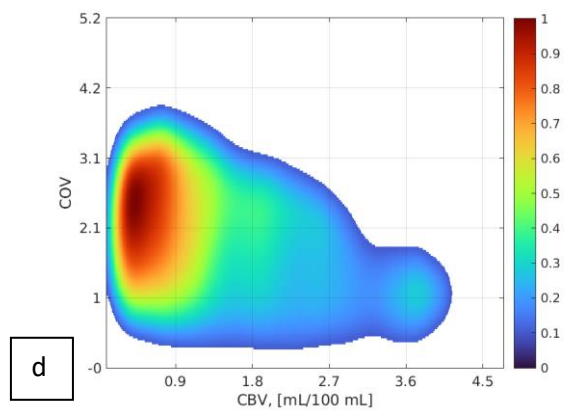
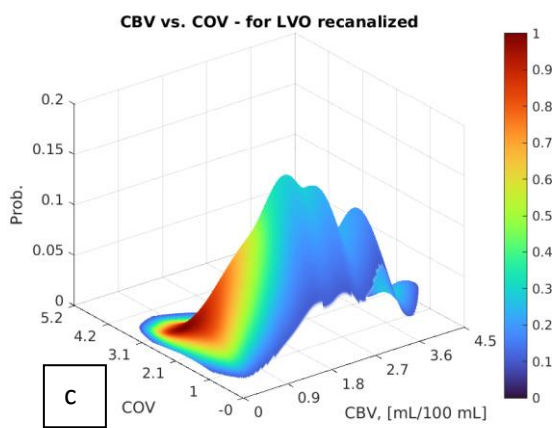
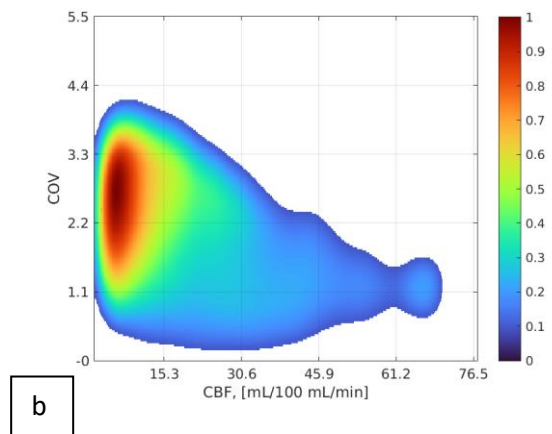
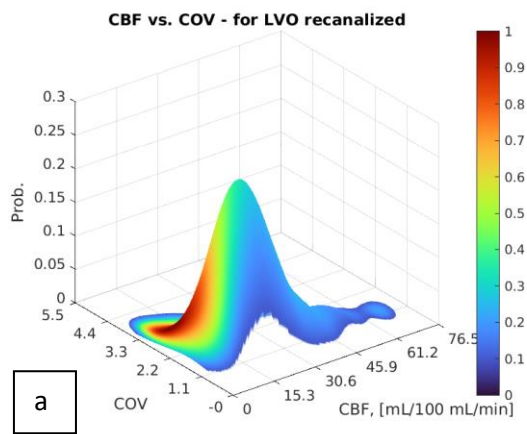


**Figure 3: Non-recanalized patients**

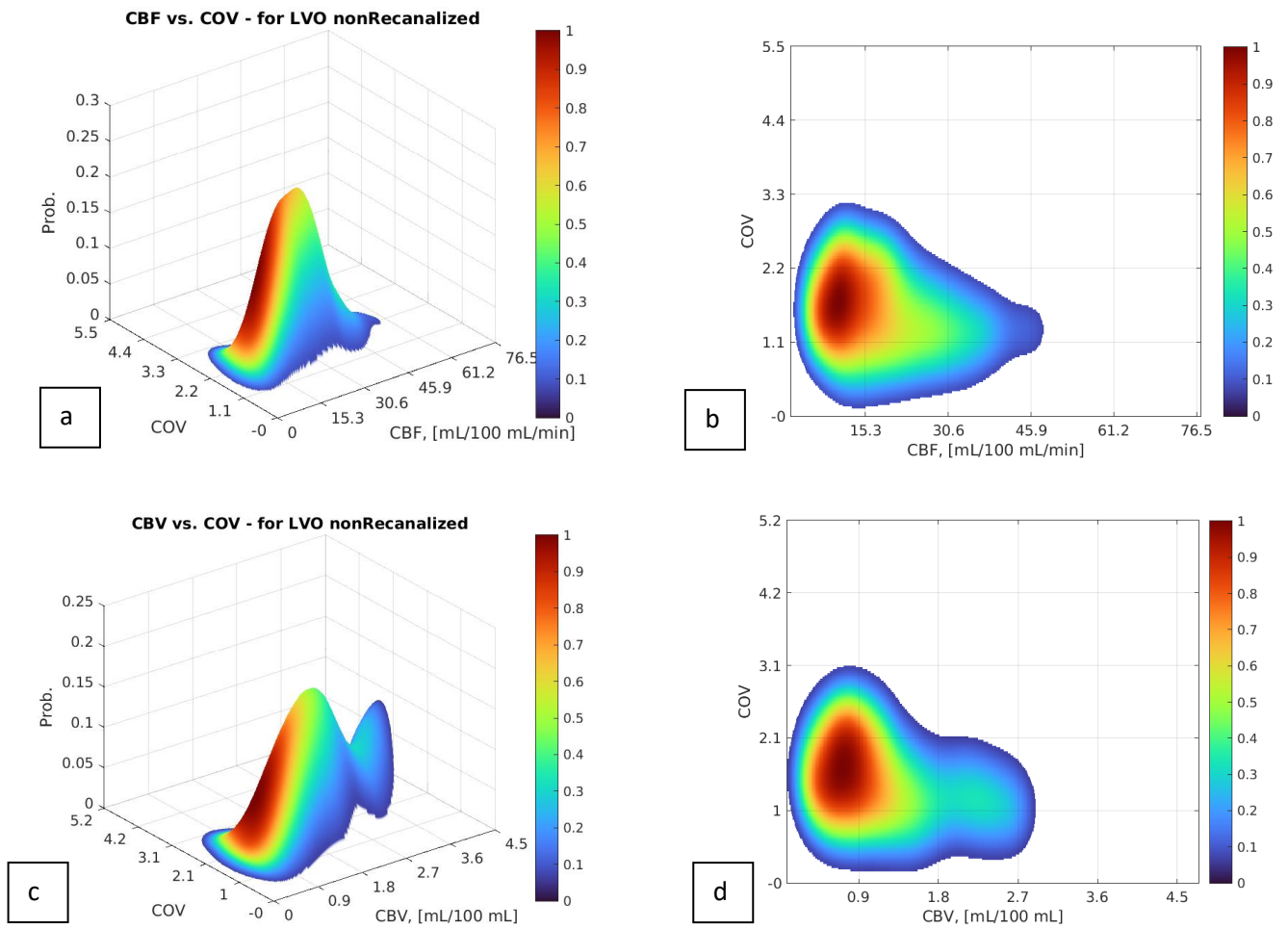


**Figure 2 and 3:** The plots show the CTP parametric measures on admission in the hyperperfused region in recanalized (figure 2) and non-recanalized patients (figure 3). The results are presented as 3D plots (a+c) and 2D plots (b+d). Values of the parametric measures are defined in the first two dimensions of each 2D and 3D plot. The third dimension in the 3D plots indicates the distribution of value combinations for the parametric measures analyzed (given as probability, values ranging between 0 and 1). Final infarct was defined as the union between the hyperperfused region from a CTP scan and the infarct area visible on a follow-up DWI scan (step 3 in Figure 1). The color dimension illustrates the likelihood of final infarct (given as probability, with values weighted to lie between 0 and 1) across all subjects in the dataset, i.e., the likelihood of having a particular combination of values in the CTP hyperperfused region, overlapping the DWI-based final infarct area. Abbreviations: CBF, cerebral blood flow (ml blood/100 g brain tissue/minute); CBV, cerebral blood volume (ml blood/100 g brain tissue); CoV, transit time coefficient variation.

## Discussion

CTP is a widely used diagnostic modality for AIS worldwide. In this study on AIS patients, different CTP-based measures were analyzed, including the non-conventional calculation CoV, which reflects the microvascular distribution of blood. Most previous imaging-based studies, exploring microvascular distribution of blood in ischemic brain tissue, are MRP based(21, 25-28). We evaluated the combination of CoV, CBF and CBV on CTP and compared the findings to final tissue outcome on follow-up DWI.

The lack of a perfectly reliable definition for ischemic core presents a major challenge in current stroke imaging. The whole concept of ischemic core was challenged in a recent paper, pointing out three fundamental problems(10): Firstly, currently used perfusion imaging cannot accurately distinguish between viable and infarcted tissue. Secondly, treatment-decisions in AIS are based on multiple factors, reducing the relative importance of single variables like imaging. And thirdly, discrepancies between core volume and clinical outcome are often observed(10). The final outcome in AIS relies on several factors including time to and degree of recanalization, the tissue type affected, collateral circulation, ischemia depth and duration, and multiple, often severe patient related factors(10). Most commonly used perfusion-based parameters struggle to accurately differentiate between salvageable and non-salvageable tissue(34, 35). Despite being considered the foremost gold standard technique, even DWI is not a perfectly reliable measurement for identifying the ischemic core(10-13). DWI can yield false negative results in the initial phase in a small but significant group of AIS patients, shown in 8% of cases in one study(14). On the other hand, DWI changes in the acute setting can also be reversible and represent penumbra in up to 15.5% of EVT-treated patients(15, 16).

Multiple studies have demonstrated a clear benefit from both IVT and EVT in extended time windows(36-39). Perfusion imaging becomes crucial in extended time windows, as treatment is recommended if the estimated infarct core is sufficiently small and there is a substantial penumbra(4, 7, 8). A significant number of patients remains ineligible for IVT or EVT within the current extended time window recommendations(4, 7, 8). Probably, some of the patients in extended time windows, that are excluded from treatment based on current guidelines, would profit from treatment, if the selection criteria were more accurate. Conversely, the clinical outcome in nearly 50 % of patients undergoing EVT is poor. Probably, there are groups of patients that are treated with EVT based on the existing selection criteria, who will not profit from treatment, even with technical optimal EVT procedures(40, 41). Research efforts, such as the present study, that explore additional parametric calculations, are therefore paving the way for improved treatment

decisions in the future. Given the widespread use of CTP, there is a growing need of CTP-based studies on tissue viability visualization(34).

In patients with subsequent recanalization, both low CBF and CBV values showed a clear relationship with infarct risk. Conversely, in patients without recanalization, infarct risk was largely dependent on CoV; a substantial proportion of tissue with reduced CoV developed into infarction, even in regions with preserved CBF and CBV values. These findings suggest that the size and site of the final infarct core can be more precisely predicted by using CoV in the acute setting, compared to analyses of conventional parameters alone, and has the potential to add valuable information to treatment decisions.

Areas with red color on the 3D curves, representing combinations of voxel values associated with a high risk of infarction, were predominantly located beside the peaks for both CBF and CBV, most evident in recanalized patients. Along with a clear relationship between both low CBF and CBV and infarct risk, this indicates that certain combinations of voxel values are destined to become infarcted regardless of recanalization. In a previous MRP-based study, it was shown that tissue with severely restricted CBF ( $\leq 6$  mL/100 mL/min) was likely to infarct regardless of recanalization status, while the destiny of tissue with preserved CBF was largely dependent on RTH (=CoV)(21). Our CTP-based findings are in alignment with these findings.

During an ischemic event in the brain, tissue damage occurs when the capacity of the autoregulation to maintain stable blood flow is exceeded(17). Impaired neurovascular coupling, characterized by the reduced ability of the brain vasculature to increase blood flow in response to increased metabolic demands, has been linked to capillary dysfunction and is thought to contribute to futile recanalization(42). The collapse of collateral blood flow or poor collateral filling is strongly associated with rapid infarct progression and futile recanalization(43, 44). Interestingly, rather than perceiving collateral failure as a cause, it has been hypothesized to consider it as an inevitable outcome resulting from escalating microvascular resistance during progressive infarction(45).

Following recanalization therapy, possible incomplete restoration of microcirculatory flow in parts of the ischemic tissue, has been referred to as the *no-reflow* phenomenon(23, 46, 47). This can result in the tissue's metabolic requirements not being fulfilled, despite complete recanalization(47, 48).

Transit time homogenization is believed to visualize capillary no-flow, i.e., regions with extreme flow homogenization, identified by CoV(21, 28). Low CoV values have been found in association with penumbral microvascular failure(21). We firmly believe that a better understanding of the microvascular environment during an ischemic event will contribute to the goal of selecting patients for treatment more precisely.

The no-flow and no-reflow phenomenon is debated. Factors beyond microvascular impairment, such as distal microvascular embolization, in situ thrombus formation, early re-occlusion, and parenchymal hemorrhage, can also contribute to compromised reperfusion after recanalization<sup>62</sup>.

The lack of a widespread standard definition for no-reflow also poses a challenge. In a recent review encompassing thirteen studies with a total of 719 patients, the no-reflow phenomenon was observed in one-third of AIS patients with successful macrovascular reperfusion, which in turn was associated with worse clinical outcome(49). Both experimental and radiological data support the notion that no-flow is an important characteristic of the ischemic penumbra(21). On the other hand, capillary flow might recover with recanalization, leading to a partial reversal of the RTH and MTT lesion(21, 23).

Considering its potential to impede the efficacy of recanalization therapy, there has been hypotheses about whether incomplete reperfusion could be a potential target for treatment to improve outcome after recanalization(24, 28, 47, 50-52). It is also questioned whether patients ineligible for recanalization therapy could benefit from such treatment alone(21). Interestingly, several factors that predispose for stroke and dementia, such as aging, hypertension, hypercholesterolemia and diabetes, have been shown to alter the autoregulation of CBF to meet the tissue's metabolic need during neuronal activity(24).

Multiple thresholds are applied to different parametric maps to estimate penumbra and core(12, 53-56). Artificial neural networks (ANN) and machine learning (ML) methods have demonstrated promising results in image analyses in AIS patients, exhibiting the capacity to accurately predict tissue outcomes. In one study, a general linear model (GLM) based on CTP and clinical data successfully identified patients who could benefit from recanalization therapy in the extended time window(57). Another study found that the ischemic core could be predicted with a sensitivity of 0.91 and a specificity of 0.65 using ANNs that integrated clinical and CTP data(58). Additionally, the entire 4D CTP data has been used as input to neural networks to segment both penumbra and core(59). Color-coded CTP parametric maps have been used to automatically segment penumbra and core using ML-based methods, showing that the best method outperforms classical thresholding approaches(13). Future studies on implementing supplementary parametric measures and clinical variables into ANN and ML methods are of great interest.

Our study has inherent limitations. Not all AIS patients during the study period were included, as this was contingent on the presence of a visible and acute ischemic lesion on CTP, satisfactory technical image quality (i.e., absence of motion artifacts, high-quality contrast bolus), and the availability of a follow-up MRI scan. Our primary focus was to collect high-quality data on combinations of parameters. A more unselected cohort, including all LVO-patients with the ischemic region



encompassed in the CTP scan, would also be of interest and is the scope of a planned study. Additionally, some of the CTP scans included are relatively old; however, our focus has been on obtaining high-quality perfusion images consistently over several years. To further assess the risk of infarction, such as employing a logistic model, might yield intriguing findings, aligning with the intended focus of an upcoming study. We included patients with both anterior and posterior circulation LVO, in both early and extended time windows, regardless of NIHSS score. Consequently, there is some heterogeneity in our study population, which may pose challenges in interpreting our results and comparing them with other studies. However, it is noteworthy that only 8 patients included in our study had a posterior circulation AIS. For normalization, we used the mean of NAWM across all patients for the different perfusion parameters, assuming that this represents a fair approximation for our study population. We did not rely on literature references for healthy NAWM, primarily because previous studies did not assess all the parameters included in our study(60, 61). Variables like age and diabetes, known to influence NAWM(61-63), were not taken into consideration. Nevertheless, there was no difference in age or diabetes between the two groups in our study (table 1). The non-recanalized group was relatively small (13 patients), yet, the voxel count in the ischemic lesions for this group is high. Our study period spans nearly 7 years, during which several factors have changed, contributing to heterogeneity in our group. Numerous randomized controlled trials have established the safety and efficacy of treatment in a larger patient population, especially in extended time windows. Nevertheless, our emphasis throughout the whole study period has been on obtaining high-quality images, as this was one of the inclusion criteria.

In summary, we assessed the CTP-based parametric maps CoV, CBF and CBV voxel-wise according to DWI-based final infarct. In patients with subsequent recanalization, a distinct correlation between infarct risk and both CBF and CBV was observed. Conversely, in patients without recanalization, infarct risk was largely dependent on CoV. These findings suggest the potential for a more accurate delineation of the ischemic core using CoV. Research initiatives, that explore additional parametric calculations, are thus paving the way for improved treatment decisions in the future.

#### **Author contribution statement**

L.J.H., L.T., K.B.M. and K.D.K. designed the experiments. L.J.H. performed data collection, statistical analyses and wrote the manuscript. L.J.H. and K.D.K. conducted manual annotations of ischemic regions on CTP and DWI images. L.T. performed image processing and created the 2D and 3D plots, which were reviewed and interpreted along with L.J.H., K.E., M.K., K.D.K. and K.B.M. K.E., M.K. and

J.S. contributed to statistical analyses. M.W.K. has the clinical responsibility for the patients. All authors contributed in conducting the discussion and in the review and editing of the manuscript.

**Conflicts of interest**

Kim Mouridsen is CEO and shareholder of Cercare Medical A/S. The other authors declare no conflicts of interest.

**Data availability statement**

The data that support the findings of this study are available from the corresponding author upon reasonable request.

## References

1. World Health Organization (WHO). Optimizing brain health across the life course: WHO position paper. 2022.
2. Collaborators GS. Global, regional, and national burden of stroke and its risk factors, 1990-2019: a systematic analysis for the Global Burden of Disease Study 2019. *Lancet Neurol*. 2021;20(10):795-820.
3. Kurz KD, Ringstad G, Odland A, Advani R, Farbu E, Kurz MW. Radiological imaging in acute ischaemic stroke. *Eur J Neurol*. 2016;23 Suppl 1:8-17.
4. Guidelines for the early management of patients with acute ischemic stroke: 2019 update to the 2018 guidelines for the early management of acute ischemic stroke a guideline for healthcare professionals from the American Heart Association/American Stroke Association, (2019).
5. McDonough R, Ospel J, Goyal M. State of the Art Stroke Imaging: A Current Perspective. *Can Assoc Radiol J*. 2021;8465371211028823.
6. Young JY, Schaefer PW. Acute ischemic stroke imaging: a practical approach for diagnosis and triage. *Int J Cardiovasc Imaging*. 2016;32(1):19-33.
7. Berge E, Whiteley W, Audebert H, De Marchis GM, Fonseca AC, Padiglioni C, et al. European Stroke Organisation (ESO) guidelines on intravenous thrombolysis for acute ischaemic stroke. *Eur Stroke J*. 2021;6(1):I-lxii.
8. Turc G, Bhogal P, Fischer U, Khatri P, Lobotesis K, Mazighi M, et al. European Stroke Organisation (ESO) - European Society for Minimally Invasive Neurological Therapy (ESMINT) Guidelines on Mechanical Thrombectomy in Acute Ischaemic Stroke Endorsed by Stroke Alliance for Europe (SAFE). *Eur Stroke J*. 2019;4(1):6-12.
9. Thomalla G, Gerloff C. Acute imaging for evidence-based treatment of ischemic stroke. *Curr Opin Neurol*. 2019;32(4):521-9.
10. Goyal M, Ospel JM, Menon B, Almekhlafi M, Jayaraman M, Fiehler J, et al. Challenging the Ischemic Core Concept in Acute Ischemic Stroke Imaging. *Stroke*. 2020;51(10):3147-55.
11. von Kummer R, Dzialowski I. Imaging of cerebral ischemic edema and neuronal death. *Neuroradiology*. 2017;59(6):545-53.
12. Cereda CW, Christensen S, Campbell BCV, Mishra NK, Mlynash M, Levi C, et al. A benchmarking tool to evaluate computer tomography perfusion infarct core predictions against a DWI standard. *J Cereb Blood Flow Metab*. 2016;36(10):1780-9.
13. Tomasetti L, Hølllesli LJ, Engan K, Kurz KD, Kurz MW, Khanmohammadi M. Machine learning algorithms vs. thresholding to segment ischemic regions in patients with acute ischemic stroke. *IEEE J Biomed Health Inform*. 2021;Pp.
14. Simonsen CZ, Madsen MH, Schmitz ML, Mikkelsen IK, Fisher M, Andersen G. Sensitivity of diffusion- and perfusion-weighted imaging for diagnosing acute ischemic stroke is 97.5%. *Stroke*. 2015;46(1):98-101.
15. Lakomkin N, Pan J, Stein L, Malkani B, Dharmoon M, Mocco J. Diffusion MRI Reversibility in Ischemic Stroke Following Thrombolysis: A Meta-Analysis. *J Neuroimaging*. 2020;30(4):471-6.
16. Yoo J, Choi JW, Lee SJ, Hong JM, Hong JH, Kim CH, et al. Ischemic Diffusion Lesion Reversal After Endovascular Treatment. *Stroke*. 2019;50(6):1504-9.
17. Smith CA, Carpenter KL, Hutchinson PJ, Smielewski P, Helmy A. Candidate neuroinflammatory markers of cerebral autoregulation dysfunction in human acute brain injury. *J Cereb Blood Flow Metab*. 2023;43(8):1237-53.
18. Ostergaard L, Jespersen SN, Engedahl T, Gutierrez Jimenez E, Ashkanian M, Hansen MB, et al. Capillary dysfunction: its detection and causative role in dementias and stroke. *Curr Neurol Neurosci Rep*. 2015;15(6):37.
19. Jespersen SN, Ostergaard L. The roles of cerebral blood flow, capillary transit time heterogeneity, and oxygen tension in brain oxygenation and metabolism. *J Cereb Blood Flow Metab*. 2012;32(2):264-77.

20. Rasmussen PM, Jespersen SN, Østergaard L. The effects of transit time heterogeneity on brain oxygenation during rest and functional activation. *J Cereb Blood Flow Metab.* 2015;35(3):432-42.
21. Engedal TS, Hjort N, Hougaard KD, Simonsen CZ, Andersen G, Mikkelsen IK, et al. Transit time homogenization in ischemic stroke - A novel biomarker of penumbral microvascular failure? *J Cereb Blood Flow Metab.* 2018;38(11):2006-20.
22. Pérez-Bárcena J, Goedhart P, Ibáñez J, Brell M, García R, Llinás P, et al. Direct observation of human microcirculation during decompressive craniectomy after stroke. *Crit Care Med.* 2011;39(5):1126-9.
23. Lee J, Gursoy-Ozdemir Y, Fu B, Boas DA, Dalkara T. Optical coherence tomography imaging of capillary reperfusion after ischemic stroke. *Appl Opt.* 2016;55(33):9526-31.
24. Ostergaard L, Jespersen SN, Mouridsen K, Mikkelsen IK, Jonsdottir KY, Tietze A, et al. The role of the cerebral capillaries in acute ischemic stroke: the extended penumbra model. *J Cereb Blood Flow Metab.* 2013;33(5):635-48.
25. Mouridsen K, Hansen MB, Ostergaard L, Jespersen SN. Reliable estimation of capillary transit time distributions using DSC-MRI. *J Cereb Blood Flow Metab.* 2014;34(9):1511-21.
26. Mundiyanapurath S, Ringleb PA, Diatschuk S, Hansen MB, Mouridsen K, Ostergaard L, et al. Capillary Transit Time Heterogeneity Is Associated with Modified Rankin Scale Score at Discharge in Patients with Bilateral High Grade Internal Carotid Artery Stenosis. *PLoS One.* 2016;11(6):e0158148.
27. Nielsen A, Hansen MB, Tietze A, Mouridsen K. Prediction of Tissue Outcome and Assessment of Treatment Effect in Acute Ischemic Stroke Using Deep Learning. *Stroke.* 2018;49(6):1394-401.
28. Ostergaard L, Sorensen AG, Chesler DA, Weisskoff RM, Koroshetz WJ, Wu O, et al. Combined diffusion-weighted and perfusion-weighted flow heterogeneity magnetic resonance imaging in acute stroke. *Stroke.* 2000;31(5):1097-103.
29. Brugnara G, Herweh C, Neuberger U, Bo Hansen M, Ulfert C, Mahmutoglu MA, et al. Dynamics of cerebral perfusion and oxygenation parameters following endovascular treatment of acute ischemic stroke. *J Neurointerv Surg.* 2022;14(1).
30. Mikkelsen IK, Jones PS, Ribe LR, Alawneh J, Puig J, Bekke SL, et al. Biased visualization of hypoperfused tissue by computed tomography due to short imaging duration: improved classification by image down-sampling and vascular models. *Eur Radiol.* 2015;25(7):2080-8.
31. Ajmi SC, Advani R, Fjetland L, Kurz KD, Lindner T, Qvindesland SA, et al. Reducing door-to-needle times in stroke thrombolysis to 13 min through protocol revision and simulation training: A quality improvement project in a Norwegian stroke centre. *BMJ Quality and Safety: BMJ Publishing Group;* 2019. p. 939-48.
32. Zaidat OO, Yoo AJ, Khatri P, Tomsick TA, von Kummer R, Saver JL, et al. Recommendations on angiographic revascularization grading standards for acute ischemic stroke: a consensus statement. *Stroke.* 2013;44(9):2650-63.
33. Soille P. *Morphological Image Analysis: Principles and Applications.* Springer-Verlag. 1999:pp. 173-4.
34. Biesbroek JM, Niesten JM, Dankbaar JW, Biessels GJ, Velthuis BK, Reitsma JB, van der Schaaf IC. Diagnostic accuracy of CT perfusion imaging for detecting acute ischemic stroke: a systematic review and meta-analysis. *Cerebrovasc Dis.* 2013;35(6):493-501.
35. Martins N, Aires A, Mendez B, Boned S, Rubiera M, Tomasello A, et al. Ghost Infarct Core and Admission Computed Tomography Perfusion: Redefining the Role of Neuroimaging in Acute Ischemic Stroke. *Interv Neurol.* 2018;7(6):513-21.
36. Nogueira RG, Jadhav AP, Haussen DC, Bonafe A, Budzik RF, Bhuva P, et al. Thrombectomy 6 to 24 Hours after Stroke with a Mismatch between Deficit and Infarct. *N Engl J Med.* 2018;378(1):11-21.
37. Albers GW, Marks MP, Kemp S, Christensen S, Tsai JP, Ortega-Gutierrez S, et al. Thrombectomy for Stroke at 6 to 16 Hours with Selection by Perfusion Imaging. *N Engl J Med.* 2018;378(8):708-18.

38. Thomalla G, Simonsen CZ, Boutitie F, Andersen G, Berthezene Y, Cheng B, et al. MRI-Guided Thrombolysis for Stroke with Unknown Time of Onset. *N Engl J Med*. 2018;379(7):611-22.
39. Ma H, Campbell BCV, Parsons MW, Churilov L, Levi CR, Hsu C, et al. Thrombolysis Guided by Perfusion Imaging up to 9 Hours after Onset of Stroke. *N Engl J Med*. 2019;380(19):1795-803.
40. Goyal M, Menon BK, van Zwam WH, Dippel DWJ, Mitchell PJ, Demchuk AM, et al. Endovascular thrombectomy after large-vessel ischaemic stroke: a meta-analysis of individual patient data from five randomised trials. *The Lancet*. 2016;387(10029):1723-31.
41. Shi ZS, Liebeskind DS, Xiang B, Ge SG, Feng L, Albers GW, et al. Predictors of functional dependence despite successful revascularization in large-vessel occlusion strokes. *Stroke*. 2014;45(7):1977-84.
42. Staehr C, Giblin JT, Gutiérrez-Jiménez E, Gulbrandsen H, Tang J, Sandow SL, et al. Neurovascular Uncoupling Is Linked to Microcirculatory Dysfunction in Regions Outside the Ischemic Core Following Ischemic Stroke. *J Am Heart Assoc*. 2023;12(11):e029527.
43. Bang OY, Saver JL, Buck BH, Alger JR, Starkman S, Ovbiagele B, et al. Impact of collateral flow on tissue fate in acute ischaemic stroke. *J Neurol Neurosurg Psychiatry*. 2008;79(6):625-9.
44. Bang OY, Saver JL, Kim SJ, Kim GM, Chung CS, Ovbiagele B, et al. Collateral flow predicts response to endovascular therapy for acute ischemic stroke. *Stroke*. 2011;42(3):693-9.
45. Pham M, Bendszus M. Facing Time in Ischemic Stroke: An Alternative Hypothesis for Collateral Failure. *Clin Neuroradiol*. 2016;26(2):141-51.
46. del Zoppo GJ, Schmid-Schönbein GW, Mori E, Copeland BR, Chang CM. Polymorphonuclear leukocytes occlude capillaries following middle cerebral artery occlusion and reperfusion in baboons. *Stroke*. 1991;22(10):1276-83.
47. Dalkara T, Arsava EM. Can restoring incomplete microcirculatory reperfusion improve stroke outcome after thrombolysis? *J Cereb Blood Flow Metab*. 2012;32(12):2091-9.
48. Alexandrov AV, Hall CE, Labiche LA, Wojner AW, Grotta JC. Ischemic stunning of the brain: early recanalization without immediate clinical improvement in acute ischemic stroke. *Stroke*. 2004;35(2):449-52.
49. Mujanovic A, Ng F, Meinel TR, Dobrocky T, Piechowiak EI, Kurmann CC, et al. No-reflow phenomenon in stroke patients: A systematic literature review and meta-analysis of clinical data. *Int J Stroke*. 2023;17474930231180434.
50. El Amki M, Wegener S. Improving Cerebral Blood Flow after Arterial Recanalization: A Novel Therapeutic Strategy in Stroke. *Int J Mol Sci*. 2017;18(12).
51. Mollet I, Marto JP, Mendonça M, Baptista MV, Vieira HLA. Remote but not Distant: a Review on Experimental Models and Clinical Trials in Remote Ischemic Conditioning as Potential Therapy in Ischemic Stroke. *Mol Neurobiol*. 2021:1-32.
52. Livne M, Kossen T, Madai VI, Zaro-Weber O, Moeller-Hartmann W, Mouridsen K, et al. Multiparametric Model for Penumbra Flow Prediction in Acute Stroke. *Stroke*. 2017;48(7):1849-54.
53. Campbell BC, Christensen S, Levi CR, Desmond PM, Donnan GA, Davis SM, Parsons MW. Comparison of computed tomography perfusion and magnetic resonance imaging perfusion-diffusion mismatch in ischemic stroke. *Stroke*. 2012;43(10):2648-53.
54. Lin L, Bivard A, Levi CR, Parsons MW. Comparison of computed tomographic and magnetic resonance perfusion measurements in acute ischemic stroke: back-to-back quantitative analysis. *Stroke*. 2014;45(6):1727-32.
55. Austein F, Riedel C, Kerby T, Meyne J, Binder A, Lindner T, et al. Comparison of Perfusion CT Software to Predict the Final Infarct Volume After Thrombectomy. *Stroke*. 2016;47(9):2311-7.
56. Dani KA, Thomas RG, Chappell FM, Shuler K, MacLeod MJ, Muir KW, Wardlaw JM. Computed tomography and magnetic resonance perfusion imaging in ischemic stroke: definitions and thresholds. *Ann Neurol*. 2011;70(3):384-401.
57. Kemmling A, Flottmann F, Forkert ND, Minnerup J, Heindel W, Thomalla G, et al. Multivariate dynamic prediction of ischemic infarction and tissue salvage as a function of time and degree of recanalization. *J Cereb Blood Flow Metab*. 2015;35(9):1397-405.

58. Kasasbeh AS, Christensen S, Parsons MW, Campbell B, Albers GW, Lansberg MG. Artificial Neural Network Computer Tomography Perfusion Prediction of Ischemic Core. *Stroke*. 2019;50(6):1578-81.
59. Tomasetti L, Engan K, Khanmohammadi M, Kurz KD. CNN Based Segmentation of Infarcted Regions in Acute Cerebral Stroke Patients From Computed Tomography Perfusion Imaging. *Proceedings of the 11th ACM International Conference on Bioinformatics, Computational Biology and Health Informatics; Virtual Event, USA: Association for Computing Machinery; 2020*. p. Article 59.
60. Ito H, Kanno I, Fukuda H. Human cerebral circulation: positron emission tomography studies. *Ann Nucl Med*. 2005;19(2):65-74.
61. Leenders KL, Perani D, Lammertsma AA, Heather JD, Buckingham P, Healy MJ, et al. Cerebral blood flow, blood volume and oxygen utilization. Normal values and effect of age. *Brain*. 1990;113 ( Pt 1):27-47.
62. Last D, Alsop DC, Abduljalil AM, Marquis RP, de Bazelaire C, Hu K, et al. Global and regional effects of type 2 diabetes on brain tissue volumes and cerebral vasoreactivity. *Diabetes Care*. 2007;30(5):1193-9.
63. Liu J, Yang X, Li Y, Xu H, Ren J, Zhou P. Cerebral Blood Flow Alterations in Type 2 Diabetes Mellitus: A Systematic Review and Meta-Analysis of Arterial Spin Labeling Studies. *Front Aging Neurosci*. 2022;14:847218.

## Appendix


	NCCT of the head	CTA of precerebral and intracranial arteries	CTP
kV	120 (CarekV off)	100 (CarekV on)	80
mAs	280 (CareDose off)	160 (CareDose on)	200
Rotation time (s)	1	0.28	0.28
Slice collimation	3 mm c 20 x 0.6 mm	0.6 mm c 128 x 0.6 mm	5 mm c 32 x 1.2 mm
Pitch	0.55	1.0	-
X-care	Yes	No	No
IV contrast	No	60 ml Omnipaque 350 mg I/ml + 40 ml NaCl	40 ml Omnipaque 350 mg I/ml + 40 ml NaCl
Flow rate	-	5 ml/s	6 ml/s
Start delay	-	4 s	4 s, ≥60 s after CTA
Scan direction	Caudocranial	Craniocaudal	Caudocranial

Computed Tomography Technical Protocol for Acute Ischemic Stroke.

Note: Spiral scan technique, head first, supine. CTA, computed tomography angiography; CTP, perfusion computed tomography; kV, kilovolt; mAs, milliampere-seconds; ml/s, milliliters per second; NCCT, Non-contrast enhanced computed tomography; s, seconds.

## ORIGINAL ARTICLE

# Simulation-based team-training in acute stroke: Is it safe to speed up?

Liv Jorunn Høllesli<sup>1,2</sup>  | Soffien Chadli Ajmi<sup>3,4</sup> | Martin W. Kurz<sup>3,5</sup> |  
 Thomas Bailey Tysland<sup>3</sup> | Morten Hagir<sup>6</sup> | Ingvild Dalen<sup>7</sup> | Sigrun Anna Qvindesland<sup>8</sup> |  
 Hege Ersdal<sup>9,10</sup> | Kathinka D. Kurz<sup>1,2</sup>

<sup>1</sup>Stavanger Medical Imaging Laboratory (SMIL), Department of Radiology, Stavanger University Hospital, Stavanger, Norway

<sup>2</sup>Department of Electrical Engineering and Computer Science, University of Stavanger, Stavanger, Norway

<sup>3</sup>Neurology Research Group, Department of Neurology, Stavanger University Hospital, Stavanger, Norway

<sup>4</sup>Department of Quality and Health Technology, University of Stavanger, Stavanger, Norway

<sup>5</sup>Department of Clinical Medicine, University of Bergen, Bergen, Norway

<sup>6</sup>Department of Radiology, Hospital of Southern Norway Kristiansand, Kristiansand, Norway

<sup>7</sup>Department of Research, Section of Biostatistics, Stavanger University Hospital, Stavanger, Norway

<sup>8</sup>Department of Research, Simulation Section, Stavanger University Hospital, Stavanger, Norway

<sup>9</sup>Critical Care and Anesthesiology Research Group, Stavanger University Hospital, Stavanger, Norway

<sup>10</sup>Faculty of Health Sciences, University of Stavanger, Stavanger, Norway

## Correspondence

Liv Jorunn Høllesli, Stavanger Medical Imaging Laboratory (SMIL), Department of Radiology, Stavanger University Hospital, Postboks 8100, 4068 Stavanger, Norway.  
 Email: [liv.jorunn.hollesli@sus.no](mailto:liv.jorunn.hollesli@sus.no)

## Abstract

**Background:** In acute ischemic stroke (AIS), rapid treatment with intravenous thrombolysis (IVT) is crucial for good clinical outcome. Weekly simulation-based team-training of the stroke treatment team was implemented, resulting in faster treatment times. The aim of this study was to assess whether this time reduction led to a higher proportion of stroke mimics (SMs) among patients who received IVT for presumed AIS, and whether these SM patients were harmed by intracranial hemorrhage (ICH).

**Methods:** All suspected AIS patients treated with IVT between January 1, 2015 and December 31, 2020 were prospectively registered. In 2017, weekly in situ simulation-based team-training involving the whole stroke treatment team was introduced. To analyze possible unintended effects of simulation training, the proportion of SMs among patients who received IVT for presumed AIS were identified by clinical and radiological evaluation. Additionally, we identified the extent of symptomatic ICH (sICH) in IVT-treated SM patients.

**Results:** From 2015 to 2020, 959 patients were treated with IVT for symptoms of AIS. After introduction of simulation training, the proportion of patients treated with IVT who were later diagnosed as SMs increased significantly (15.9% vs. 24.4%,  $p = .003$ ). There were no ICH complications in the SM patients treated before, whereas two SM patients suffered from asymptomatic ICH after introduction of simulation training ( $p = 1.0$ ). When subgrouping SMs into prespecified categories, only the group diagnosed with peripheral vertigo increased significantly (2.5% vs. 8.6%,  $p < .001$ ).

**Conclusions:** Simulation training of the acute stroke treatment team was associated with an increase in the proportion of patients treated with IVT for a suspected AIS who were later diagnosed with peripheral vertigo. The proportion of other SM groups

This is an open access article under the terms of the [Creative Commons Attribution](https://creativecommons.org/licenses/by/4.0/) License, which permits use, distribution and reproduction in any medium, provided the original work is properly cited.

© 2022 The Authors. *Brain and Behavior* published by Wiley Periodicals LLC.



among IVT-treated patients did not change significantly. No sICH was detected in IVT-treated SM patients.

**KEYWORDS**

intracranial hemorrhages, ischemic stroke, patient safety, simulation training, thrombolytic therapy

## 1 | INTRODUCTION

Ischemic stroke is a major cause of morbidity and mortality worldwide (Feigin et al., 2017; Wafa et al., 2020). The global burden of stroke is increasing, especially in younger age groups in low–moderate-income countries (Katan & Luft, 2018; Virani et al., 2020). The main therapeutic target in acute ischemic stroke (AIS) is timely recanalization of the occluded vessel. Rapid recognition of stroke symptoms, patient transfer, diagnostics, and acute treatment, including intravenous thrombolysis (IVT) and/or endovascular thrombectomy (EVT), are of vital importance and significantly improve outcomes in stroke patients (Powers et al., 2019). The therapy should be given as fast as possible, as the clinical outcome improves if therapy is given timely (Advani et al., 2017; Meretoja et al., 2014, 2017). In order to reduce treatment times in AIS patients, we have introduced weekly in situ simulation-based team-training sessions for the stroke treatment team. This led to a reduction of the median door-to-needle time (DNT) from 27 to 13 minutes and reduced patient morbidity and mortality (Ajmi et al., 2019).

Stroke mimics (SMs) are common and comprise up to 43% of patients presenting with acute neurological symptoms in the prehospital phase (McClelland et al., 2019; Tarnutzer et al., 2017). Due to the possibility of bleeding complications, IVT treatment of SMs poses a potential risk for the patients (Hacke et al., 2008; National Institute of Neurological Disorders and Stroke rt-PA Stroke Study Group, 1995); furthermore, the treatment is associated with an increased resource and cost burden to hospitals and society (Goyal et al., 2015).

The aim of this study was to evaluate whether simulation training for the stroke treatment team led to a higher proportion of SMs among patients who received IVT for presumed AIS, and whether these patients were harmed by intracranial hemorrhage (ICH).

## 2 | MATERIALS AND METHODS

### 2.1 | Patients

All patients with suspected AIS treated with IVT between January 1, 2015 and December 31, 2020 were prospectively registered in a local research database. All relevant data-endpoints, including ICH and the final diagnosis, were registered in this database. On February 1, 2017, repeated clusters with weekly in situ simulation-based team-training involving the stroke treatment team were introduced. Patients treated

before the introduction of the simulation training served as control group.

Vertigo patients were IVT treated if the symptoms were deemed to be of cerebrovascular origin. The IVT decision was made by the neurologic team on call (resident and senior consultant) and comprised both clinical findings and results of the radiological investigations.

### 2.2 | Simulation training

We performed clusters of in situ simulation-based team-training using acute stroke scenarios, simulating both the emergency medical services (EMS) and the in-hospital stroke care pathway from calling the EMS to administration of IVT. The simulated cases presented with FAST symptoms (face–arm–speech, and aphasia or dysarthria). Vertigo symptoms were not simulated. All in-hospital stroke treatment team members and paramedics on-call participated in the simulation training. Our primary aims were to reduce treatment times, to enhance protocol adherence, and to improve communication skills. Details of the simulation training have been described previously (Ajmi et al., 2019).

### 2.3 | Radiological evaluation

Patients with suspected AIS were routinely investigated with a CT protocol comprising non-contrast CT of the head, CT angiography of the precerebral and intracranial arteries and CT perfusion immediately after hospital admission. In most cases, this is followed by magnetic resonance imaging (MRI), including diffusion-weighted imaging (DWI) during the first days after hospital admission. Supplementary CT or MRI examinations were performed in patients with clinical deterioration. In most patients with suspected wake-up stroke or with unknown symptom onset time, MRI, including DWI and fluid-attenuated inversion recovery, was routinely used as a first-line diagnostic tool. If the neurological symptoms were deemed to be of cerebrovascular origin, patients were IVT treated also in cases of negative initial MRI (Edlow et al., 2017).

### 2.4 | Clinical evaluation

Neurological impairment on admission was assessed using the National Institutes of Health Stroke Scale (NIHSS). NIHSS was performed at

hospital admission, repeatedly after IVT, and on the day of hospital discharge. Functional outcome at 3 months was evaluated using modified Rankin Scale (mRS) assessed by a certified stroke nurse by means of a telephone interview. Good functional outcome was defined as mRS score 0–2, and poor functional outcome was defined as mRS score 3–6.

SMs were defined as patients who presented with stroke-like symptoms, but after diagnostic work-up were determined not to have suffered from a stroke episode. Evaluation of the clinical course, examination by all specialists involved (typically neurologists, ear, nose and throat specialists, or cardiologists), and evaluation with MRI were all part of the diagnostic work-up. SMs were diagnosed during their hospital stay and then retrospectively categorized into eight different subgroups: psychiatric disorders, peripheral vertigo, epilepsy, migraine, infectious diseases, intoxication, peripheral facial palsy and other.

ICH was classified according to the European Cooperative Acute Stroke Study II (ECASS II) (Hacke et al., 1998); symptomatic ICH (sICH) was defined as ICH associated with a NIHSS deterioration of four points or more.

## 2.5 | Statistics

All statistical analyses were performed using SPSS Statistics version 24 (IBM Cooperation, Armonk, NY, USA). Categorical variables are presented as count (percent, %) and continuous variables as median (interquartile range, IQR). Changes in proportions were evaluated using Pearson Chi-squared test or Fisher's exact test, as appropriate. Changes in continuous variables were evaluated using the Mann-Whitney test.

## 2.6 | Ethical approval

All procedures involving human participants were performed in accordance with the ethical standards of the institutional and/or national research committee and with the 1964 Helsinki Declaration and its later amendments or comparable ethical standards. This study was approved by the regional ethical committee and the local hospital authorities. Informed consent was waived, after approval of the regional ethical committee.

## 3 | RESULTS

From 2015 to 2020, 959 patients were treated with IVT under suspicion of AIS (Table 1). The proportion of IVT treatments varied between 22.8% and 30.8%.

In 2015 and 2016, the years before introduction of simulation-based team-training, the proportion of SMs among IVT-treated patients was 12.6% and 18.5%, respectively. In 2017, the year simulation training started, the proportion of SMs was 14.8%. Between 2018 and 2020, years with ongoing simulation training, the proportion of

SMs was 27.8% (24.0%–32.1%, Table 1). A significant increase was registered between 2017 and 2018 ( $p = .003$ ). 2018 was the first complete year with simulation training. Treatment times dropped significantly between 2016 and 2017, after introduction of the simulation training ( $p < .001$ ) (Table 1).

Baseline characteristics and cerebrovascular risk factors of patients treated with IVT are described in Table 2. Before introduction of simulation-based team-training in February 2017, 320 patients were treated with IVT, 639 patients thereafter (Table 1). Patients treated with IVT after introduction of simulation-based team-training had significantly less atrial fibrillation ( $p = .004$ ); otherwise, there were no statistically significant differences in baseline variables (Table 2).

The clinical outcome of the patients before and after implementation of simulation-based team-training did not differ in our patient group (Table 3). The proportion of SMs among IVT-treated patients rose from 51 (15.9%) before introduction of simulation-based team-training to 156 (24.4%) thereafter ( $p = .003$ ). There were no bleeding complications in the SM patients treated before introduction of simulation-based team-training, whereas two (1.3% of 156) SM patients suffered from asymptomatic ICH after introduction of simulation training ( $p = 1.0$ ). The ICH in one patient had a diameter of 5 mm and was located in the right frontal lobe, whereas the other patient was diagnosed with a small amount of blood in the subarachnoid space parieto-occipitally on the right side. None of the hemorrhages were accompanied with neurological deterioration. The two SM patients with ICH had a DNT of 22 and 49 min, respectively.

When subgrouping SMs into prespecified categories, there was a significantly higher proportion of patients with peripheral vertigo (8 patients/2.5% vs. 55 patients/8.6%,  $p < .001$ ) among IVT-treated patients (Table 4) after implementation of simulation training. There were no significant changes in the proportion of other SM categories.

## 4 | DISCUSSION

Introduction of simulation-based team-training in 2017 was accompanied by a significant increase in the proportion of patients treated with IVT for a presumed AIS who were later diagnosed as SMs (15.9% vs. 24.4%,  $p = .003$ ), consisting mainly of patients with peripheral vertigo. This increase was not seen during the first year of simulation training (Ajmi et al., 2019). Possibly, the rise has been supported by an evolving fear to harm patients by withholding IVT in ambiguous cases, by some insecurity in the clinical evaluation of vertigo patients, and by the recognition that IVT in SMs is rarely associated with complications (Moulin & Leys, 2019).

The overall number of stroke admissions showed a tendency to increase during the period 2015–2020, with an exception of 2019, whereas the proportion of IVT treatments fluctuated. The increasing number of stroke admissions may be explained by a general increased awareness of stroke symptoms and the importance of rapid treatment. We do not have a clear explanation for the decrease in the number of stroke admissions in 2019, nor the fluctuation in the proportion of IVT treatments.

**TABLE 1** Number of stroke admissions, intravenous thrombolysis (%) and stroke mimics (%) between 2015 and 2020

	2015	2016	2017	2018	2019	2020
Stroke admissions	438	578	674	614	498	627
IVT treatments (%)	127 (29.0)	178 (30.8)	182 (27.0)	140 (22.8)	140 (28.1)	192 (30.6)
Stroke mimics (%)	16 (12.6)	33 (18.5)	27 (14.8)	40 (28.6)	45 (32.1)	46 (24.0)
DNT, median (IQR)	30 (22, 45) (n = 113)	25 (17, 37) (n = 175)	15 (9, 29) (n = 174)	17 (11, 30) (n = 136)	16 (11, 30) (n = 137)	20 (13, 35) (n = 184)

Note: Stroke mimics: Percent is calculated from the number of patients IVT treated for suspected acute ischemic stroke. Simulation-based team-training started on February 1, 2017.

Abbreviations: DNT, door-to-needle time (all IVT-treated patients, including wake-up and in-house stroke); IQR, interquartile range; IVT, intravenous thrombolysis.

**TABLE 2** Patient baseline characteristics and cerebrovascular risk factors before and after implementation of simulation training

	Before simulation training (n = 320)	After simulation training (n = 639)	p-Value
Age, median (IQR)	71 (59, 81)	69 (55, 80)	.076
Sex—female	135 (42.2)	296 (46.3)	.23
Hypertension	145 (45.3)	259 (40.5)	.16
Diabetes	40 (12.5)	89 (13.9)	.54
Atrial fibrillation	47 (14.7)	55 (8.6)	.004
Prior stroke	71 (22.2)	132 (20.7)	.58

Note: Data presented as count (%) unless otherwise stated.

Abbreviation: IQR, interquartile range.

**TABLE 3** Clinical outcome before and after implementation of simulation training

	Before simulation training (n = 320)	After simulation training (n = 639)	p-Value
NIHSS score at admission. Median, (IQR)	3 (2, 7) (n = 313)	3 (1, 6) (n = 627)	.023
NIHSS score at dismissal. Median, (IQR)	0 (0, 1) (n = 279)	0 (0, 1) (n = 579)	.50
mRS score 0–2 at 3 months. N (%)	179 (72.8) (n = 246)	321 (75.2) (n = 428)	.49

Abbreviations: IQR, interquartile range; mRS, modified Rankin Scale; N = number of patients; NIHSS, National Institutes of Health Stroke Scale.

**TABLE 4** Intravenous thrombolysis (IVT)-treated stroke mimic patients and final diagnoses before and after implementation of simulation training

	Before simulation training (n = 320)	After simulation training (n = 639)	p-Value
Stroke mimics total	51 (15.9)	156 (24.4)	.003
Psychiatric disorders	8 (2.5)	18 (2.3)	.88
Peripheral vertigo	8 (2.5)	55 (8.6)	<.001
Epilepsy	3 (0.9)	15 (2.3)	.13
Migraine	9 (2.8)	23 (3.6)	.69
Infectious diseases	3 (0.9)	6 (0.9)	1.00
Intoxication	2 (0.6)	3 (0.5)	1.00*
Peripheral facial palsy	2 (0.6)	3 (0.5)	1.00*
Other	16 (5.0)	33 (5.2)	.54

Note: Data presented as count (%). p-Values from Chi-squared test, except \* Fisher's exact test.

Before the start of simulation-based team-training, SM rates at our center were in the range of centers with CT-based patient selection (Kvistad et al., 2019). Although the numbers increase thereafter, they are still comparable to other centers (Pohl et al., 2021; Sporns et al., 2021). It is well known that the proportion of SMs among IVT-treated patients under the suspicion of AIS varies considerably and also depends on the initial imaging modality used. Centers with initial CT examination, and centers actively reducing treatment times, in general have higher SM rates ranging up to 30% (Burton et al., 2017; Liberman et al., 2015). The increase of SM rates is likely to be multifactorial and related to a focus on time, the acceptance of lower diagnostic specificity, and an increased comfort to perform IVT in SMs (Psychogios & Tsvigoulis, 2021). This comfort is probably a result of the overwhelming evidence on the benefit from early treatment (Advani et al., 2017; Ajmi et al., 2019; Liberman et al., 2015; Meretoja et al., 2014) combined with the low bleeding risk in IVT-treated SMs (Kvistad et al., 2019; Pohl et al., 2021). Probably, this has influenced the increasing IVT rates in SMs also at our center, shaping a culture where IVT treatment of SMs is more accepted than avoiding to give IVT to true stroke patients who could have been treated. Yet, as our study period spans over 6 years, other factors may have contributed to the increase of SM rates: Randomized controlled trials established the safety and efficacy of EVT in patients with large vessel occlusions (Berkhemer et al., 2015; Campbell et al., 2015; Jovin et al., 2015; Saver et al., 2015), MRI-guided thrombolysis for stroke with unknown time of onset was introduced (Thomalla et al., 2018), and thrombolysis in the extended time window was established (Ma et al., 2019; Nogueira et al., 2018). These developments have surely contributed to change the culture of acute stroke treatment toward less restrictions for giving IVT treatment. Simulation training is a tool helping to adapt in this cultural change. It is important to underline that the learning effect of simulation is optimized if directly connected to health service priorities and patient outcomes (translational simulation) (Nickson et al., 2021).

Introduction of MRI in the initial stroke diagnosis algorithm reduces the proportion of SMs treated, increasing the initial diagnostic specificity (Bhattacharya et al., 2013; Burton et al., 2017). Most departments with both modalities available in the emergency room setting have adopted a stroke imaging algorithm containing both CT and MRI modalities (Hetts & Khangura, 2019). This seems unavoidable as imaging of the ischemic penumbra has become increasingly complex, and advanced imaging protocols have been introduced, not only for the extended time window (Albers et al., 2018; Goyal et al., 2020; Ma et al., 2019; Nogueira et al., 2018). Yet, a small but significant percentage of patients with AIS have initial negative MRI scans, and thus, we have IVT treated some SM patients without DWI lesion on initial MRI (Burton et al., 2017; Edlow et al., 2017).

The increase of SMs treated with IVT at our center was not associated with a significant increase in bleeding complications. During the 4-year study period, only 2 of 156 IVT-treated SMs were diagnosed with ICH after IVT, and both were clinically asymptomatic. The rate of ICH in SMs is generally low. In the NOR-TEST study, none of the IVT-treated SMs exhibited a sICH (Kvistad et al., 2019). A current review concluded with an overall ICH rate as low as 0.7% (Pohl et al., 2021).

Peripheral vertigo was the most frequent SM thrombolysed in this cohort and the only SM category with a significant increase after implementation of simulation training. In the literature, peripheral vertigo accounts for 23.2% of SMs (Pohl et al., 2021). Before the introduction of simulation-based team-training, peripheral vertigo accounted for 2.5% of our patients, rising to 8.6% afterwards ( $p < .001$ ). Peripheral vertigo seems to be a main challenge for stroke physicians and is frequently misinterpreted as stroke in the initial phase. Patients with acute vertigo account for about 4% of all emergency room visits and 20% of emergency room neurological consultations (Newman-Toker et al., 2008). Although most of the patients presenting with vertigo suffer from benign disorders, up to 27% can end up with serious diagnoses, and cerebral stroke is the underlying cause in 4%–15% of these patients (Newman-Toker et al., 2008; Royle et al., 2011). The clinical differentiation between peripheral and central causes of vertigo is posing a challenge in the acute setting. Usually, vertigo of cerebrovascular causes is accompanied by other neurological symptoms. Yet, stroke in the posterior circulation can mimic peripheral vestibular syndromes, especially infarction in the territory of the anterior inferior cerebellar artery can present clinically with neuro-otological symptoms as combined loss of auditory and vestibular functions (Lee et al., 2009).

In order to support clinical decision-making, the three-step bedside oculomotor examination HiNTS (Head impulse, Nystagmus, Test of Skew) is a useful tool discriminating central and peripheral causes of vertigo (Kattah et al., 2009). The study emphasizes that the HiNTS examination is more sensitive for stroke than early MRI, the latter potentially being false negative in up to 12% of stroke patients presenting with acute vestibular syndrome during the first 48 h. Systematic testing with HiNTS of patients presenting with dizziness and vertigo has not been part of our clinical routine. We plan to add HiNTS for this patient group with implementation in the clinical routine through simulation training.

The proportion of IVT-treated SM patients in the other SM categories in our study did not change significantly after the introduction of simulation-based training. Migraine was the second most common SM, followed by psychiatric disorders and epilepsy (Table 4). Migraine accounts for about 8% of SMs (Pohl et al., 2021). Accompanying aura symptoms can easily be interpreted as a possible stroke, especially if present before or without headache (Otlivanchik & Liberman, 2019). Basilar migraine can present with symptoms from the posterior cerebral artery territory, hemiplegic migraine is rare but poses an obvious challenge in the initial assessment of the patients (Pohl et al., 2021). Psychiatric disorders are responsible for about 10% of all SMs (Pohl et al., 2021). Symptoms are often atypical and fluctuating. Previous psychiatric history is common, and physical examination often reveals inconsistent findings with repeated examinations. The prognosis for full recovery is rather poor with more than one third of patients reporting the same or worse deficits during follow-up (Gelauff et al., 2014). Seizures are responsible for 13% of SMs (Pohl et al., 2021). Postictal paresis and dysphasia can be misinterpreted as an acute stroke, especially if the seizure was unwitnessed. Early seizures occur in 3.8% of all ischemic stroke cases and 1.5% present with a seizure at the onset of stroke symptoms (Feher et al., 2020). Multimodal brain imaging and the

use of MRI in the acute phase may aid in the differentiation of ischemia versus seizure.

Although IVT in SMs is considered to be safe and the cost of under-treatment in acute stroke is high, the high number of IVT-treated SMs poses a potential medical risk (i.e., ICH) and an economical challenge. Administration of IVT to patients with SM is associated with excess costs, including costs of unnecessary hospital admission, drug-cost, and the excess cost of a higher care level. The total cost of IVT-treated SMs in the US (based on 2013 financial estimates) was approximately 15 million dollars per year with an average hospital direct cost of \$3600 per admission (Goyal et al., 2015). Understanding which patients constitute the biggest challenge and implementing adequate measures might therefore have important implications. Some patients present with suspected AIS, with symptoms resolving after IVT and with no DWI lesion on follow-up MRI. MRI can also be false negative in patients with AIS, especially in the posterior fossa (Edlow et al., 2017). This might cause a diagnostic challenge, with some patients actually having suffered from an ischemic event being diagnosed as SM, contributing to some overestimation of SM rates (Edlow et al., 2017). This emphasizes the critical importance of taking a complete medical history and doing a thorough clinical evaluation in the work-up of patients with suspected SM. An incorrect SM diagnosis may have serious implications for the patients (acute treatment and secondary prophylactic therapy).

This study has several limitations. It is a single center analysis and although we have analyzed over several years, the numbers presented are rather small. Additionally, patients treated with IVT after introduction of simulation-based team-training had significantly less atrial fibrillation, possibly lowering the number of true strokes in our study group. Yet, we are presenting consecutive patient treatment result data spanning over several years in the only stroke-treating hospital in the study's geographical area. Thus, we are able to present population-based numbers and avoid selection and patient transfer bias. However, a challenge in simulation training in general is to firmly establish a cause-effect relationship. We found a significant increase in the proportion of SMs among patients who received IVT for presumed AIS after implementation of simulation training. However, as previously discussed, other factors could also have contributed to this increase.

In summary, implementation of in situ simulation-based team-training for the acute stroke treatment team seems to be safe, but was associated with a significant increase in the proportion of patients treated with IVT who were later diagnosed as SMs, constituted mainly of patients with peripheral vertigo. This emphasizes the need of accompanying and correcting quality improvement measures tailored to patients presenting with dizziness and vertigo.

#### CONFLICT OF INTEREST

The authors declare no conflict of interest.

#### DATA AVAILABILITY STATEMENT

The data that support the findings of this study are available from the corresponding author upon reasonable request.

#### ORCID

Liv Jorunn HølleSLI  <https://orcid.org/0000-0001-9311-0476>

#### PEER REVIEW

The peer review history for this article is available at <https://publons.com/publon/10.1002/brb3.2814>

#### REFERENCES

- Advani, R., Naess, H., & Kurz, M. W. (2017). The golden hour of acute ischemic stroke. *Scandinavian Journal of Trauma, Resuscitation and Emergency Medicine*, 25(1), 54. <https://doi.org/10.1186/s13049-017-0398-5>
- Ajmi, S. C., Advani, R., Fjetland, L., Kurz, K. D., Lindner, T., Qvindesland, S. A., Ersdal, H., Goyal, M., Kvaløy, J. T., & Kurz, M. (2019). Reducing door-to-needle times in stroke thrombolysis to 13 min through protocol revision and simulation training: A quality improvement project in a Norwegian stroke centre. *BMJ Quality & Safety*, 28(11), 939–948. <https://doi.org/10.1136/bmjqs-2018-009117>
- Albers, G. W., Marks, M. P., Kemp, S., Christensen, S., Tsai, J. P., Ortega-Gutierrez, S., Mctaggart, R. A., Torbey, M. T., Kim-Tenser, M., Leslie-Mazwi, T., Sarraj, A., Kasner, S. E., Ansari, S. A., Yeatts, S. D., Hamilton, S., Mlynash, M., Heit, J. J., Zaharchuk, G., Kim, S., ... Lansberg, M. G. (2018). Thrombectomy for stroke at 6 to 16 hours with selection by perfusion imaging. *New England Journal of Medicine*, 378(8), 708–718. <https://doi.org/10.1056/NEJMoa1713973>
- Berkhemer, O. A., Fransen, P. S. S., Beumer, D., Van Den Berg, L. A., Lingsma, H. F., Yoo, A. J., Schonewille, W. J., Vos, J. A., Nederkoorn, P. J., Wermer, M. J. H., Van Walderveen, M. A. A., Staals, J., Hofmeijer, J., Van Oostayen, J. A., Lycklama à Nijeholt, G. J., Boiten, J., Brouwer, P. A., Emmer, B. J., De Bruijn, S. F., ... Dippel, D. W. J. (2015). A randomized trial of intraarterial treatment for acute ischemic stroke. *New England Journal of Medicine*, 372(1), 11–20. <https://doi.org/10.1056/NEJMoa1411587>
- Bhattacharya, P., Nagaraja, N., Rajamani, K., Madhavan, R., Santhakumar, S., & Chaturvedi, S. (2013). Early use of MRI improves diagnostic accuracy in young adults with stroke. *Journal of the Neurological Sciences*, 324(1–2), 62–64. <https://doi.org/10.1016/j.jns.2012.10.002>
- Burton, T. M., Luby, M., Nadareishvili, Z., Benson, R. T., Lynch, J. K., Latour, L. L., & Hsia, A. W. (2017). Effects of increasing IV tPA-treated stroke mimic rates at CT-based centers on clinical outcomes. *Neurology*, 89(4), 343–348. <https://doi.org/10.1212/WNL.0000000000004149>
- Campbell, B. C. V., Mitchell, P. J., Kleinig, T. J., Dewey, H. M., Churilov, L., Yassi, N., Yan, B., Dowling, R. J., Parsons, M. W., Oxley, T. J., Wu, T. Y., Brooks, M., Simpson, M. A., Miteff, F., Levi, C. R., Krause, M., Harrington, T. J., Faulder, K. C., Steinfurt, B. S., ... Davis, S. M. (2015). Endovascular therapy for ischemic stroke with perfusion-imaging selection. *New England Journal of Medicine*, 372(11), 1009–1018. <https://doi.org/10.1056/NEJMoa1414792>
- Edlow, B. L., Hurwitz, S., & Edlow, J. A. (2017). Diagnosis of DWI-negative acute ischemic stroke: A meta-analysis. *Neurology*, 89(3), 256–262. <https://doi.org/10.1212/WNL.0000000000004120>
- Feher, G., Gurdan, Z., Gombos, K., Koltai, K., Pusch, G., Tibold, A., & Szapary, L. (2020). Early seizures after ischemic stroke: Focus on thrombolysis. *CNS Spectrums*, 25(1), 101–113. <https://doi.org/10.1017/s1092852919000804>
- Feigin, V. L., Norrving, B. o., & Mensah, G. A. (2017). Global burden of stroke. *Circulation Research*, 120(3), 439–448. <https://doi.org/10.1161/CIRCRESAHA.116.308413>
- Gelauff, J., Stone, J., Edwards, M., & Carson, A. (2014). The prognosis of functional (psychogenic) motor symptoms: A systematic review. *Journal of Neurology, Neurosurgery, and Psychiatry*, 85(2), 220–226. <https://doi.org/10.1136/jnnp-2013-305321>
- Goyal, M., Ospel, J. M., Menon, B., Almekhlafi, M., Jayaraman, M., Fiehler, J., Psychogios, M., Chapot, R., Van Der Lugt, A., Liu, J., Yang, P., Agid, R.,

- Hacke, W., Walker, M., Fischer, U., Asdaghi, N., Mctaggart, R., Srivastava, P., Nogueira, R. G., ... Fisher, M. (2020). Challenging the ischemic core concept in acute ischemic stroke imaging. *Stroke: A Journal of Cerebral Circulation*, 51(10), 3147–3155. <https://doi.org/10.1161/strokeaha.120.030620>
- Goyal, N., Male, S., Al Wafai, A., Bellamkonda, S., & Zand, R. (2015). Cost burden of stroke mimics and transient ischemic attack after intravenous tissue plasminogen activator treatment. *Journal of Stroke and Cerebrovascular Diseases*, 24(4), 828–833. <https://doi.org/10.1016/j.jstrokecerebrovasdis.2014.11.023>
- Hacke, W., Kaste, M., Bluhmki, E., Brozman, M., Dávalos, A., Guidetti, D., Larrue, V., Lees, K. R., Medeghri, Z., Machnig, T., Schneider, D., Von Kummer, R., Wahlgren, N., & Toni, D. (2008). Thrombolysis with alteplase 3 to 4.5 hours after acute ischemic stroke. *New England Journal of Medicine*, 359(13), 1317–1329. <https://doi.org/10.1056/NEJMoa0804656>
- Hacke, W., Kaste, M., Fieschi, C., Von Kummer, R., Dávalos, A., Meier, D., Larrue, V., Bluhmki, E., Davis, S., Donnan, G., Schneider, D., Diez-Tejedor, E., & Trouillas, P. (1998). Randomised double-blind placebo-controlled trial of thrombolytic therapy with intravenous alteplase in acute ischaemic stroke (ECASS II). Second European-Australasian acute stroke study investigators. *Lancet*, 352(9136), 1245–1251. [https://doi.org/10.1016/s0140-6736\(98\)08020-9](https://doi.org/10.1016/s0140-6736(98)08020-9)
- Hettis, S., & Khangura, R. (2019). Imaging of acute stroke: Current state. *Radiologic Clinics of North America*, 57(6), 1083–1091. <https://doi.org/10.1016/j.rcl.2019.07.009>
- Jovin, T. G., Chamorro, A., Cobo, E., De Miquel, M. -A. A., Molina, C. A., Rovira, A., San Román, L., Serena, J. -N., Abilleira, S., Ribó, M., Millán, M., Urra, X., Cardona, P., López-Cancio, E., Tomasello, A., Castaño, C., Blasco, J., Aja, L. -A., Dorado, L., ... Dávalos, A. (2015). Thrombectomy within 8 hours after symptom onset in ischemic stroke. *New England Journal of Medicine*, 372(24), 2296–2306. <https://doi.org/10.1056/NEJMoa1503780>
- Katan, M., & Luft, A. (2018). Global burden of stroke. *Seminars in Neurology*, 38(2), 208–211. <https://doi.org/10.1055/s-0038-1649503>
- Kattah, J. C., Talkad, A. V., Wang, D. Z., Hsieh, Y. -H., & Newman-Toker, D. E. (2009). HINTS to diagnose stroke in the acute vestibular syndrome: Three-step bedside oculomotor examination more sensitive than early MRI diffusion-weighted imaging. *Stroke: A Journal of Cerebral Circulation*, 40(11), 3504–3510. <https://doi.org/10.1161/strokeaha.109.551234>
- Kvistad, C. E., Novotny, V., Næss, H., Hagberg, G., Ihle-Hansen, H., Waje-Andreassen, U., Thomassen, L., & Logallo, N. (2019). Safety and predictors of stroke mimics in the Norwegian tenecteplase stroke trial (NOR-TEST). *International Journal of Stroke*, 14(5), 508–516. <https://doi.org/10.1177/1747493018790015>
- Lee, H., Kim, J. S., Chung, E. -J., Yi, H. -A., Chung, I. -S., Lee, S. -R., & Shin, J. -Y. (2009). Infarction in the territory of anterior inferior cerebellar artery: Spectrum of audiovestibular loss. *Stroke: A Journal of Cerebral Circulation*, 40(12), 3745–3751. <https://doi.org/10.1161/STROKEAHA.109.564682>
- Lieberman, A. L., Liotta, E. M., Caprio, F. Z., Ruff, I., Maas, M. B., Bernstein, R. A., Khare, R., Bergman, D., & Prabhakaran, S. (2015). Do efforts to decrease door-to-needle time risk increasing stroke mimic treatment rates? *Neurology Clinical Practice*, 5(3), 247–252. <https://doi.org/10.1212/CPJ.0000000000000122>
- Ma, H., Campbell, B. C. V., Parsons, M. W., Churilov, L., Levi, C. R., Hsu, C., Kleinig, T. J., Wijeratne, T., Curtze, S., Dewey, H. M., Miteff, F., Tsai, C.-H., Lee, J.-T., Phan, T. G., Mahant, N., Sun, M.-C., Krause, M., Sturm, J., Grimley, R., ... Donnan, G. A. (2019). Thrombolysis guided by perfusion imaging up to 9 hours after onset of stroke. *New England Journal of Medicine*, 380(19), 1795–1803. <https://doi.org/10.1056/NEJMoa1813046>
- Mcclelland, G., Rodgers, H., Flynn, D., & Price, C. I. (2019). The frequency, characteristics and aetiology of stroke mimic presentations: A narrative review. *European Journal of Emergency Medicine*, 26(1), 2–8. <https://doi.org/10.1097/MEJ.0000000000000550>
- Meretoja, A., Keshkaran, M., Saver, J. L., Tatlisumak, T., Parsons, M. W., Kaste, M., Davis, S. M., Donnan, G. A., & Churilov, L. (2014). Stroke thrombolysis: Save a minute, save a day. *Stroke: A Journal of Cerebral Circulation*, 45(4), 1053–1058. <https://doi.org/10.1161/strokeaha.113.002910>
- Meretoja, A., Keshkaran, M., Tatlisumak, T., Donnan, G. A., & Churilov, L. (2017). Endovascular therapy for ischemic stroke: Save a minute-save a week. *Neurology*, 88(22), 2123–2127. <https://doi.org/10.1212/wnl.0000000000003981>
- Moulin, S., & Leys, D. (2019). Stroke mimics and chameleons. *Current Opinion in Neurology*, 32(1), 54–59. <https://doi.org/10.1097/WCO.0000000000000620>
- National Institute of Neurological Disorders and Stroke rt-PA Stroke Study Group. (1995). Tissue plasminogen activator for acute ischemic stroke. *New England Journal of Medicine*, 333(24), 1581–1588. <https://doi.org/10.1056/NEJM199512143332401>
- Newman-Toker, D. E., Hsieh, Y.-H., Camargo, C. A., Pelletier, A. J., Butchy, G. T., & Edlow, J. A. (2008). Spectrum of dizziness visits to US emergency departments: Cross-sectional analysis from a nationally representative sample. *Mayo Clinic Proceedings*, 83(7), 765–775. <https://doi.org/10.4065/83.7.765>
- Nickson, C. P., Petrosniak, A., Barwick, S., & Brazil, V. (2021). Translational simulation: From description to action. *Advances in Simulation (Lond)*, 6(1), 6. <https://doi.org/10.1186/s41077-021-00160-6>
- Nogueira, R. G., Jadhav, A. P., Haussen, D. C., Bonafe, A., Budzik, R. F., Bhuya, P., Yavagal, D. R., Ribo, M., Cognard, C., Hanel, R. A., Sila, C. A., Hassan, A. E., Millan, M., Levy, E. I., Mitchell, P., Chen, M., English, J. D., Shah, Q. A., Silver, F. L., ... Jovin, T. G. (2018). Thrombectomy 6 to 24 hours after stroke with a mismatch between deficit and infarct. *New England Journal of Medicine*, 378(1), 11–21. <https://doi.org/10.1056/NEJMoa1706442>
- Otlivanchik, O., & Liberman, A. L. (2019). Migraine as a stroke mimic and as a stroke chameleon. *Current Pain and Headache Reports*, 23(9), 63. <https://doi.org/10.1007/s11916-019-0801-1>
- Pohl, M., Hessesberger, D., Kapus, K., Meszaros, J., Feher, A., Varadi, I., Pusch, G., Fejes, E., Tibold, A., & Feher, G. (2021). Ischemic stroke mimics: A comprehensive review. *Journal of Clinical Neuroscience*, 93, 174–182. <https://doi.org/10.1016/j.jocn.2021.09.025>
- Powers, W. J., Rabinstein, A. A., Ackerson, T., Adeoye, O. M., Bambakidis, N. C., Becker, K., Biller, J., Brown, M., Demaerschalk, B. M., Hoh, B., Jauch, E. C., Kidwell, C. S., Leslie-Mazwi, T. M., Ovbiagele, B., Scott, P. A., Sheth, K. N., Southerland, A. M., Summers, D. V., & Tirschwell, D. L. (2019). Guidelines for the early management of patients with acute ischemic stroke: 2019 update to the 2018 guidelines for the early management of acute ischemic stroke: A guideline for healthcare professionals from the American heart association/American stroke association. *Stroke: A Journal of Cerebral Circulation*, 50(12), e344–e418. <https://doi.org/10.1161/STR.0000000000000211>
- Psychogios, K., & Tsvigoulis, G. (2021). Intravenous thrombolysis for acute ischemic stroke: Why not? *Current Opinion in Neurology*, 35, 10–17. <https://doi.org/10.1097/WCO.0000000000001004>
- Royle, G., Ploner, C. J., & Leithner, C. (2011). Dizziness in the emergency room: Diagnoses and misdiagnoses. *European Neurology*, 66(5), 256–263. <https://doi.org/10.1159/000331046>
- Saver, J. L., Goyal, M., Bonafe, A., Diener, H.-C., Levy, E. I., Pereira, V. M., Albers, G. W., Cognard, C., Cohen, D. J., Hacke, W., Jansen, O., Jovin, T. G., Mattle, H. P., Nogueira, R. G., Siddiqui, A. H., Yavagal, D. R., Baxter, B. W., Devlin, T. G., Lopes, D. K., ... Jahan, R. (2015). Stent-retriever thrombectomy after intravenous t-PA vs. t-PA alone in stroke. *New England Journal of Medicine*, 372(24), 2285–2295. <https://doi.org/10.1056/NEJMoa1415061>
- Sporns, P. B., Brehm, A., Hilgers, C., Ntoulis, N., Tsogkas, I., & Psychogios, M. (2021). Distribution of diagnoses and clinical and imaging characteristics in 1,322 consecutive suspected stroke patients. *Frontiers in Neurology*, 12, 753183. <https://doi.org/10.3389/fneur.2021.753183>
- Tarnutzer, A. A., Lee, S.-H., Robinson, K. A., Wang, Z., Edlow, J. A., & Newman-Toker, D. E. (2017). ED misdiagnosis of cerebrovascular events in the era of modern neuroimaging: A meta-analysis. *Neurology*, 88(15), 1468–1477. <https://doi.org/10.1212/WNL.0000000000003814>

- Thomalla, G., Simonsen, C. Z., Boutitie, F., Andersen, G., Berthezene, Y., Cheng, B., Cheripelli, B., Cho, T.-H., Fazekas, F., Fiehler, J., Ford, I., Galinovic, I., Gellissen, S., Golsari, A., Gregori, J., Günther, M., Guibernau, J., Häusler, K. G., Hennerici, M., ... Gerloff, C. (2018). MRI-Guided thrombolysis for stroke with unknown time of onset. *New England Journal of Medicine*, 379(7), 611–622. <https://doi.org/10.1056/NEJMoa1804355>
- Virani, S. S., Alonso, A., Benjamin, E. J., Bittencourt, M. S., Callaway, C. W., Carson, A. P., Chamberlain, A. M., Chang, A. R., Cheng, S., Delling, F. N., Djousse, L., Elkind, M. S. V., Ferguson, J. F., Fornage, M., Khan, S. S., Kissela, B. M., Knutson, K. L., Kwan, T. W., Lackland, D. T., ... Stroke Statistics Subcommittee. (2020). Heart disease and stroke statistics-2020 update: A report from the American heart association. *Circulation*, 141(9), e139–e596. <https://doi.org/10.1161/CIR.0000000000000757>
- Wafa, H. A., Wolfe, C. D. A., Emmett, E., Roth, G. A., Johnson, C. O., & Wang, Y. (2020). Burden of stroke in Europe: Thirty-year projections of incidence, prevalence, deaths, and disability-adjusted life years. *Stroke: A Journal of Cerebral Circulation*, 51(8), 2418–2427. <https://doi.org/10.1161/STROKEAHA.120.029606>

**How to cite this article:** Hølllesli, L. J., Ajmi, S. C., Kurz, M. W., Tysland, T. B., Hagir, M., Dalen, I., Qvindesland, S. A., Ersdal, H., & Kurz, K. D. (2022). Simulation-based team-training in acute stroke: Is it safe to speed up?. *Brain and Behavior*, e2814. <https://doi.org/10.1002/brb3.2814>